Doctoral Dissertation

Mitigation of ammonia and/or salt inhibition in anaerobic digestion process through bioaugmentation with tolerant microbial community

耐性微生物群を用いたバイオオーグメンテーションによる嫌気性消化へのアンモニアおよび塩分阻害の緩和

LI ZIYAN

(李 子言)

July 2024

Division of Sustainable Energy and Environmental Engineering

Graduate School of Engineering

Osaka University

Content

Abbreviations

AD: Anaerobic digestion

AM: Acetoclastic methanogens

ANOVA: Analysis of variance

ASVs: Amplicon sequencing variants

DNA: Deoxyribonucleic acid

EPS: Extracellular polymeric substances

FAN: Free ammonia nitrogen

FO: Forward osmosis

HM: Hydrogenotrophic methanogens

KEGG: Kyoto Encyclopedia of Genes and Genomes

MSC: Marine sediment-derived microbial consortia

NH_4^+: Ammonium ions

PCA: Principal component analysis

PICRUSt: Phylogenetic investigation of communities by the reconstruction of unobserved states

RMSE: Root mean square error

SAO: Syntrophic acetate oxidation

sCOD: Soluble chemical oxygen demand

SMA: Specific methanogenetic activity

SPOB: Syntrophic propionate-oxidizing bacteria

TAN: Total ammonia nitrogen

TCOD: Total chemical oxygen demand

TS: Total solids

VFA: Volatile fatty acids

VS: Volatile solids

VSS: Volatile suspended solids

Lists of Tables

Lists of Figures

Fig. 2-7. Microbial network patterns in (a) the controls (non-bioaugmentation) under 5 g NH_4-N L^{-1} and 30 g NaCl L^{-1} treatments, (b) augmented cultures under NH_4^+ treatment, and (c) augmented cultures under salt treatment. Network with labeled connections between *Aminobacterium*, *Mariniphaga*, and *Methanoculleus* in the augmented cultures under salt treatment is shown in panel (d) and its sub-network is shown in panel (e). Other nodes that belong to a large number of smaller modules are colored gray for simplification. The node size is proportional to the betweenness centrality corresponding to the importance of the node. The top 5 major modules with the highest number of nodes were distinguished by distinct colors. Fruchterman Reingold's layout is applied to all networks. Positive and negative connections are expressed with green and red lines, respectively.

Fig. 3-1 CH_4 production profile of the two enrichments under the respective inhibition conditions. Enr-A represents the enrichment used in the ammonium-inhibited experiment, and Enr-S represents the enrichment used in the salt-inhibited experiment. The dotted line represents the cumulative CH_4 production level without inhibition.

Fig. 3-2 CH_4 production profile in repeated batch experiments of the (a) ammonium-inhibited and (b) salt-inhibited groups. The error bars represent the standard deviation of the mean for each duplicate experiment.

Fig. 3-3 Parameters estimated by modified Gompertz equation in the second and third batch of (a) ammonium-inhibited experiment and (b) salt-inhibited experiment. Solid lines indicate significant differences between different groups with *: $p < 0.05$; **: $p < 0.01$; ***: $p < 0.001$; ns: no significance.

Fig. 3-4 The total VFA concentration profile in the repeated batch experiment of (a) ammonium-inhibited experiment and (c) salt-inhibited experiment. The accumulated concentrations of different VFAs at the end of each batch of (b) ammonium-inhibited experiment and (d) salt-inhibited experiment, the three bars in the same cluster represent the results of, from left to right, first batch, second batch and third batch.

Fig. 3-5 Relative abundance of archaeal communities in the repeated batch experiment of (a) ammonium-inhibited experiment and (b) salt-inhibited experiment at the genus level. Genera under 1% relative abundance were allocated to "Others". "b" in the

sample names stands for “batch”.

Fig. 3-6 Relative abundance of bacterial communities in the repeated batch experiment of (a) ammonium-inhibited experiment and (b) salt-inhibited experiment at the genus level. Genera under 5% relative abundance were allocated to “Others”. “b” in the sample names stands for “batch”.

Fig. 3-7 The predicted relative abundance of key enzymes related to acidogenesis, acetogenesis and methanogenesis steps in anaerobic digestion of (a) ammonium-inhibited experiment and (b) salt-inhibited experiment using PICRUSt2 method. Error bars represent the standard deviation of the mean for each duplicate experiment.

Fig. 3-8 Principal component analysis (PCA) based on the 16S rRNA amplicon sequencing results for different experimental groups in different batches: (a) archaeal communities in the ammonium-inhibited group, (b) bacterial communities in the ammonium-inhibited group, (c) archaeal communities in the salt-inhibited group, and (d) bacterial communities in the salt-inhibited group. “b” stands for “batch.” PC1 and PC2 represent the principal components 1 and 2, respectively.

Chapter 1

Introduction

1.1 Anaerobic digestion

1.1.1 Principles and current status of anaerobic digestion process

Anaerobic digestion (AD) refers to a biochemical process in which organic waste is stepwise degraded to CH_4, CO_2 and H_2O by the synergistic action of various types of anaerobic microorganisms (Holm-Nielsen et al., 2009). With end products including biomass, biogas (mainly a mixture of CH_4 and CO_2), and effluent fertilizer, AD can simultaneously control pollution and produce bioenergy (Westerholm et al., 2012) thus widely considered a promising method for recovering bioenergy from organic waste. In the AD process, the degradation of organics to produce biogas is achieved by the combined efforts of various obligate and facultative anaerobes in a cascade form. AD is broadly recognized to be carried out in four steps: hydrolysis, acidogenesis, acetogenesis, and methanogenesis (Angelidaki et al., 2011; Khanal, 2008). In hydrolysis step, the polymers in organic waste are degraded to soluble organic monomers such as monosaccharides (from carbohydrates), amino acids (from proteins), glycerol and long-chain fatty acids (from oils and fats) by hydrolytic enzymes. In acidogenesis step, further conversion of monomers to volatile fatty acids (VFAs) with fewer than five carbon atoms, including acetic acid, propionic acid, butyric acid and

valeric acid, and alcohols. In acetogenesis step, VFAs and alcohols are further decomposed into acetic acid, accompanied by the production of formic acid, CO_2 and H_2. Finally, in methanogenesis step, acetic acid, formic acid, methanol, CO_2 and H_2 are converted into CH_4, CO_2 and H_2O by methanogens. Methanogenesis in AD can be divided into three different pathways: acetoclastic methanogenesis, syntrophic acetate oxidation (SAO) coupled with hydrogenotrophic methanogenesis, and methylotrophic methanogenesis (Harirchi et al., 2022; Pan et al., 2021; Zhang et al., 2016). Methylotrophic methanogenesis pathway is often neglected due to its limited contribution (Chandra et al., 2012). In acetoclastic methanogenesis, acetic acid is directly metabolized to produce CH_4 by acetoclastic methanogens (AM), as shown in Eq. (1-1).

$$CH_3COO^- + H_2O \rightarrow CH_4 + HCO_3^- \qquad \Delta G^0 = 31.0 \text{ kJ/mol} \qquad (1\text{-}1)$$

In SAO coupled with hydrogenotrophic methanogenesis, acetic acid is firstly oxidized to produce CO_2 and H_2, as shown in Eq. (1-2). Then, CO_2 and H_2 are utilized by hydrogenotrophic methanogens (HM) to produce CH_4, as shown in Eq. (1-3).

$$CH_3COO^- + 4H_2O \rightarrow 4H_2 + 2HCO_3^- + H^+ \qquad \Delta G^0 = +104.6 \text{ kJ/mol} \qquad (1\text{-}2)$$

$$4H_2 + HCO_3^- + H^+ \rightarrow CH_4 + 3H_2O \qquad \Delta G^0 = -135.6 \text{ kJ/mol} \qquad (1\text{-}3)$$

Microbes involved in each step utilize different types of substrates and have different optimum environmental factors for growth; thus, a delicate balance is maintained in the complex system in an AD reactor (Chen et al., 2008).

AD technology have been applied in energy recovery from waste/wastewater treatment for over a century, with numerous full-scale anaerobic digesters operating globally (Bencoova et al., 2021). Data released by Korean government shows that 110 centralized full-scale anaerobic digesters are being operated in Korea (MoE of Korea, 2021). However, process imbalance was frequently encountered during the operation of anaerobic digesters, which became the biggest problem hindering the application of AD process. Nielsen and Angelidaki (2008) surveyed 20 full-scale anaerobic digesters in Denmark and reported process imbalance in AD process could last for up to a few months, resulting in 20-30% loss in CH_4 production while the cause remained unclear. This results in a daily loss of roughly 650–1000 kWh of electricity for a biogas plant with daily CH_4 production of 300 m^3 (Maroušek et al., 2020), which reduces competitiveness of AD technology against other alternative technologies.

1.1.2 Influencing factors of AD process

As AD process is mediated by the combined efforts of a balanced and diversified microorganism community in a cascade form, the misfunction of any of the step will finally lead to the deterioration of the CH_4 production performance. Thus, attentive management is needed for the AD systems to keep various influencing factors in control.

(1) Temperature: Temperature imposes huge impact on the characteristics of the substrates and the thermodynamic equilibrium of biochemical reactions (Leven et al., 2007), also regulates the composition and activity of the microbial community (Hupfauf et al., 2018). AD systems are generally operated under psychrophilic

(<20 °C) (Tiwari et al., 2021), mesophilic (20–43 °C, optimum at 35 –37 °C) (Fernández-Rodríguez et al., 2016) or thermophilic conditions (50–60 ◦C, optimum at 55 °C) (Madigou et al., 2019). Psychrophilic conditions are generally considered inappropriate for AD processes because of the detrimental effect on bacterial metabolism. Recently, psychrophilic AD systems have drawn increasing attention in cold regions due to the low external energy input and easy implementation (X. Xu et al., 2022). Mesophilic AD systems are the most widely applied because of their relatively low investment and stable operation. Mesophilic conditions are suitable for the growth of the vulnerable methanogens, as most methanogens have optimal growth temperatures in the mesophilic range (Harirchi et al., 2022). Thermophilic AD systems suffer from requiring high energy input and having unstable operating conditions, while recent studies have suggested that a high organic removal rate and CH_4 yield can confer thermophilic AD a better energy balance compared with mesophilic AD (De Vrieze et al., 2016).

(2) pH: pH plays important role in the influencing the rate of biochemical reactions. For hydrolysis and acidogenic bacteria, a wide range of pH from 3 to 10 is suitable for degradation and metabolism of organics. While methanogens are more sensitive to pH, with optimal pH ranging from 6.5–8.5 (Liu et al., 2008).

(3) Organic loading: Organic loading refers to the total amount of organic substrate added to the AD reactor per unit volume per day, which strongly influence the growth and activity of associated microbial communities within an anaerobic system (Christou et al., 2021). If the organic loading rate in the AD reactor is too

high, intermediate products (e.g., VFAs) may accumulate, leading to a reduction in CH_4 production.

(4) Inhibitors: Inhibitory substances are often found to be the leading cause of anaerobic reactor upset. A wide variety of substances have been reported to be inhibitory to the biochemical reactions and the growth of the AD associated microorganisms (Chen et al., 2008). For organics, VFAs are the common inhibitors that deteriorate AD performance. When VFAs produced in the acidogenesis and acetogenesis step cannot be utilized in methanogenesis in time, the accumulation of VFAs occur. This reduces the pH in the system, and the excess acidification further inhibits the methanogenic community in a feedback loop that eventually leads to process failure (Li et al., 2023). For inorganics, ammonia and salt are common inhibitors because of their ubiquitous presence and frequent high concentrations in waste. The reported threshold of total ammonia nitrogen (TAN) inhibiting CH_4 production varies from 3.0 to 5.7 g NH_4^+-N L^{-1} (Climenhaga and Banks, 2008; Fotidis et al., 2013). It is also reported that salt levels >1% lead to cell disintegration and reduce metabolic enzyme activity and CH_4 production (Duc et al., 2022).

1.2 Ammonia inhibition in AD process

Ammonia is the basic nitrogen source for microorganisms in AD process. When in low concentration, ammonia not only promotes the microbial growth, but also enhances the buffering capabilities of the system. However, when its concentration exceeds a certain threshold, significant inhibitory effect occurs to the microorganisms associated to the

AD process. Free ammonia nitrogen (FAN) and ammonium ions (NH_4^+) are two forms of ammonia in AD system. A balance among FAN, TAN, as well as NH_4^+ exists and is governed by the following Eq. (1-4) (Hansen et al., 1998).

$$NH_3(\text{Free}) = \text{TAN} * \left(1 + \frac{10^{-pH}}{10^{-(0.09018 + \frac{2729.92}{T(K)})}}\right)^{-1} \quad (1\text{-}4)$$

where NH_3 (Free) is FAN (g L^{-1}), and T (K) is the temperature (Kelvin).

Inhibitory thresholds of TAN concentrations, ranging from 3.4 to 5.77 g L^{-1}, have been reported, resulting in severe CH_4 yield losses in the AD process ranging from 39 to 100 % (Climenhaga and Banks, 2008; Gallert and Winter, 1997; Liu and Sung, 2002; Sung and Liu, 2003), which can be ascribed to different temperatures, reactor configuration/operation modes adopted in AD systems (Alsouleman, 2019).

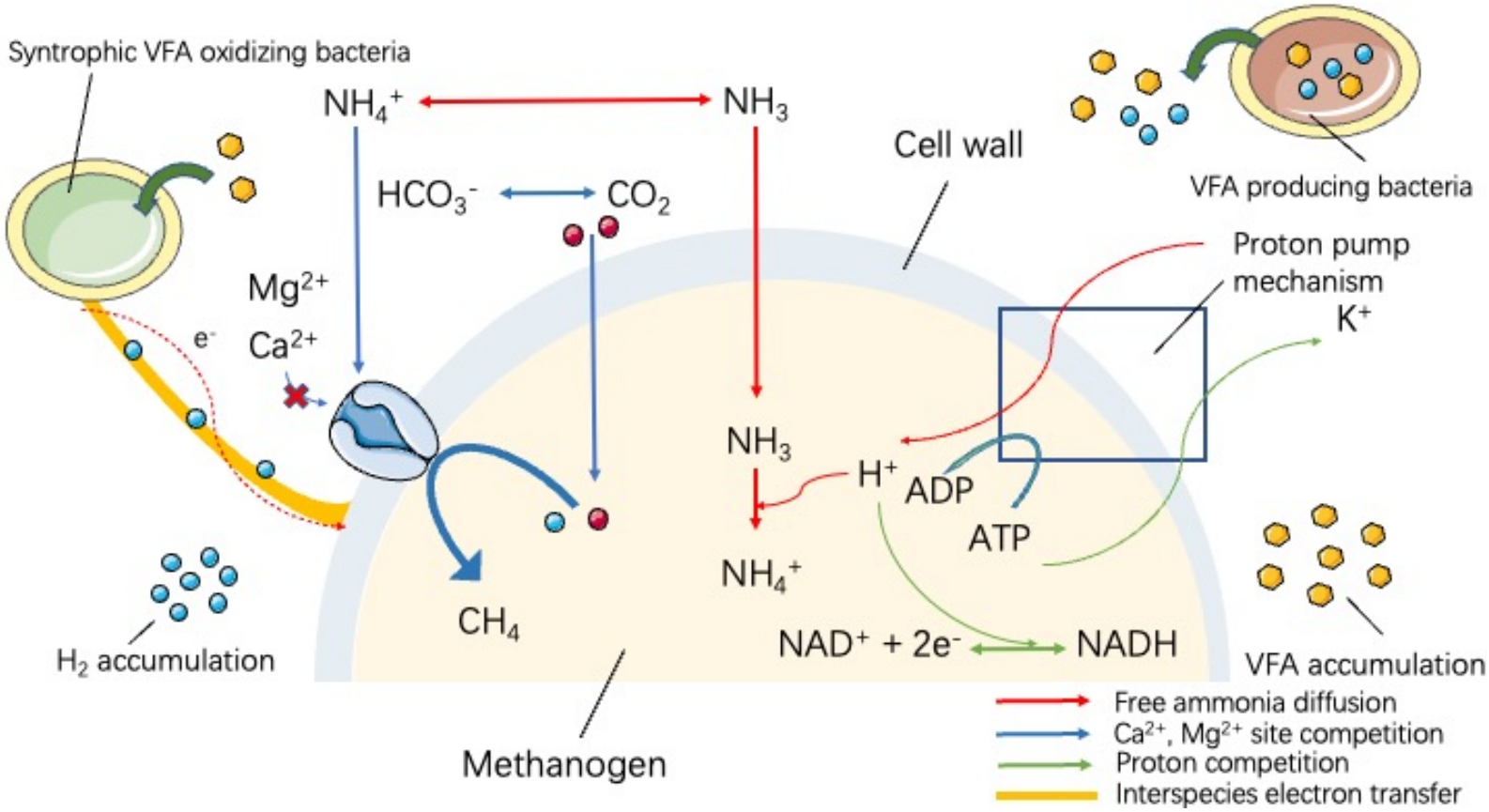

Fig. 1-1 Schematic of various ammonia inhibition mechanisms in the AD process. (adapted from (Yu et al., 2021))

1.2.1 Mechanisms proposed for ammonia inhibition of AD process

The two forms of ammonia (i.e., FAN and NH_4^+) are reported to be inhibit methanogenesis in different ways, as shown in Fig. 1-1. For FAN, the mechanism is proposed as "proton pump mechanism" as it diffuses through the plasma membrane due to the concentration gradient and competes for intracellular protons with enzymatic reactions such as NADH formation from NAD^+ (Wang et al., 2015). The proton pump is forced to pump more H^+ to maintain proton balance, thus results in a higher ATP energy cost and K^+ loss. Furthermore, when NH_4^+ formed from FAN that diffuses into the cell accumulates, it significantly influences intracellular pH, which further disturbs the enzymatic reactions involved in methanogenesis (Jiang et al., 2019). The concentration of FAN is influenced by pH as shown in Eq. (1-4). FAN concentration is 44.27 times higher in a solution with a pH of 9 than in one with a pH of 7 when both systems have the same TAN concentration and are operated at 37°C, indicating the importance of keeping a near-neutral pH in the AD process.

Sprott and Patel (1986) proposed that an essential enzyme participating in CH_4 synthesis spans the cytoplasmic membrane and relies on interactions with Ca^{2+} and Mg^{2+}, while a high concentration of NH_4^+ interferes with those interactions at Ca^{2+} and Mg^{2+} sites, thus impairing CH_4-producing activity. However, more direct evidence is required to support this hypothesis. Besides, high TAN concentrations can also result in secondary inhibition by the accumulation of intermediate products such as hydrogen and forementioned VFAs in AD reactors (Yuan and Zhu, 2016; Harirchi et al., 2022), which aggravated the inhibition level.

Table 1-1 Examples of physicochemical properties of various wastes and their inhibition of AD.

Waste type	TS (%)	VS (%)	TCOD (g L^{-1})	TN (mg L^{-1})	TAN (mg L^{-1})	Inhibition effect	Reference
Animal waste (chicken manure)	11.2 ±0.53	8.27 ±0.83	102.6 ±3.2	6450 ±810	3850 ±200	20% decrease of biogas yield at TAN of 10 g L^{-1} 100% loss of biogas yield at TAN of 16 g L^{-1} 0.35–0.4 L g^{-1} VS (biogas yield) under uninhibited conditions	Niu et al., 2015
Animal waste (pig manure)	5.9	4.6	N.A.	6700	4000	50% decrease of CH_4 yield at TAN of 11 g L^{-1}	Nakakubo et al., 2008
Food waste (school canteen)	28.41 ±0.62	26.46 ±0.67	N.A.	N.A.	3516 ±111	53% decrease of CH_4 yield at FAN of 0.3 g L^{-1} 0.53±0.02 L g^{-1} VS (CH_4 yield) under uninhibited conditions	Peng et al., 2018
Food waste (school canteen)	24.30 ±2.11	22.50 ±1.32	181.05 ±0.24	5950 ±130	330 ±8	94% decrease of CH_4 yield at TAN of 2.87 g L^{-1} 100% loss of CH_4 yield at TAN of 4.69 g L^{-1} 0.4 L g^{-1} VS (CH_4 yield) under uninhibited conditions	Chen et al., 2016
Municipal waste (sewage sludge)	1.34	0.95	N.A.	N.A.	791	20% decrease of cumulative CH_4 yield at TAN of 1.434 g L^{-1} 40% decrease of cumulative CH_4 yield at TAN of 2.339 g L^{-1}	Berninghaus and Radniecki, 2022
Municipal waste (sewage sludge)	2.14	1.56	N.A.	N.A.	1336	10% decrease of cumulative CH_4 yield at TAN of 1.954 g L^{-1} 18% decrease of cumulative CH_4 yield at TAN of 2.917 g L^{-1}	Berninghaus and Radniecki, 2022
Municipal waste (FO concentrated sewage)	N.A.	N.A.	2.714-3.289	N.A.	190-224	50% decrease of CH_4 yield at TAN of 2 g L^{-1}	Gao et al., 2019

TS, total solids; VS, volatile solids; TCOD, total chemical oxygen demand; N.A., not available.

1.2.2 Waste with the potential to cause ammonia inhibition in AD process

Ammonia inhibition is a common problem for AD process despite the different characteristics and nitrogen sources of the various target wastes. Previous studies have examined the physicochemical parameters and ammonia inhibition effects of several wastes prone to excess ammonia on the AD process, as summarized in Table 1-1.

(1) Animal waste: Animal waste consists mainly of animal bodies, manure, urine, and flushing water, and is characterized by high nitrogen content attributed to the decomposition of urea and proteins. For example, chicken manure is reported to contain an average of 3.85 g L^{-1} of TAN (Niu et al., 2015).

(2) Food waste: Food waste is rich in saccharides, proteins, and fats. The decomposition of proteins is the main cause of ammonia overabundance, whereas fats produce large amounts of hydrogen during hydrolysis (Hajjaji et al., 2016). A high hydrogen partial pressure in the system is undesirable for both the reaction thermodynamics and interspecies electron transfer (Tian et al., 2019).

(3) Municipal sewage sludge: Municipal sewage sludge is mainly composed of microorganisms and extracellular polymeric substances (EPS) excreted by them. Proteins and saccharides are the main constituents of EPS (Wilén et al., 2003), making AD a promising choice for municipal sewage sludge treatment. However, the composition of organic matter varies greatly depending on the source of wastewater. Efficiency of the digestion process is reported to deteriorate as the nitrogen content increases, and total CH_4 production ceases at a chemical oxygen demand to nitrogen ratio of 50 (Poggi-Varaldo et al., 1997).

(4) Municipal wastewater: Municipal wastewater concentrated by forward osmosis (FO) has recently been used as a feedstock for AD (Ortega-Bravo et al., 2022). The FO process significantly enhances the organic concentration of municipal wastewater, while ammonia, salt, and other nutrients are concentrated because of the non-selective characteristics of the FO process.

1.2.3 Technologies to relieve ammonia inhibition in AD process

(1) Physical/chemical methods: Physical/chemical methods aiming to relieve ammonia inhibition mainly focus on reducing ammonia concentration, adjusting pH and temperature of the system. Substrate dilution is regarded as a valid method to relieve ammonia inhibition. Nielsen and Angelidaki (2008) investigated the mitigating effort of three different dilution methods: with 50% of water, with 50% digested manure, or with 50% fresh manure on the performance of AD reactor treating cow manure. The results suggested that these different dilution methods were able to enhance CH_4 yield by 30–60%. Besides of dilution, adjustment of the carbon-to-nitrogen ratio, pH control, and ammonia recovery by membrane distillation were also applied in mitigating ammonia inhibition. However, physical/chemical methods are generally considered either energy/cost-intensive or difficult to implement (Rajagopal et al., 2013).

(2) Biological methods: Biological methods have been tested to strengthen biological processes, including bioaugmentation and acclimation, adding various supporting materials, such as biochar, activated carbon, and magnetite (Li et al., 2018; H. Peng et al., 2018; Zhang et al., 2017), and supplying trace elements. Peng et al. (2018)

investigated the effect of various kinds of supporting materials on enhancing the performance of AD process treating sludge. Results showed that average CH_4 production increased by 7.3% for magnetite, 13.1% for granular activated carbon, and 20% for the combination of above two materials. Among the biological methods, bioaugmentation, with advantages such as fast microbial community response and ease of implementation, has been intensively studied for the treatment of various types of waste. Bioaugmentation is a technology that delivers specialized microorganisms into the system and improves a specific function in the system, thus ameliorating reactor performance (Tale et al., 2015). Bioaugmentation using both pure strains and enriched mixed cultures has been proven to be efficient in mitigating ammonia inhibition in the AD process by Fotidis et al. (2017, 2014), despite the underlying mechanisms being different from each other.

1.3 Salt inhibition in AD process

Salt originates mainly from the NaCl used in food processing (especially in regions where people prefer salty food), breakdown of organic matter, or pH-adjustment chemicals (Grady et al., 1999). Salt is known to be the necessary component for microbial growth, thus when in moderate concentrations, it stimulates the growth of microorganisms, whereas excessive amounts cause severe inhibition (Soto et al., 1993). It is reported by Wood (2015) that salt levels >1% will lead to reduction of metabolic enzyme activity and CH_4 production (Duc et al., 2022).

1.3.1 Mechanisms proposed for salt inhibition of AD process

The Mechanisms of salt inhibition is closely related to the osmotic pressure change caused by high concentrations of salt (Yerkes et al., 1997). Dehydration and disintegration of microbial cells occur when under severe salt inhibition. Despite the co-occurrence of anions and cations in the solution, the toxicity of salt was reported to be predominantly determined by the cation, i.e., Na^+, in AD systems (McCarty and McKinney, 1961). It is reported by Liu and Boone (1991) that by comparing within VFA-degrading bacteria, Na^+ was more toxic to propionic acid-utilizing bacteria than to acetic acid-utilizing ones. Antagonistic effect exists between Na^+ and low-molecular-weight organic compounds, known as compatible solutes, which mitigates salt inhibition when the extracellular solute concentration exceeds that of the cell cytoplasm (Lai and Gunsalus, 1992). Besides, antagonism also exists between and other cations such as K^+ and Mg^{2+}, as Kugelman and McCarty (1965) reported the tolerance of microorganisms to Na^+ was highly increased when K^+ and Mg^{2+} co-existed.

1.3.2 Technologies to relieve salt inhibition in AD process

(1) Physical/chemical method: Physical/chemical methods are also applied in relieving salt inhibition. The main target of those method is to reduce salt concentration in the system, with technologies such as dilution with substrates containing less salt and membrane processes, which selectively remove salts from the digestate or recirculate low-salinity streams. Turcios et al. (2021) proposed co-digestion with other biomass feedstocks to dilute the salt concentration contained in halophyte plants and their residues, which will largely expand renewable energy production.

(2) Biological methods: Biological methods applied in mitigating salt inhibition in AD

process include acclimation of microorganisms to high salt concentrations and adding various supporting materials (Aramrueang et al., 2022). Ali et al. (2021) examined the performance of anaerobic reactors with salt-adapted microorganisms. The results showed efficient performance was achieved with >99.9% phenol removal at salt level of 10 g NaCl L^{-1}. However, successful application of bioaugmentation was not reported in mitigating salt inhibition in AD reactors.

1.4 Bioaugmentation as a promising method to mitigate inhibition effect

1.4.1 Principles and merits of bioaugmentation

Bioaugmentation, with advantages such as fast microbial community response and ease of implementation, has been intensively studied for the treatment of various types of waste by AD. By delivering specialized microorganisms into the system, bioprocesses associated to AD process are strengthened by exotic microorganisms introduced as bioaugmentation inocula, and the effect may be even enhanced when the inoculum targets weak steps (i.e., acetogenesis and methanogenesis) in the AD process or is pre-acclimated to specific inhibitors (Venkiteshwaran et al., 2016).

Among the various methods developed to strengthen different aspects of the AD process in the presence of different inhibitors, bioaugmentation stands out on the following merits:

(1) Economic feasibility and easy implementation: Compared to bioaugmentation, physical/chemical methods such as the C:N ratio and pH adjustment require large

amounts of substrate/pH regulators, whereas membrane distillation relies on the use of membrane modules, the operation and maintenance of which are complicated, energy-intensive, and expensive (Darestani et al., 2017; Shanmugam and Horan, 2009).

(2) Fast microbial community response: The alternative use of acclimation and/or fixation of microorganisms requires a long time for shifts in species composition and dominance to occur and for biofilms or granules to form (Gao et al., 2015; Sasaki et al., 2011).

(3) Long-term stability: For example, over 140 days of stable operation were achieved after bioaugmentation (Yang et al., 2020).

(4) Ease of customization: Various combinations of strains and consortia with different optimal environmental factors can be used to provide case-customized strategies.

1.4.2 Bioaugmentation focusing on different steps of AD process

Given the cascade form of microbial reactions in AD process, the decline in activity in any step will lead to the problematic reactor performance. Various bioaugmentation strategies aimed at mitigating ammonia inhibition by strengthening the different steps of the AD process are summarized in Fig. 1-2.

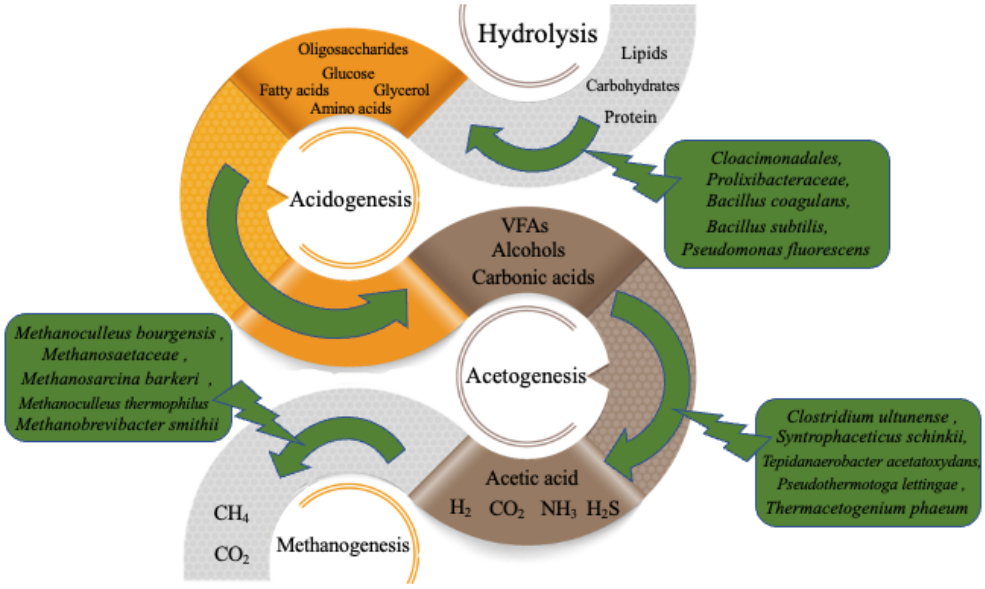

Fig. 1-2 Schematic diagram of bioaugmentation strategies for improving AD performance under high ammonia conditions.

(1) Methanogenesis: As forementioned, acetoclastic methanogenesis and SAO coupled with hydrogenotrophic methanogenesis are two main methanogenesis pathways in AD process. A lot more focus has been placed on strengthening hydrogenotrophic methanogenesis using HM as a bioaugmentation inoculum, since HM is reported to be more tolerant to ammonia toxicity than other microbes involved (Hardy et al., 2021). Fotidis et al. (2014) chose a fast-growing HM, *Methanoculleus bourgensis* MS2^{T} as the bioaugmentation inoculum for AD operated at high ammonia levels (5 g NH_4^+-N L^{-1}). Compared with the control group, the bioaugmentation group achieved a 31.3 % increase in yield of CH_4 production. Microbial community analyses revealed that the augmented species were well established in the system, demonstrating a 5-fold increase in relative abundance after bioaugmentation.

Bioaugmentation aimed at reinforcing acetoclastic methanogenesis also draws attention from researchers due to the ubiquity of the acetoclastic pathway and the high affinity of AM to acetate (Tao et al., 2020). Li et al. (2017) launched bioaugmentation using an enriched culture dominated by obligate AM *Methanosaetaceae,* which consists of over 90 % archaeal groups. An enhanced average volumetric CH_4 production of 70 mL L^{-1} d^{-1} and an enhanced propionate degradation rate of 51 % were observed 45 d after dosing, while the non-bioaugmentation reactor almost failed to generated CH_4 under ammonia stress at a TAN of 3.0 g N L^{-1}. In addition, a double dosage of bioaugmentation culture enabled efficient recovery of the failing group. Microbial analyses after bioaugmentation showed a significant increase in *Methanosaetaceae*, which proved the establishment of the bioaugmentation culture. This research demonstrated that despite the susceptibility of AMs to ammonia, prevention and recovery from an ammonium-inhibited state is possible by dosing the system with AMs. However, because a relatively mild ammonia inhibition (3.0 g N L^{-1}) was selected in this study, whether the mitigation effect is still valid at higher ammonia levels requires further investigation.

(2) Acetogenesis: VFA accumulation problems are commonly encountered in AD reactors with excess levels of ammonia inhibition, since acidogenic bacteria are reported to endure higher levels of ammonia than other guilds, such as acetogenic bacteria and methanogenic archaea (Niu et al., 2014). Li et al. (2022) introduced propionate-degrading methanogenic cultures to relieve the accumulation of VFAs

resulting from treating chicken manure, which is a typical high-ammonia waste. The results suggested an effective improvement in reactor performance, as propionate accumulation was almost eliminated, and the CH_4 yield in the bioaugmented digester was enhanced by 17–26 %. Furthermore, long lasting bioaugmentation effect was observed even after the cease of introducing microorganisms from 90 days, which lasted for 180 days, as CH_4 yield was improved by 15–18 % under high ammonia concentration of 5.0–8.4 g NH_4^+-N L^{-1} when a higher organic loading rate was implemented. According to an analysis of the microbial community, the syntrophic propionate-oxidizing bacteria *Syntrophobacter* was regarded as the key contributor to the improved AD process, as its relative abundance experienced an evident increase. The relative abundances of HM *Methanobacterium* and AM *Methanothrix* also increased, which may be due to the more suitable environment for proliferation after bioaugmentation.

(3) Hydrolysis: For high-solids (>20 %) AD reactors treating food and vegetable waste, hydrolysis may be the rate-limiting step (Wilson, 2016). Jo et al. (2021) applied a rumen culture, which is characterized by large populations of microbes capable of degrading particulate matter, as a bioaugmentation inoculum to mitigate the effects of excess ammonia and cellulose due to fluctuations in feed composition. The one-time bioaugmented reactor maintained better and more stable performance than the control reactor over 1000 d, particularly during periods in which the ammonia concentration reached nearly 3.0 g N L^{-1} of TAN. Bioaugmentation with rumen culture increased not only the relative abundance of potential hydrolyzing bacteria,

such as *Cloacimonadales* and *Prolixibacteraceae*, but also the diversity and resilience of the whole microbial community. Microorganisms that contribute to hydrolysis are reported not to be inhibited by ammonia even at high concentrations (Fernandes et al., 2012), thus the mitigation effect at high ammonia concentration periods may be due to improved interactions and cooperation within the microbial community.

1.4.3 Current status and perspectives of bioaugmentation

Since bioaugmentation as a technology to mitigate ammonia inhibition is still at the stage of exploration and development, most bioaugmentation experiments have been conducted at the laboratory scale (Romero-Güiza et al., 2016). However, within the same scale, the reactor configuration appears to be a crucial factor for the successful implementation of bioaugmentation. Most of successful bioaugmentation attempts were obtained in batch mode (Kovács et al., 2015; Town and Dumonceaux, 2016; Yan et al., 2021). A comparative study by Tian et al. (2017) revealed that a continuous reactor is unfavorable for bioaugmentation owing to a washout effect, in comparison to batch and fed-batch reactors. In the research by Westerholm et al. (2012), where bioaugmentation with SAO culture was conducted in continuous reactors under extreme ammonia levels of up to 11.0 g NH_4^+-N L^{-1}, the reactor performance deteriorated as the ammonia concentration increased and finally collapsed completely, in spite of the daily addition of the inoculum to avoid the SAO culture being washed out. Despite extensive studies verifying the usefulness of bioaugmentation to mitigate ammonia inhibition, full-scale demonstration trials are still scarce (Schmack and Reuter, 2010). This might be

attributed to the large volume of bioaugmentation inoculum needed for trials, as full-scale facilities usually work continuously with a large working volume. To further reduce the cost of acquiring bioaugmentation inoculum, the use of a mixed culture is recommended because of the relatively low requirements for cultivation compared to pure strains. To mitigate the washout effect, the addition of supporting materials and application of membrane reactors enabling biofilm formation and biomass retention are potential means of realizing successful bioaugmentation. Furthermore, bioaugmentation regimes (i.e., dosage, repetition, and timing) also need to be optimized to ensure its effectiveness.

1.5 Objective of this study

Previous studies have proved that bioaugmentation is a promising method in mitigating inhibition effect in AD process. Successful attempts of applying bioaugmentation on mitigating ammonia inhibition were reported, whereas no such attempts were reported in mitigating salt inhibition in AD process. Moreover, bioaugmentation regimes (i.e., dosage, repetition, and timing) also need to be optimized in bioaugmentation to ensure its effectiveness, as well as to reduce its cost. Thus, the objective of this study is to investigate the feasibility of applying bioaugmentation on mitigating salt inhibition in AD process and further to optimize bioaugmentation regimes in both ammonium- and salt-inhibited conditions.

In Chapter 1, the principles and current status of AD process and bioaugmentation were introduced. Technologies proposed for mitigating ammonia/salt inhibition were also

introduced. Based on the review of previous studies, the objective of this study was proposed as mentioned above.

In Chapter 2, the feasibility of applying bioaugmentation on mitigating salt inhibition in AD process was investigated using marine sediment-derived microbial consortia (MSC) as bioaugmentation inoculum under salt, as well as under ammonia stress.

In Chapter 3, a variety of bioaugmentation regimes in both ammonium- and salt-inhibited conditions were investigated using repeated-batch mode reactors for their optimization.

In Chapter 4, the summary and conclusions of this study were given.

Chapter 2

Bioaugmentation with marine sediment-derived consortia in mesophilic anaerobic digestion for enhancing CH_4 production under high salt/ammonium condition

2.1 Introduction

Bioaugmentation applied on mitigating salt inhibition in AD process is seldomly reported. Also, the potential of using MSCs as bioaugmentation agents to relieve the inhibitory effects of salt, as well as of ammonia stresses in AD systems has not been explored. In addition, key phylotypes and microbial interactions (e.g., symbiosis and competition) for effective bioaugmentation under ammonia or salt stress remain to be determined. Thus, this chapter was conducted aiming to evaluate the effectiveness of using pre-acclimated MSCs as a novel augmented agent to alleviate the inhibitory effects of high ammonia and salt concentrations on CH_4 production. Two MSCs pre-acclimated to high ammonia and salt concentrations were used for bioaugmentation in batch AD experiments. Microbial cooccurrence networks with and without bioaugmentation were analyzed to identify key phylotypes for efficient CH_4 production under ammonia or salt stress.

2.2 Material and methods

2.2.1 Seed sludge and pre-acclimated microbial consortia

Table 2-1 Characteristics of the seed sludge and the pre-acclimated marine sediment-derived microbial consortia (MSCs).

Parameters	Seed sludge	MSCs	
		MSC-A	MSC-B
pH	6.91	8.25	8.35
TS (mg L^{-1})	21465	53925	52503
VS (mg L^{-1})	16325	19289	15262
TCOD (mg L^{-1})	25750	27533	31900
sCOD (mg L^{-1})	821	27933	30467
NH_4-N (mg L^{-1})	692	5281	4821
NaCl (g L^{-1})	3.05	40.4	41.9

Seed AD sludge was collected from a mesophilic continuous anaerobic digester in the central part of Japan. Two MSCs pre-acclimated to high ammonia (5 g NH_4-N L^{-1}) and salt (30 g NaCl L^{-1}) concentrations were constructed using marine sediment samples collected from saline environments, the tidal flat of the Ariake Sea in Japan (33°04′28.1″ N, 130°08′47.1″ E) and the bottom of the brackish water of Lake Hamanako in Japan (34°4′12.4″ N, 137°36′38.9″ E), as the microbial sources and designated as MSC-A and MSC-B, respectively. Each sediment sample was suspended in an 800 mL bottle containing 200 mL of synthetic medium (2.3 g L^{-1} glucose, 1.1 g L^{-1} yeast extract, 0.9 g L^{-1} peptone, 2 g NH_4-N L^{-1}, 30 g NaCl L^{-1}, and 10 g L^{-1} $NaHCO_3$) to yield a final volatile solids (VS) concentration of 10 g L^{-1}. After sealing with a rubber stopper and purging with N_2 gas, the cultures were anaerobically incubated at 37℃ with rotary shaking at 120 rpm. The cultivation was continued for over 20 weeks with a stepwise increment of ammonia concentration to 5 g NH_4-N L^{-1}. The physicochemical properties

of the seed sludge and two MSCs were summarized (Table 2-1).

2.2.2 Anaerobic digestion experiment

Prior to use in AD experiments, the seed sludge and MSCs were centrifuged (3000 × g, 10 min), washed twice with 0.9% NaCl solution, and resuspended in pure water. The suspended seed sludges and synthetic wastewater were mixed and fed into 50 mL serum bottles as control (non-bioaugmentation) to yield a final VS concentration of 5 g L^{-1} in a 20 mL culture volume. In the other bottles, 7.5% and/or 15% VS of the seed sludge were replaced with MSC-A or MSC-B, which were designated as A (15%), B (7.5%), and B (15%), for bioaugmentation. At the onset of all AD experiments, the ratio of the soluble chemical oxygen demand (sCOD) of synthetic wastewater to the VS of the seed sludge was approximately 1:1. Duplicate bottles were prepared for the control and each augmented culture. The synthetic wastewater consisted of glucose (2.3 g L^{-1}), yeast extract (1.1 g L^{-1}), peptone (0.9 g L^{-1}), and $KHCO_3$ (4.5 g L^{-1}). NH_4Cl or NaCl was amended at 5 g NH_4-N L^{-1} or 30 g NaCl L^{-1} (11.8 g L^{-1} Na^+), respectively, as the inhibitory factor, considering their inhibitory concentrations in AD systems.

The anaerobic condition was obtained by sealing the serum bottles with a butyl rubber stopper and flushing with N_2 gas for 5 min. All the prepared cultures were cultivated at 37°C with rotary shaking at 120 rpm for 40 days without pH control. On day 14, one of the duplicate cultures was sacrificed for the determination of pH, ammonia, VFA concentrations, and microbial community. From day 14, only one culture was run for each condition because comparable CH_4 production ($p > 0.05$; Student's t-test) was

observed between the duplicate cultures. The CH_4 production was monitored periodically until 40 days when the daily CH_4 production for 3 consecutive days was < 1% of the cumulative CH_4 production. In addition, pH, ammonia, VFAs, and microbial community were analyzed on day 40.

2.2.3 Chemical analyses

Total solids (TS) and VS were determined following standard methods (APHA, 2012). ammonia was measured using an HIC-NS/HIC-SP dual flow-line ion chromatography system (Shimadzu, Japan) equipped with a Shim-pack IC-C4 cation exchange column (Shimadzu). To analyze the concentration of ammonia, a mixture of 3.0 mM oxalic acid and 4.0 mM 18-crown-6 was used as the eluent. Salt concentration was measured using an MM-42DP portable water quality meter (DKK-TOA, Japan). The TCOD and sCOD were measured using a Merck COD Spectroquant test kit and a Move 100 colorimeter (Merck, Germany). Before measuring the sCOD, the samples were filtered through a cellulose acetate filter (0.45 μm pore size, Advantec, Japan). The biogas produced in the headspace of the serum bottles was collected with a 100 μL gas-tight syringe (Hamilton, USA), and the CH_4 concentration was determined using a GC-2010 Plus gas chromatography system (Shimadzu) equipped with a barrier discharge ionization detector and MICROPACKED-ST capillary column (Shinwa Chemical Industries, Japan). VFA concentrations in the culture liquid were measured using a GC-2014 gas chromatography system (Shimadzu, Japan) equipped with a flame ionization detector and Stabilwax-DA capillary column (Restek, USA). The concentrations of VFAs,

including propionate, butyrate, and valerate, were calculated as mg of acetic acid equivalent per L (mg L^{-1}).

2.2.4 Microbial community analyses

A FastDNA Spin Kit for Soil (MP Biomedicals, USA) was used to extract DNA from the samples (0.25 mL for each), including the seed sludge, two MSCs (MSC-A and MSC-B), and sludge samples on days 14 and 40. A 2-step tailed PCR was performed to construct amplicon libraries targeting the V4 hypervariable region of the 16S rRNA genes with the 515F and 806R primer set (Peiffer et al., 2013). At the second PCR, the resulting amplicon was barcoded using the Index PCR primers. The amplicon libraries were subjected to Illumina Miseq sequencing (Illumina, USA) at the Bioengineering Lab. Co. Ltd. (Japan). The raw sequence reads were registered to the DNA Data Bank of Japan Sequence Archive database under accession number DRA015451.

The sequencing reads were quality filtered and chimera checked using QIIME 2 (version 2021.2) and grouped into amplicon sequencing variants (ASVs) using the DADA2 algorithm. The taxonomic classification was assigned based on SILVA database release 132 with 97% identity. Dendrograms were constructed based on the Bray–Curtis similarity matrix using the "vegan" package in RStudio (version 1.3.1056; R Foundation, USA) to compare the similarity of archaeal and bacterial communities between samples with and without bioaugmentation. Two microbial cooccurrence networks were constructed by grouping 16S rRNA datasets obtained from six augmented cultures (A (15%), B (7.5%), and B (15%)) collected on days 14 and 40 for

each treatment of 5 g NH_4-N L^{-1} and 30 g NaCl L^{-1}. This step was performed to identify key phylotypes in bioaugmentation. Another microbial cooccurrence network was constructed by grouping 16S rRNA datasets from the controls (non-bioaugmentation) with ammonia and salt treatments obtained on days 14 and 40. Only ASVs with an abundance of 0.1% and greater, which occurred in more than two samples, were included in the analysis to minimize the impact of rare ASVs. The correlation matrix for the ASVs was calculated using Spearman's rank-based correlation generated by the "corr.test" function of the "psych" package. Only ASVs with Spearman's correlation coefficients $r > 0.6$ and p-values < 0.01 were considered statistically significant and used for microbial cooccurrence network analysis using the "igraph" and "psych" packages in RStudio. The networks were further analyzed and visualized using Gephi 0.9.7 (Bastian et al., 2009). The modularity-based Louvain algorithm was applied to optimize, sort, and detect distinct modules of microbial communities of closely connected nodes within each network.

2.2.5 Predictive model and statistical analyses

The observed data of cumulative CH_4 production were fitted to kinetic models to evaluate the effects of inhibitory factors (ammonia and salt) and bioaugmentation on CH_4 production. The modified Gompertz model (Eq. (2-1)) (Lay et al., 1997), which is commonly used to describe a mono-sigmoidal pattern in batch AD experiments, was applied to fit the cumulative CH_4 production data under salt stress. By contrast, it did not fit the CH_4 production data under ammonia stress, where CH_4 production occurred

biphasically (i.e., a double-sigmoidal pattern). Due to the different effects of ammonia on kinetics and metabolic pathways, different response parameters (e.g., two different kinetic constants for lag time) have been recently suggested to describe the cumulative CH_4 production under this stress (Agyeman et al., 2021). In addition, Yu et al. (2020) reported that the kinetic constants of CH_4 production are likely to vary because of a shift in metabolic pathways in the second phase of CH_4 production by high ammonia concentrations. For these reasons, the observed data with high ammonia stress were fitted to a double-Gompertz model (Eq. (2-2)) as described by (Pardilhó et al., 2022) to evaluate the effects of bioaugmentation on metabolic pathways for CH_4 production. All the kinetic constants were estimated simultaneously through non-linear curve fitting using the solver tool in MS Excel (version 16.54) with the generalized reduced gradient algorithm, the central derivative, and convergence of 1 × 10-6. Root mean square error (RMSE) was calculated by the difference between the observed and predicted CH_4 production to evaluate the accuracy of the models.

$$M = P * exp\{-exp[\frac{B*R'*e}{P}(\lambda - t) + 1]\} \quad (2\text{-}1)$$

where M is the cumulative CH_4 production (mL) at time t, P is the maximal CH_4 production (mL), B is the biomass contained in the serum bottle (g volatile suspended solids (VSS)), R' is the maximal CH_4 production rate (mL CH_4 g VSS^{-1} day^{-1}), λ is the lag time of CH_4 production (day), and e is 2.71828.

$$M = \sum_{i=1}^{2} P_i * exp\{-exp[\frac{B*R_i'*e}{P_i}(\lambda_i - t) + 1]\} \quad (2\text{-}2)$$

where P_i (mL), R_i' (mL CH_4 g VSS^{-1} day^{-1}), and λ_i (day) represent the kinetic parameters of the double-Gompertz model for each phase of CH_4 production. Lag time of the second phase was calculated as the difference (day) between λ_2 and λ_1.

2.3 Results and discussion

2.3.1 Effects of bioaugmentation on CH_4 production

Fig. 2-1 shows the cumulative CH_4 production with or without bioaugmentation using MSC-A or MSC-B under 5 g NH_4-N L^{-1} or 30 g NaCl L^{-1} treatment. ammonia and salt stresses exerted different patterns in cumulative CH_4 production: a mono-sigmoidal pattern under salt stress and a biphasic pattern under ammonia stress. Reference cultures without ammonia or salt stress were not prepared in this study owing to experimental limitations. However, the inhibition of CH_4 production under ammonia or salt stress was confirmed by referring to the data of a previous study (Duc et al., 2022) that employed the same medium and seed sludge collected from the same digester (Fig. 2-2). On day 30, the cumulative CH_4 production in the controls was only 83.8% (27.5 mL) and 62.5% (20.5 mL) of those without ammonia and salt stresses in the study by Duc et al. (2022), respectively. By contrast, bioaugmentation with MSC-A or MSC-B allowed efficient CH_4 production of 33.7 ± 1.4 mL with a specific yield of 336.6 ± 13.9 mL CH_4 g $sCOD^{-1}$ on day 30, which was comparable to those without ammonia and salt stresses (Fig. 2-2) and the theoretical CH_4 production of 340.7 mL CH_4 g $sCOD^{-1}$. The cumulative CH_4 production nearly reached an asymptotic value on days 36–40. During this period, the daily CH_4 production was <1% (0.3–0.8%) of the cumulative

CH_4 production in each sample, indicating stabilization (Holliger et al., 2016). Therefore, the results suggested that bioaugmentation using the MSCs alleviated the inhibitory effects of ammonia and salt stresses on CH_4 production. By contrast, extension of the experimental period further enhanced CH_4 production in the controls, which eventually showed a small difference to those in the augmented cultures on day 40. This result may be ascribed to the relatively high tolerance of the seed sludge to ammonia stress (Agyeman et al., 2021).

Compared with 5 g NH_4-N L^{-1}, 30 g NaCl L^{-1} caused significantly greater inhibition (p <0.05; Student's t-test) of the cumulative CH_4 production. By contrast, bioaugmentation using the MSCs enhanced CH_4 production from day 22 onward and improved up to 25% of the cumulative CH_4 production compared with the controls (Figs. 2-1 and 2-2).

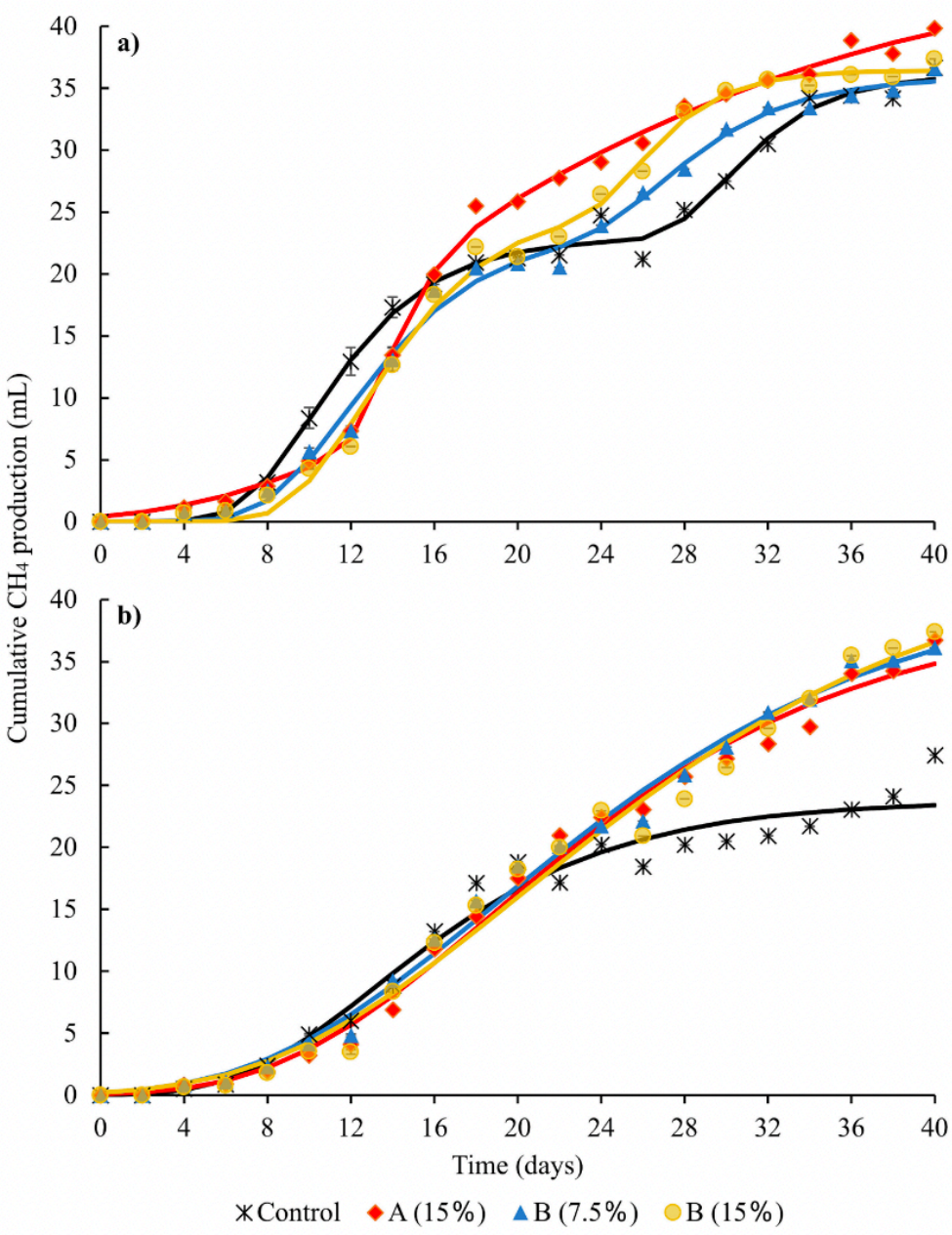

Fig. 2-1 Observed (symbols) and predicted (solid lines) cumulative CH_4 production in the controls (non-bioaugmentation) and augmented cultures under (a) 5 g NH_4-N L^{-1} and (b) 30 g NaCl L^{-1} treatments. A and B indicate the augmented sources that were added to the AD systems, while 7.5% and 15% VS refer to the augmented dosages. Error bars represent standard deviation of the mean for each duplicate experiment until day 14.

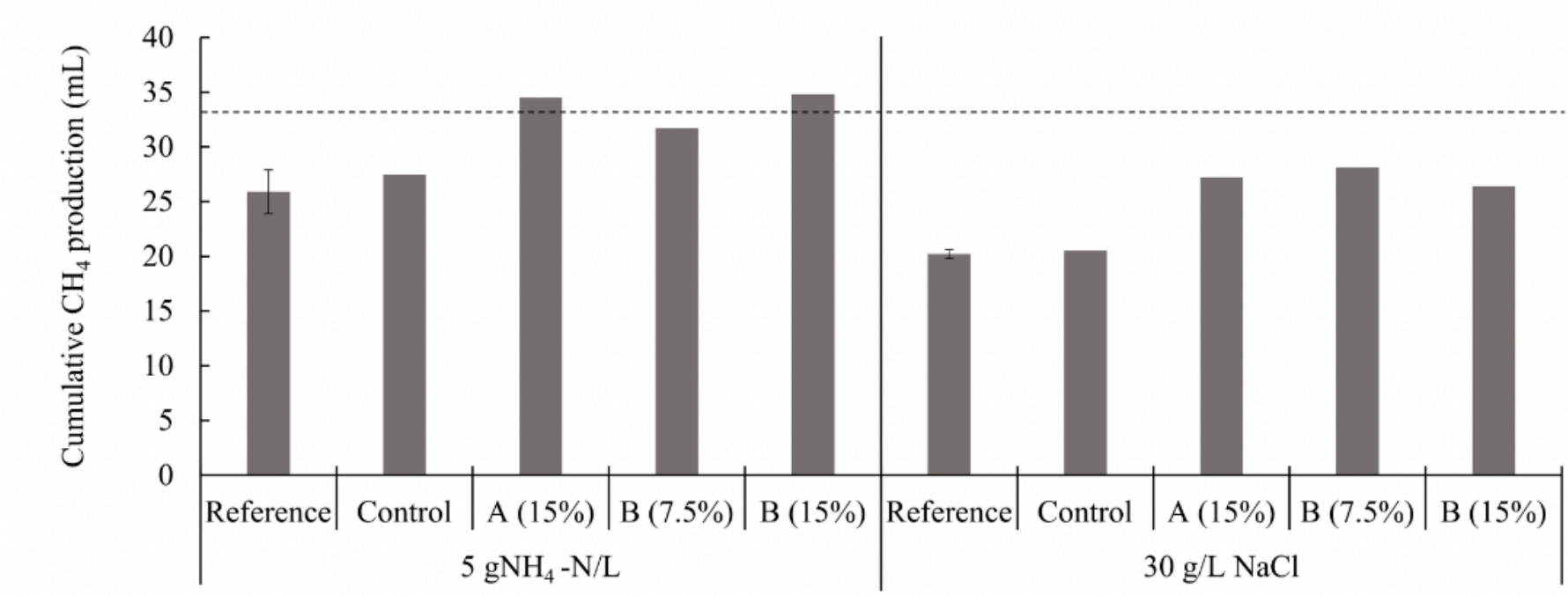

Fig. 2-2 Comparison of the cumulative CH_4 production on day 30 in the augmented cultures and controls under 5 g NH_4-N L^{-1} and 30 g NaCl L^{-1} treatments. Data of the 30-day CH_4 production experiment in a previous study (Duc et al., 2022) that employed the same synthetic wastewater and seed sludge collected from the same digester without (dashed line) and with the same ammonia or salt treatment ("Reference" bar) are shown for comparison.

Table 2-2 Kinetic constants and statistical results of the models applied for the controls (non-bioaugmentation) and the augmented cultures under 5 g NH_4-N L^{-1} or 30 g NaCl L^{-1} treatment.

Treatment	Model	Parameter	Control	Augmented culture		
				A (15%)*	B (7.5%)*	B (15%)*
30 g NaCl L^{-1}	Modified Gompertz model	*P* (mL)	23.8	39.4	41.9	44.3
		*B*R'* (mL/day)	1.3	1.4	1.4	1.4
		λ (day)	6.6	8.6	7.8	8.3
		R^2	0.974	0.992	0.994	0.986
		RMSE	1.5	1.2	1.0	1.6
5 g NH_4-N L^{-1}	Double-Gompertz model	P_1 (mL)	22.9	31.1	23.5	25.5
		$B*R_1'$ (mL/day)	2.5	0.9	2.3	2.6
		λ_1 (day)	6.7	5.9	7.9	9.0
		P_2 (mL)	13.2	13.4	12.4	10.9
		$B*R_2'$ (mL/day)	1.8	3.2	1.3	1.7
		λ_2 (day)	27.2	12.0	23.5	23.5
		R^2	0.996	0.998	0.996	0.996
		RMSE	0.8	0.7	0.9	0.9

* A (15%), B (7.5%), and B (15%) indicate the bioaugmentation dosages, in which 7.5% or 15% VS of the seed sludge used in controls was replaced with MSC A or B.

Kinetic constants of CH_4 production in the augmented cultures and the controls were estimated using the modified Gompertz model and the double-Gompertz model for high salt and ammonia concentrations, respectively, to understand further the effects of bioaugmentation. The models showed a good fit with the observed cumulative CH_4 production in all samples (R^2 = 0.974–0.998 with a low RMSE) (Fig. 2-1 and Table 2-2). The *P* values in the augmented cultures were notably greater (165.3–186.3%) than those in the control under salt stress (Table 2-2). Under ammonia stress, the *P* value

(the sum of P_1 and P_2) in the culture augmented using MSCA was greater (123.5%) than that in the control. After bioaugmentation, the lag time of the second phase was also shortened by 4.9–14.4 days as compared with the controls under ammonia stress (Table 2-2). These results suggested that the tolerant populations in the MSCs adapted well to ammonia stress and complemented the impaired AD steps in the seed sludge, allowing smooth CH_4 production with a shortened lag time. By contrast, bioaugmentation with MSC-B at different doses (7.5% and 15% as VS) showed minor effects on the kinetic parameters under both stresses (Fig. 2-1 and Table 2-2). However, the dose–effect relationship and the optimum dosage of augmented consortia warrant further analyses to determine the practical applications of bioaugmentation.

2.3.2 Effects of bioaugmentation on volatile fatty acids accumulation

Fig. 2-3 shows the accumulation of VFAs on days 14 and 40. On day 14, propionate and acetate were mainly accumulated. Greater average concentrations of VFAs (1573 ± 239 and 2120 ± 174 mg as acetic acid equivalent L^{-1}) accumulated in the augmented cultures under ammonia and salt stresses, respectively, than in the controls. The ammonia or salt stress possibly inhibited hydrolysis reactions and consequently suppressed VFA production in the controls (Wilson et al., 2013), whereas bioaugmentation enhanced hydrolysis and acidogenesis.

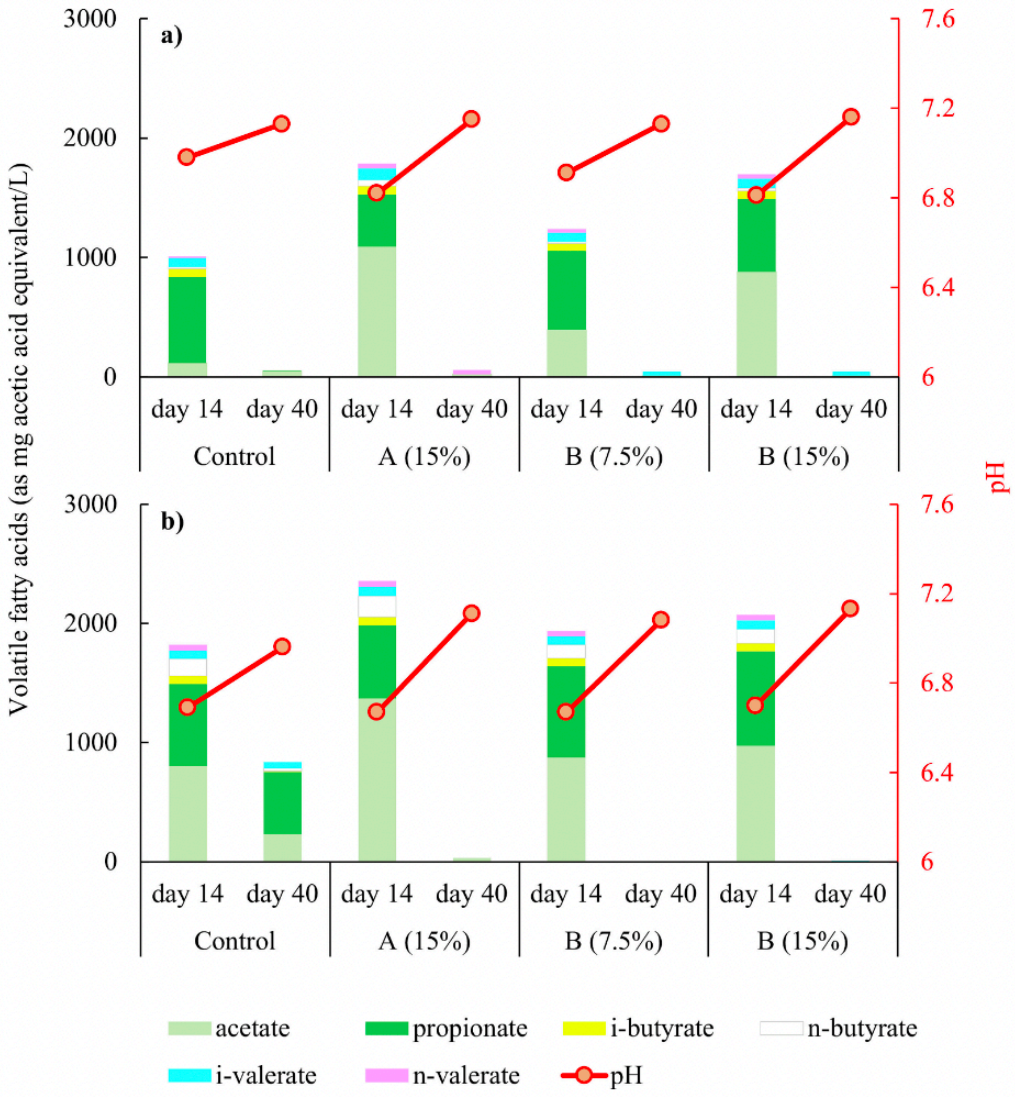

Fig. 2-3 Changes in VFA concentrations and pH during anaerobic digestion with and without bioaugmentation under (a) 5 g NH_4-N L^{-1} and (b) 30 g NaCl L^{-1} treatments.

On day 40, VFAs were almost degraded in the augmented cultures with efficient CH_4 production (Figs. 2-1 and 2-3). VFAs were also degraded in the controls, which eventually resulted in a small difference in the cumulative CH_4 production compared with those in the augmented cultures under ammonia stress (Figs. 2-1a and 2-3a). However, in the control under salt stress, where CH_4 production was low, VFAs (mainly, propionate) still accumulated on day 40 (Fig. 2-3b). These results indicated that efficient propionate degradation is important to enhance CH_4 production under ammonia or salt stress. Similarly, Zhang et al. (2022) reported that propionate accumulates under 4.8 g NH_4-N L^{-1} treatment, which seriously decreases CH_4 production. In addition, Li et al. (2017) enhanced CH_4 production by reducing propionate accumulation under ammonia inhibition through augmenting propionate-oxidizing consortia. Nevertheless, excess propionate accumulation under ammonia and salt stresses is difficult to alleviate because of the unfavorable thermodynamics of propionate oxidation (Zhang et al., 2022). The results of this study demonstrated the usefulness of pre-acclimated MSCs as bioaugmentation agents to allow efficient CH_4 production through alleviating propionate accumulation under ammonia and salt stresses.

2.3.3 Effects of bioaugmentation on microbial composition

Fig. 2-4 shows the archaeal community compositions in the controls and the augmented cultures. Although the acetoclastic methanogen *Methanosaeta* dominated in the seed sludge, its population declined in all of the cultures, indicating that its growth was inhibited by ammonia or salt stress. By contrast, the relative abundance of versatile

methanogens and HMs increased. The versatile methanogen *Methanosarcina* predominated (30–45%) in the controls and augmented cultures on day 40, indicating the relatively high tolerance of this genus to ammonia and salt (Zeb et al., 2019). In addition, HMs *Methanoculleus* (7.7–90.9%) and *Methanomassiliicoccus* (8.9–51.4%), which predominated in MSC-A and MSC-B, were minor in the seed sludge and most of the augmented cultures treated with salt on day 14 but became dominant in the augmented cultures with greater proportion than those in the controls on day 40 (*Methanoculleus* at 4.6–18.4% and *Methanomassiliicoccus* at 2.8–4.7%). These genera can tolerate the toxicity of 9.8 g NH_4-N L^{-1} or greater (Hardy et al., 2021) and the combination of 4 g L^{-1} Na^+ and 6.5 g NH_4-N L^{-1} (Lee et al., 2021). These results indicated the successful complement of *Methanoculleus* and *Methanomassiliicoccus* through bioaugmentation. In addition, the dominance of the hydrogen-consuming pathway through the complement of HMs by bioaugmentation with MSCs might contribute to the enhancement of CH_4 production in the augmented cultures.

Among bacteria, *Atopostipes* (33.8–45%), *Jeotgalibaca* (1.6–26.5%), *Tepidimicrobium* (6.1–11.6%), *Aminobacterium* (4.8–11%), *Anaerosalibacter* (3–5%), and *Fermentimonas* (0.7–4.6%) predominated in MSC-A and MSC-B (Fig. 2-5). Although *Atopostipes*, *Jeotgalibaca*, *Tepidimicrobium*, *Aminobacterium*, and *Fermentimonas* were not detected in the seed sludge, they became abundant after bioaugmentation. *Atopostipes*, *Jeotgalibaca*, and *Tepidimicrobium* are hydrolytic and acetogenic bacteria (Kim et al., 2018; Sohail et al., 2022). These genera were likely responsible for the increased VFA production in the augmented cultures (Fig. 2-3). By contrast,

Fermentimonas and *Aminobacterium* were considerably enriched on day 40. *Fermentimonas* is a candidate for syntrophic VFA-degrading bacteria (Usman et al., 2020). *Aminobacterium* is another potential syntrophic propionate-oxidizing bacteria (SPOB) (Cao et al., 2021), accounting for a greater proportion in the augmented cultures (0.9–7.6%) than in the controls (0.4–1.9%). The increased abundance of these VFA-degrading bacteria may explain the efficient degradation of VFAs, especially propionate, in the augmented cultures (Fig. 2-3).

A similarity analysis of archaeal and bacterial compositions was performed to understand the regulatory factors of microbial transitions (Fig. 2-6). The archaeal and bacterial communities were separated into three clusters, irrespective of the treatment with ammonia or salt. One cluster comprised both pre-acclimated MSCs. The other clusters separated microbial communities on days 14 and 40, irrespective of the augmented cultures and the controls. These results indicated the temporal transition with similar microbial compositions under ammonia and salt stresses. In addition, similar microbial compositions and transitions independent from bioaugmentation suggested decisive process parameters, such as high ammonia and salt or propionate accumulation, determining the archaeal and bacterial compositions (Peces et al., 2018).

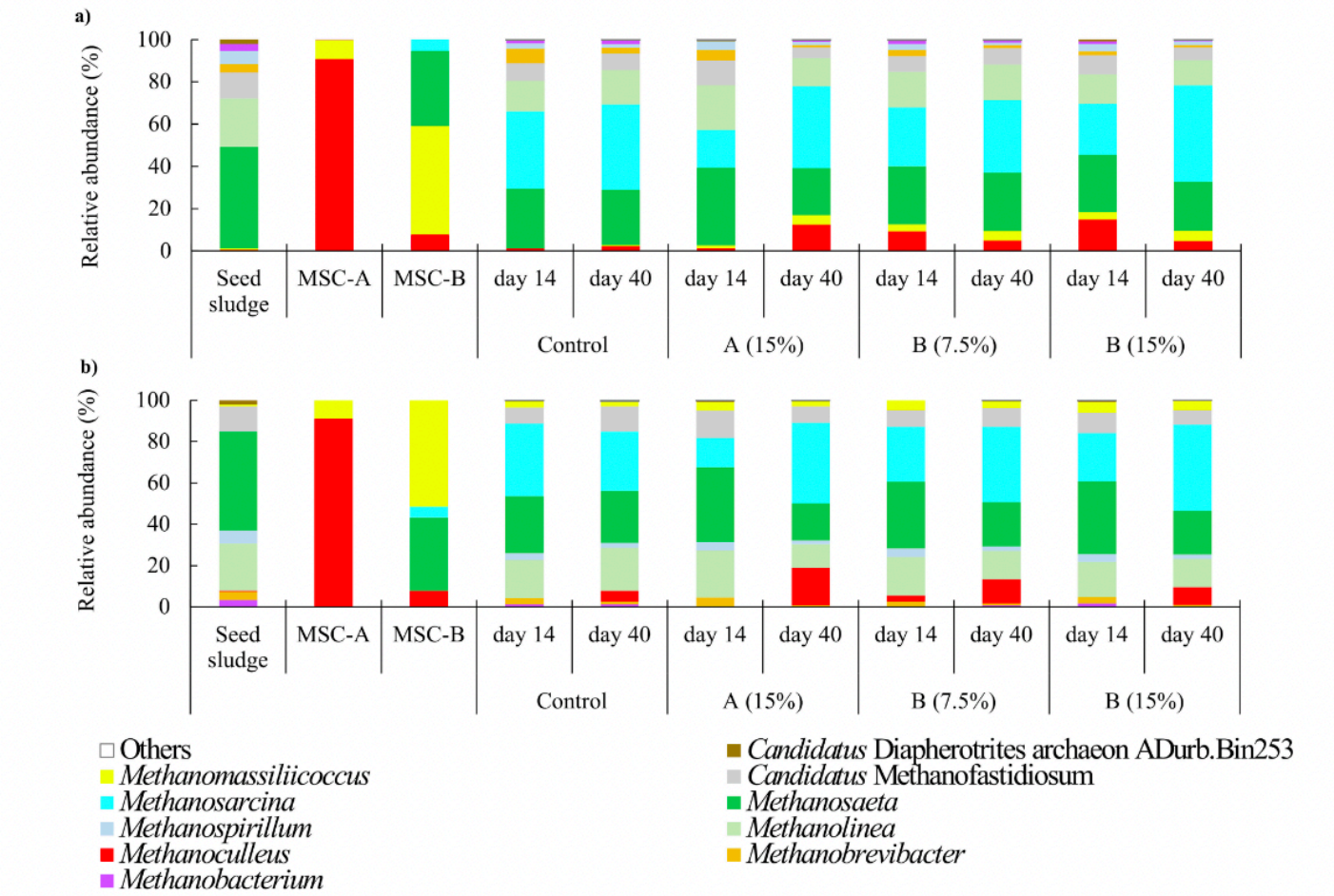

Fig. 2-4 Relative abundance of archaeal communities at the genus level under (a) 5 g NH_4-N L^{-1} and (b) 30 g NaCl L^{-1} treatments. Unclassified genera were allocated to “Others”.

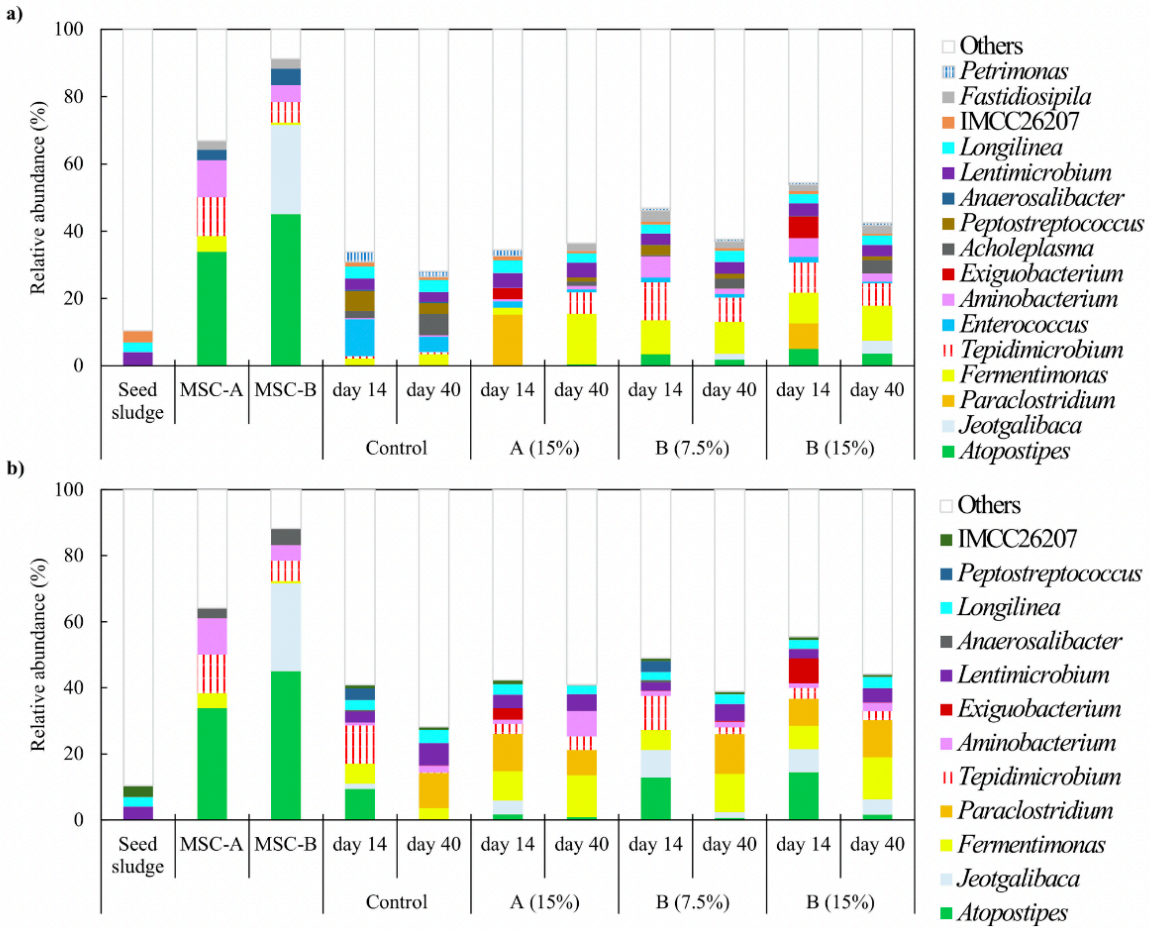

Fig. 2-5 Relative abundance of bacterial communities at the genus level under (a) 5 g NH_4-N L^{-1} and (b) 30 g NaCl L^{-1} treatments. Unclassified genera or the genera with <3% relative abundance were allocated to "Others".

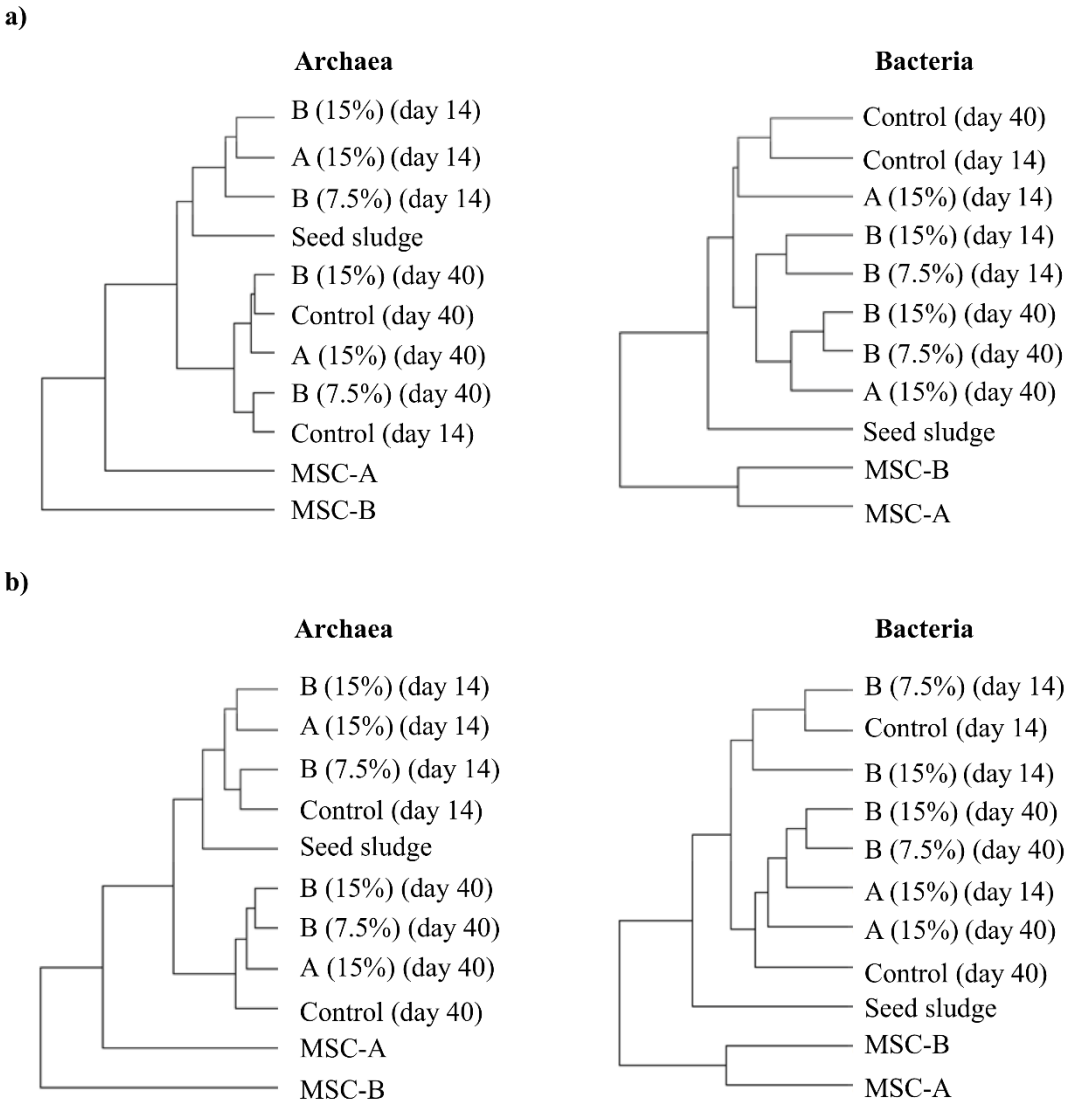

Fig. 2-6. Clustering tree of archaeal (left) and bacterial (right) communities under (a) ammonia and (b) salt treatments.

2.3.4 Mechanism for enhanced CH_4 production through bioaugmentation

Topological properties and influential phylotypes (keystone) with high impact on the microbial community were characterized through microbial cooccurrence network analysis to unveil the mechanisms for efficient CH_4 production by bioaugmentation (Fig. 2-7). Different network properties were observed in the microbial communities with and without bioaugmentation. The controls showed a greater modularity index (1.2) with more modules (28) than the augmented cultures (0.6 modularity and 10 modules). The modules are functional units or niches in a microbial community (Wu et al., 2016). Therefore, the greater modularity likely indicated the fragmentation/segregation of microbial community structure into functional units under the stresses. In addition, negative connections accounted for 30% of the total connections (Fig. 2-7a), indicating the antagonism or competition between microbes under ammonia or salt stress (Freilich et al., 2018). By contrast, positive inter-community connections between nodes were dominant in the augmented cultures (Figs. 2-7b and 2-7c), indicating the mutualism between populations through bioaugmentation.

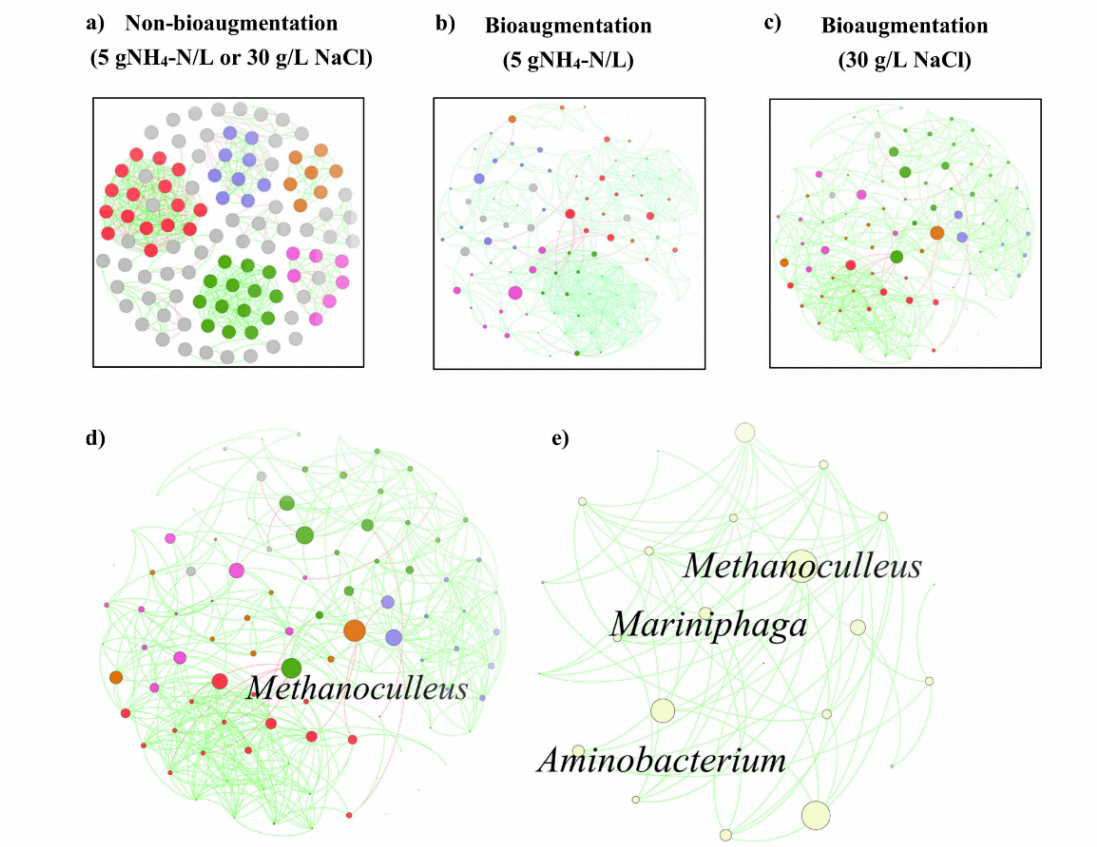

Fig. 2-7. Microbial network patterns in (a) the controls (non-bioaugmentation) under 5 g NH_4-N L^{-1} and 30 g NaCl L^{-1} treatments, (b) augmented cultures under ammonia treatment, and (c) augmented cultures under salt treatment. Network with labeled connections between *Aminobacterium*, *Mariniphaga*, and *Methanoculleus* in the augmented cultures under salt treatment is shown in panel (d) and its sub-network is shown in panel (e). Other nodes that belong to a large number of smaller modules are colored gray for simplification. The node size is proportional to the betweenness centrality corresponding to the importance of the node. The top 5 major modules with the highest number of nodes were distinguished by distinct colors. Fruchterman Reingold's layout is applied to all networks. Positive and negative connections are expressed with green and red lines, respectively.

Methanoculleus, which was complemented through bioaugmentation (Fig. 2-4), had the highest betweenness centrality. This result indicated that *Methanoculleus* was the influential phylotype, i.e., a keystone in the augmented cultures (Banerjee et al., 2018). The keystone phylotype is vital for maintaining the stability of a microbial community (Banerjee et al., 2018; Liao et al., 2023). Liao et al. (2023) reported that the toxic effects of tetracycline and polystyrene microbeads on the keystone phylotype lead to fragmentation in the gut microbiome of marine medaka. Thus, the augmentation of *Methanoculleus* was the key to the reinforcement of inter-community connections, ensuring efficient CH_4 production under ammonia and salt stresses (Fig. 2-1). The tolerance of *Methanoculleus* to high NH_4^+ (Hardy et al., 2021), propionate (Cao et al., 2021), and Na^+ (Lee et al., 2021) contributed to their proliferation. In addition, the tolerance of *Methanoculleus* likely allowed a smooth progress of methanogenesis pathways, leading to a shortened lag time in the second phase of CH_4 production in the augmented culture (Fig. 2-1 and Table. 2-2), as previously reported (Agyeman et al., 2021).

In addition, a positive connection was observed between *Methanoculleus*, SPOB (*Aminobacterium*), and *Mariniphaga* (Fig. 2-7e) (Saha et al., 2021). In the same module, *Methanosarcina* positively connected with SPOB (*Syntrophobacter* and *Syntrophothermus*) and *Desulfobulbus*. *Mariniphaga* and *Desulfobulbus* are involved in interspecies and extracellular electron transfers, respectively (Lei et al., 2019; Saha et al., 2021). *Desulfobulbus* and *Mariniphaga* were undetected in the seed sludge; thus, their increased abundance in the augmented cultures possibly originated from the MSCs

(Miura et al., 2015; Shi et al., 2015). The complement of *Mariniphaga* and *Desulfobulbus* possibly benefited the syntrophic relationships of SPOB and methanogens. These interspecies and extracellular electron transfers likely facilitated the electron flux between SPOB, *Mariniphaga*, and HMs, which allowed efficient propionate degradation and CH_4 production (Saha et al., 2021). Taken together, the results underlined the stress mitigation mechanisms through the complement of SPOB, electron transfers, and *Methanoculleus* in bioaugmentation (Figs. 2-1, 2-2, and 2-3). Although several studies recognized that electron transfers can alleviate the inhibitory effects of ammonia and salt on CH_4 production (Chen et al., 2020; J. Xu et al., 2022), few studies attempted to enhance microbial electron transfers by using bioaugmentation (Zhang et al., 2018). The present study indicated that the enhanced electron transfers to promote the syntrophic relationships between SPOB and methanogens are a key bioaugmentation strategy for efficient CH_4 production under ammonia and salt stresses. Cooccurrence network analysis is useful in identifying influential phylotypes in a complex microbial community to establish a suitable bioaugmentation strategy (De Vrieze and Verstraete, 2016). However, the effects of bioaugmentation on the topological properties of AD microbial networks remain unclear. In this study, cooccurrence network analysis unveiled the fragmentation of a microbial network under ammonia or salt stress and the inter-community joint connections of *Methanoculleus* for efficient CH_4 production. The results of this study could serve as a basis for elucidating the mechanisms underlying the inhibition of CH_4 production in AD and its mitigation through bioaugmentation.

The success of bioaugmentation largely depends on the choice of bioaugmentation agent. The MSCs pre-acclimated to high ammonia and salt concentrations robustly mitigated the inhibitory effects of ammonia and salt on CH_4 production. The successful bioaugmentation was attributed to the co-presence of tolerant hydrolytic, VFAs-degrading, and methanogenic populations in the MSCs. In marine sediment, salt tolerant anaerobes coexist naturally. In addition, the ammonium tolerance of microbes is likely associated with the salt-detoxification system based on their capacity to maintain an osmotic pressure balance between the cells and surrounding environment by potassium and osmolyte uptake systems (Manzoor et al., 2016; Maus et al., 2015). Collectively, the pre-acclimated MSCs would be ideal bioaugmentation agents in AD under ammonia and salt stresses.

2.4 Summary

Bioaugmentation using pre-acclimated MSCs was conducted to alleviate the inhibitory effects of ammonia and salt stresses on CH_4 production in AD. Compared with non-bioaugmentation, bioaugmentation increased cumulative CH_4 production by 25% under salt stress. It also shortened the lag time of the second phase under ammonia stress. The complement of SPOB, interspecies electron transfers, and *Methanoculleus* through bioaugmentation with MSCs possibly allowed efficient propionate degradation and CH_4 production. This chapter provides novel insights into establishing effective bioaugmentation strategies under ammonia and salt stresses.

Chapter 3

Different bioaugmentation regimes for mitigating ammonium/salt inhibition in repeated batch anaerobic digestion

3.1 Introduction

The feasibility of applying bioaugmentation on mitigating salt, as well as ammonia inhibition in AD process was proved in Chapter 2. However, anaerobic digester bioaugmentation is still in a nascent stage, in which the bioaugmentation regimes (i.e., dosage, repetition, and timing) need to be optimized to ensure its effectiveness. Although some previous studies have investigated the optimal dosage and meliority of single or routine dosing, most have focused only on short-term effects (Linsong et al., 2022) and some have reached conflicting conclusions (Lee et al., 2022; Yang et al., 2016). Thus, in this chapter, a comprehensive investigation of the performance of different bioaugmentation regimes, considering dosage, repetition, and timing of bioaugmentation, was conducted under both ammonium- and salt-inhibited conditions. Three consecutive batches lasting over 80 days were used to assess the sustainability of each bioaugmented group. The biomass of each group was collected during the operation, and the microbial community transition of different bioaugmentation regimes was scrutinized to provide a microbial perspective using 16S rRNA amplicon sequencing. Remarks on the different bioaugmentation regimes were made by

analyzing two independent sets of data from both ammonia and salt inhibitors.

3.2 Material and methods

3.2.1 Feedstock, seed sludge, and bioaugmentation inoculum

The feedstock used for CH_4 production was selected as synthetic wastewater consisting of glucose (2.3 g L^{-1}), yeast extract (1.1 g L^{-1}), peptone (0.9 g L^{-1}), and $KHCO_3$ (4.5 g L^{-1}). The seed AD sludge was collected from a mesophilic continuous anaerobic digester of a municipal wastewater treatment plant in northern Japan, which was stabilized in synthetic wastewater at 37°C with rotary shaking at 120 rpm for 30 days and adjusted to 5 g VSS L^{-1} before use.

The bioaugmentation inoculum were two kinds of enrichments pre-acclimated to high ammonia (5 g NH_4-N L^{-1}) and salt (30 g NaCl L^{-1}) concentrations. Both enrichments were constructed from mesophilic AD sludge in a municipal wastewater treatment plant in southern Japan through cultivation in the same synthetic wastewater for over six months with stepwise increments of ammonia and salt concentrations to the final level. Repeated batch mode was adopted for cultivation, with a batch time of 10 days. The CH_4 production activity of both enrichment systems was confirmed prior to the experiment (Fig. 3-1).

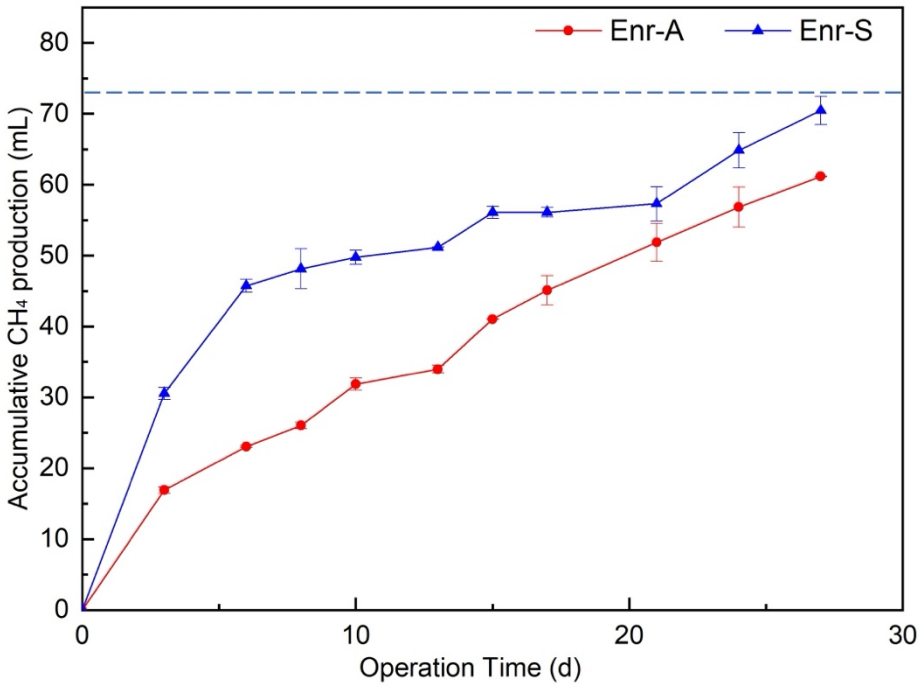

Fig. 3-1 CH_4 production profile of the two enrichments under the respective inhibition conditions. Enr-A represents the enrichment used in the ammonium-inhibited experiment, and Enr-S represents the enrichment used in the salt-inhibited experiment. The dotted line represents the cumulative CH_4 production level without inhibition.

3.2.2 Repeated batch AD experiment

The AD reactors were operated in repeated-batch mode with total and working volumes of 117 and 40 mL, respectively. Mesophilic temperature (37°C) and rotary shaking (120 rpm) conditions were maintained during the operation. The selected inhibition conditions were consistent with the pre-acclimated enrichments, which were 5 g NH_4-N L^{-1} for ammonia and 30 g NaCl L^{-1} for salt. Anaerobic conditions were maintained by sealing the serum bottles with a butyl rubber stopper and flushing with N_2 gas for 8

min. Five experimental groups were set up as follows in duplicate for both ammonium- and salt-inhibited conditions: (1) 2.5 I: one-time introduction of 2.5% (VSS base, the same below) bioaugmentation inoculum in the first batch; (2) 2.5 RB: repeated introduction of 2.5% bioaugmentation inoculum in all three batches, making total dosage reach 7.5%; (3) 5 I: one-time introduction of 5% bioaugmentation inoculum in the first batch; (4) 7.5 I: one-time introduction of 7.5% bioaugmentation inoculum in the first batch; and (5) 5 II: one-time introduction of 5% bioaugmentation inoculum in the second batch. The Control group, in which no inhibition or bioaugmentation inoculum was introduced into the system, and the Inhibited group, with inhibited conditions and no introduction of bioaugmentation inoculum, were prepared in duplicate. The detailed bioaugmentation regimes are listed in Table 3-1. Three consecutive batches of 81 d (27 d per batch) were conducted. CH_4 production was monitored every 2–3 d. Liquid samples were collected on days 8, 15, and 27 from each batch for VFAs measurements. The pH, ammonium/salt concentration, and sCOD of the liquid samples were measured, and biomass samples were collected at the end of each batch. When starting the next batch, the bulk liquid in each group was centrifuged under anaerobic conditions, the supernatant was discarded, and feedstock (together with bioaugmentation inoculum, if applicable) was replenished to the working volume. N_2 flushing was repeated before the reactors were placed in an incubator.

Table 3-1 Bioaugmentation strategy regimes of each experimental group.

Group	First batch	Second batch	Third batch	Inhibitor
Control	0	0	0	0
Inhibited	0	0	0	1
2.5 I	2.5%	0	0	1
2.5 RB	2.5%	2.5%	2.5%	1
5 I	5%	0	0	1
7.5 I	7.5%	0	0	1
5 II	0	5%	0	1

In the column of "Inhibitor", "1" represents with inhibitor addition; "0" represents without inhibitor addition.

3.2.3. Chemical analyses

Total suspended solids, VSS, as well as CH_4 concentration were determined using methods introduced in Chapter 2. The modified Gompertz model (Eq. (2-1)) was used to describe the cumulative CH_4 production in each batch test. Kinetic parameters were estimated by nonlinear curve fitting using the solver tool in Microsoft Excel (version 16.70).

NH_4^+ and Na^+ were both measured using an HIC-NS/HIC-SP dual flow-line ion chromatography system (Shimadzu) equipped with a Shim-pack IC-C4 cation exchange column (Shimadzu). Concentrations of sCOD and VFAs were determined using methods introduced in Chapter 2. The concentrations of VFAs were calculated as COD (mg L^{-1}) with conversion coefficients of 1.07, 1.51, 1.82, and 2.04 for acetate, propionate, butyrate, and valerate, respectively.

3.2.4. Microbial community analyses

A FastDNA Spin Kit for Soil (MP Biomedicals, USA) was used to extract DNA from the samples, including the seed sludge, two types of pre-acclimated enrichments, and biomass samples at the end of each batch. PCR primers 515F (5'-GTGCCAGCMGCCGCGGTAA-3') and 806R (5'-GGACTACHVGGGTWTCTAAT-3') were used to target the V4 region of the 16S rRNA genes. The amplicon libraries were subjected to Illumina MiSeq sequencing (Illumina, USA) at the Bioengineering Lab. Co. Ltd. (Japan). The sequencing reads were filtered, and chimeras were checked using QIIME 2 (version 2021.2), which were then grouped into ASVs using the DADA2 algorithm. The SILVA database (v. 138) was used for taxonomic classification, with 97% identity. Based on the sequencing results, a phylogenetic investigation of communities by the reconstruction of unobserved states (PICRUSt) was used to predict the gene abundance of key enzymes in the microbial community. The total sequencing reads were analyzed using the PICRUSt2 software (Caicedo et al., 2020) and annotated according to the Kyoto Encyclopedia of Genes and Genomes (KEGG) database. The abundant metabolic genes related to glycolysis, fatty acid synthesis, propionic and butyric acid degradation, and aceticlastic and hydrogenotrophic methanogenesis were selected based on the KEGG CH_4 metabolic pathways (Map: 00010, Map: 00061, Map:00013, Map:00357, and Map:00567) and evaluated accordingly.

3.2.5. Statistical analyses

GraphPad Prism (v. 10, GraphPad Software Inc., USA) was used to plot the parameters estimated by modified Gompertz equation in the second and third batches. Multiple

comparisons of ordinary two-way analysis of variance (ANOVA) were selected for the significance analysis among results of different groups. A significance level of 0.05 was used. Principal component analysis (PCA) using the plug-in unit of Principal Component Analysis App in OriginLab program (v. 9.8.0.200, OriginLab Corporation, USA) was conducted to compare the microbial communities collected in different experimental groups, as well as to show the succession of the microbial community in one group.

3.3 Results and discussion

3.3.1 CH_4 production

The reactor performance and kinetic parameters estimated using the modified Gompertz equation for each experimental group are shown in Fig. 3-2 and Table 3-2. Bioaugmentation at all dosages exerted an instant mitigating effect in the first batch compared to the Inhibited groups in both the ammonium- and salt-inhibited experiments. For example, the final cumulative CH_4 production in the 7.5 I group reached 1.43-fold and 1.55-fold compared to their respect Inhibited group under ammonium and salt stress. Moreover, the mitigation performance was positively correlated with the dosage of the introduced inoculum for both inhibitors. The *P* values (see Table 3-2) estimated by the modified Gompertz equation for the 2.5 I (87.5%, compared to the Control group), 5 I (91.4%), and 7.5 I (97.1%) groups increased as the dosage increased under salt-inhibited conditions. The same trend was also observed under ammonium stress, as *P* values increased from 85.5% in the 2.5 I group to 96.5% and 100.0% in the 5 I and 7.5

I groups, respectively, as the dosage increased. This intuitive result also conforms to previous studies conducted by Linsong et al. (2022) and Yang et al. (2016), who reported enhanced bioaugmentation efficiency as dosages increased when operating batch reactors for digesting chicken manure and potato slurry, respectively.

However, the positive correlation between reactor performance and bioaugmentation inoculum dosage did not persist in the second and third batches for either inhibitor. More specifically, in the salt-inhibited condition, the CH_4 production curves of the 2.5 I, 5 I, and 7.5 I groups in Fig. 3-2b overlapped with each other in the second and third batches, indicating no evident difference in bioaugmentation efficiency among groups with different dosages. Quantitative results were verified as demonstrated in Table 3-2 and Fig. 3-3: *P* values of the aforementioned three groups in the salt-inhibited experiment varied in a small range from 37.64 to 38.49 mL in the second batch and from 55.44 to 56.40 mL in the third batch with no significant difference ($p > 0.05$; ANOVA) in both batches. Moreover, the *P* value of the 2.5 RB and 5 II groups in the third batch also showed no significant difference ($p > 0.05$; ANOVA) with other bioaugmented groups, suggesting that all the bioaugmented groups performed similar mitigating effects regardless of the bioaugmentation dosage, repetition, and timing after a period of stabilization under salt stress. For the ammonium-inhibited condition, a distinct difference from the salt experiment was observed, except for the 2.5 I group. In both the second and third batches, the 2.5 I group showed a significantly better mitigating performance ($p < 0.05$; ANOVA), with the lowest dosage introduced to the system. The final cumulative CH_4 production in the 2.5 I group were 12% and 10%

higher than those in the 7.5 I group in the second and third batches, respectively, which completely overturned the positively correlated relationship between the dosages and mitigating performances observed in the first batch. To the best of our knowledge, these results have not been reported previously. Except for the 2.5 I group, the remaining bioaugmented groups exhibited no significant difference ($p > 0.05$; ANOVA) in performance in the third batch, which indicated that the stabilized performance of the bioaugmented groups also partly applied to the ammonium-inhibited condition. In summary, the above results indicate the temporality of the positive correlation between reactor performance and bioaugmentation inoculum dosages, as well as a trend of convergence of different bioaugmented groups as operation time was extended under both inhibited conditions.

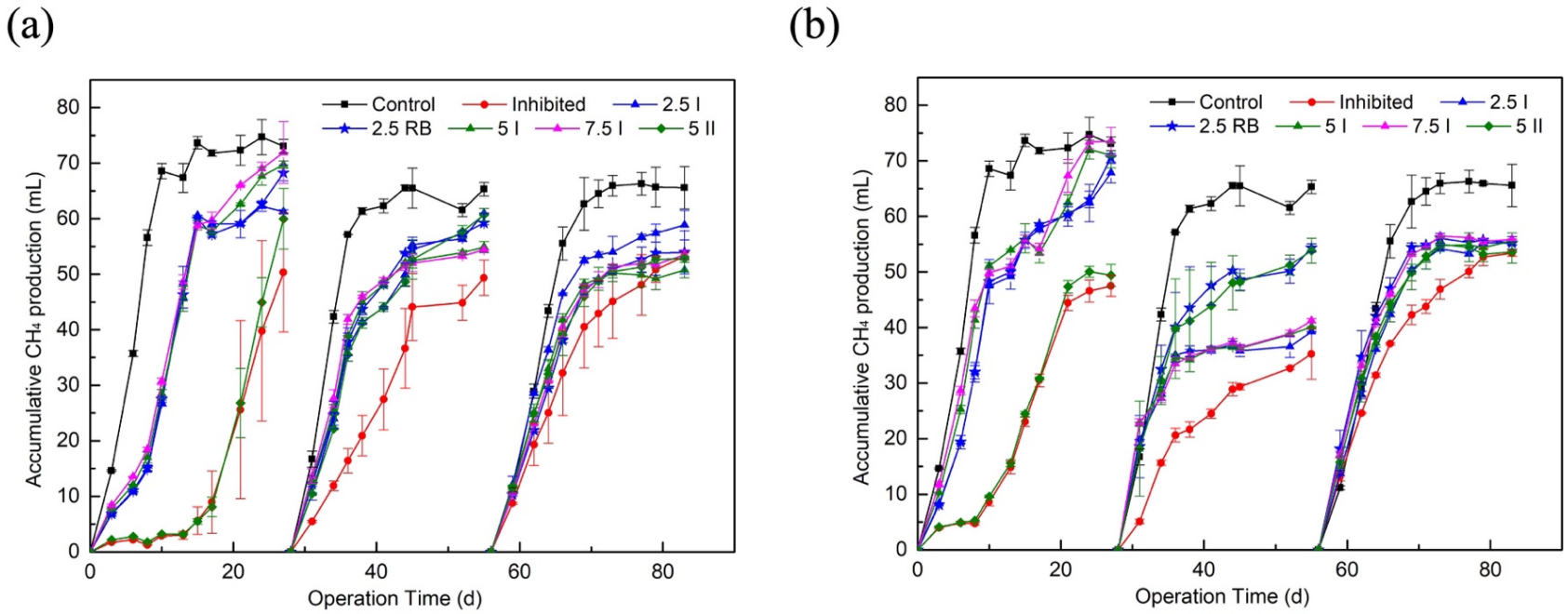

Fig. 3-2 CH_4 production profile in repeated batch experiments of the (a) ammonium-inhibited and (b) salt-inhibited groups. The error bars represent the standard deviation of the mean for each duplicate experiment.

Table 3-2 Kinetic parameters of repeated batch experiments estimated by modified Gompertz equation and their respective ratios compared to the Control group, (A) first batch, (B) second batch, and (C) third batch. Data for the Inhibited and 5 II groups in the first batch are not shown because the modified Gompertz equation was not applicable.

(A)

Group		P (mL)	R' (mL CH_4 g VSS^{-1} day^{-1})	λ (day)	R^2	P (%)	R' (%)
Control		73.69	9.88	1.87	0.991	100%	100%
Ammonia	2.5 I	63.01	7.34	5.76	0.977	85.5%	74.3%
	2.5 RB	66.18	6.20	5.09	0.979	89.8%	62.8%
	5 I	71.08	5.42	4.29	0.986	96.5%	54.9%
	7.5 I	73.71	5.37	3.86	0.990	100.0%	54.3%
Salt	2.5 I	64.44	5.45	2.00	0.987	87.5%	55.2%
	2.5 RB	65.66	5.46	2.01	0.983	89.1%	55.3%
	5 I	67.36	5.41	0.98	0.965	91.4%	54.8%
	7.5 I	71.54	4.72	0.07	0.961	97.1%	47.8%

(B)

Group		P (mL)	R' (mL CH_4 g VSS^{-1} day^{-1})	λ (day)	R^2	P (%)	R' (%)
Control		64.61	10.40	1.48	0.995	100%	100%
Ammonia	Inhibited	52.23	2.92	2.39	0.983	80.8%	28.1%
	2.5 I	58.30	4.64	0.74	0.984	90.2%	44.7%
	2.5 RB	57.99	5.22	0.95	0.995	89.8%	50.2%
	5 I	54.23	5.68	1.04	0.995	83.9%	54.6%
	7.5 I	53.34	6.20	1.04	0.994	82.6%	59.6%
	5 II	58.54	4.43	0.72	0.985	90.6%	42.6%
Salinity	Inhibited	33.60	2.43	0.37	0.978	52.0%	23.3%
	2.5 I	36.87	6.24	0.12	0.982	57.1%	60.0%
	2.5 RB	51.01	5.73	0.10	0.989	79.0%	55.1%
	5 I	36.96	6.43	0	0.967	57.2%	61.8%
	7.5 I	37.65	5.54	0	0.954	58.3%	53.3%
	5 II	50.54	5.12	0	0.981	78.2%	49.2%

(C)

Group		P (mL)	R' (mL CH_4 g VSS^{-1} day^{-1})	λ (day)	R^2	P (%)	R' (%)
Control		66.88	7.78	2.02	0.997	100%	100%
Ammonia	Inhibited	52.80	3.62	0.92	0.996	78.9%	46.6%
	2.5 I	57.67	5.74	1.08	0.997	86.2%	73.8%
	2.5 RB	54.63	4.68	1.29	0.997	81.7%	60.2%
	5 I	51.36	5.00	0.89	0.994	76.8%	64.3%
	7.5 I	53.33	4.97	1.29	0.997	79.7%	63.9%
	5 II	53.00	4.71	0.80	0.998	79.3%	60.5%
Salinity	Inhibited	52.43	3.90	0	0.991	78.4%	50.1%
	2.5 I	55.42	5.29	0.71	0.996	82.9%	68.0%
	2.5 RB	55.98	6.35	0.41	0.995	83.7%	81.6%
	5 I	55.54	5.25	0.31	0.995	83.0%	67.5%
	7.5 I	56.38	6.01	0.43	0.996	84.3%	77.2%
	5 II	54.45	5.65	0.50	0.995	81.4%	72.7%

The effect of repetition was evaluated by comparing the performance of the 2.5 RB group to that of the group with the same overall dosage at that time (i.e., the 5 I group in the second batch and the 7.5 I group in the third batch). In the salt-inhibited condition, the *P* value in the 2.5 RB group was 1.38-fold higher than that in 5 I group, whereas the ratio decreased to 0.99-fold that of the 7.5 I group in the third batch (Table 3-2). Under ammonium-inhibited conditions, the *P* value of the 2.5 RB group was 1.07-fold that of the 5 I group, whereas the ratio decreased to 1.02-fold that of the 7.5 I group in the third batch (Table 3-2). The results of both the inhibition experiments indicated that the advantageous effects of repetition were weakened as the number of batches increased. In addition, if the repeated introduction of a 2.5% bioaugmentation inoculum was regarded as a separate event in each batch, a diminishing marginal effect could be intuitively perceived as the level of performance enhancement declined as the number

of repetitions increased. Eventually, no distinguishable enhancement in performance was achieved by the newly introduced bioaugmentation inoculum, as no significant difference ($p > 0.05$; ANOVA) in performance was observed for the 2.5 RB group compared to the other bioaugmented groups (Fig. 3-3) in the third batch of both inhibited conditions. These results contradict the findings of Yang et al. (2016), who claimed that the repeated bioaugmentation group continued to outcompete the one-time bioaugmentation group in all three consecutive batches. More specifically, Yang et al. (2016) employed propionate-degrading paddy soil enrichments incubated with various individual VFA mixtures to accelerate the utilization of VFAs in anaerobic systems with an every-time dosage of 0.045 g VS/L. This discrepancy may be attributed to the short batch time (15 days for each batch) selected by Yang et al. (2016), as 45 days may not be enough to observe the declining performance of the repeated bioaugmentation group.

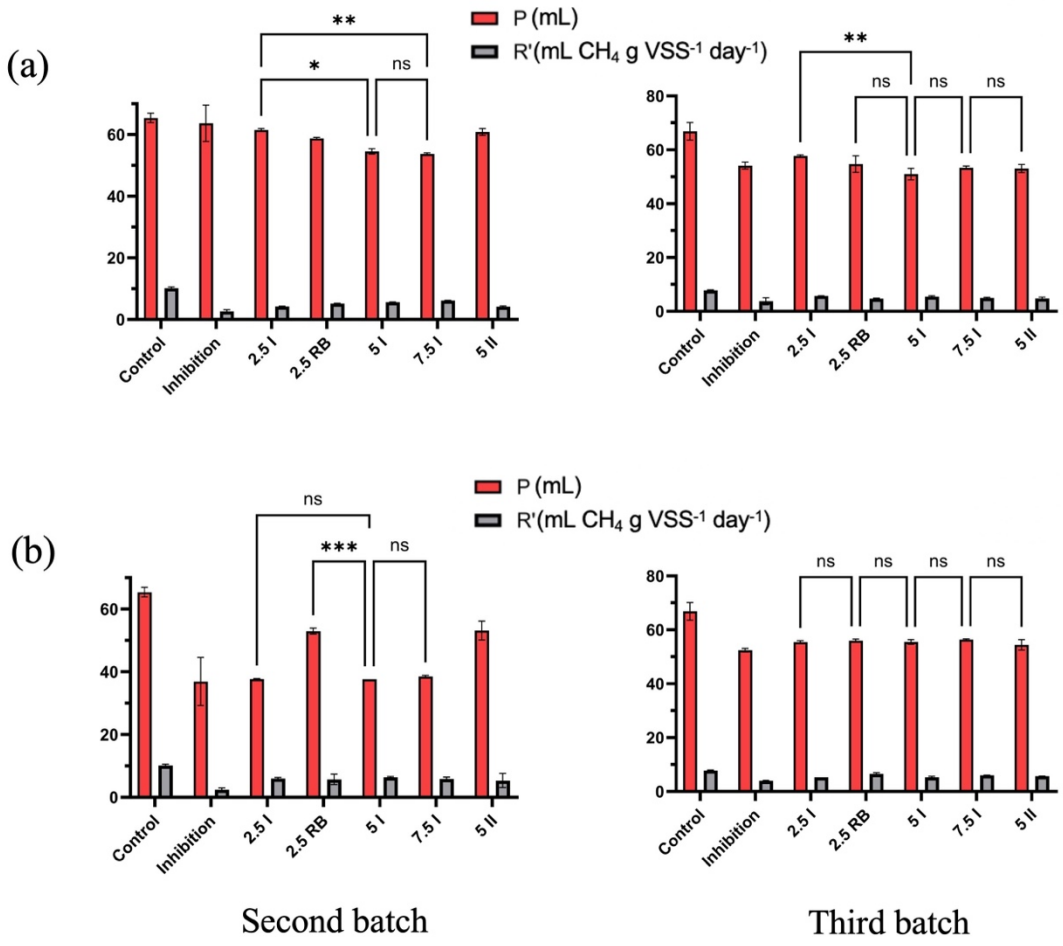

Fig. 3-3 Parameters estimated by modified Gompertz equation in the second and third batch of (a) ammonium-inhibited experiment and (b) salt-inhibited experiment. Solid lines indicate significant differences between different groups with *: $p < 0.05$; **: $p < 0.01$; ***: $p < 0.001$; ns: no significance.

The effect of bioaugmentation timing was also evaluated by comparing the performances of the 5 I, 5 II, and Inhibited groups. Of note, both 5 I and 5 II groups showed substantial improvements in CH_4 production after the introduction of the bioaugmentation inoculum. In the salt-inhibited experiment, the cumulative CH_4 production of the 5 I and 5 II groups was 1.50-fold and 1.53-fold higher than that of their respective Inhibited groups in the first and second batches, respectively. However,

in ammonium-inhibited experiment, the corresponding values were 1.38-fold and 1.23-fold higher, respectively. These results indicate that the bioaugmentation inoculum could exert its mitigating effect either by simultaneous or delayed introduction compared to the inhibitors. Supporting evidence has also been reported in the literature that the recovery of reactor performance occurs after the introduction of a bioaugmentation inoculum to systems where inhibitors already exist (Cai et al., 2021; Li et al., 2017). Moreover, for both ammonium- and salt-inhibited conditions, the difference in the performance of groups 5 I and 5 II eventually disappeared in the third batch, as shown in Figs. 3-2 and 3-3. This may indicate that convergence occurred as the operation progressed, regardless of the timing of inoculum introduction.

3.3.2 Volatile fatty acids accumulation

VFAs are important intermediates in the AD process as they connect soluble organic monomers to the final methanogenic phase by acidogenesis and acetogenesis. Consequently, VFAs, including acetate, propionate, butyrate, and valerate, are often used as indicators to evaluate the performance of AD processes (Yuan and Zhu, 2016). Given that the utilization of VFAs is thermodynamically unfavorable (Mao et al., 2015), with downstream aceticlastic methanogens vulnerable to various inhibitors, the accumulation of VFAs is often observed in problematic AD systems.

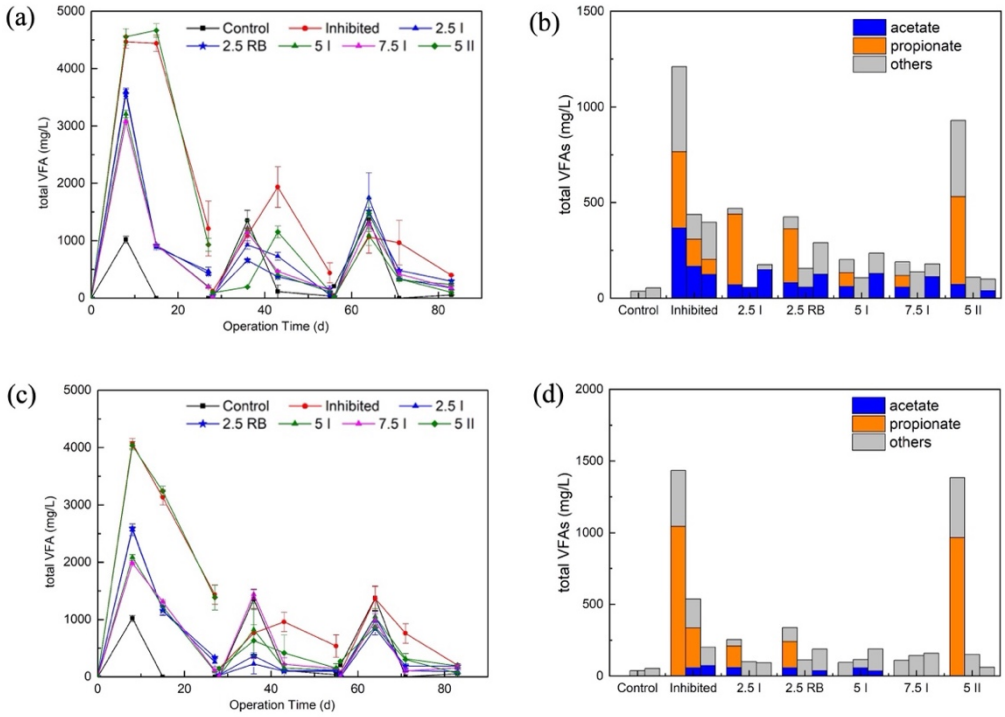

Fig. 3-4 The total VFA concentration profile in the repeated batch experiment of (a) ammonium-inhibited experiment and (c) salt-inhibited experiment. The accumulated concentrations of different VFAs at the end of each batch of (b) ammonium-inhibited experiment and (d) salt-inhibited experiment, the three bars in the same cluster represent the results of, from left to right, first batch, second batch and third batch.

The total VFA concentration profiles during the operation period of the ammonium- and salt-inhibited groups are shown in Fig. 3-4a and 3-4c. In the salt-inhibited experiment, the accumulation of total VFA in the first batch was much higher than that in the subsequent batches in all experimental groups, with the maximum concentration of the Inhibited group reaching over 4000 mg COD L^{-1}. This can be attributed to the stalled status of the downstream conversion of VFAs, as relatively low CH_4 production was observed in the first eight days in the first batch compared to that in the following

batches (Fig. 3-2). In addition, the accumulation of total VFA reached its peak on day 8 in all three batches of almost all experimental groups and then decreased continuously on days 15 and 27. In the ammonium-inhibited experiment, the overall accumulation of total VFA was greater than that in the salt-inhibited experiment. The maximum accumulation of total VFA reached over 4500 mg COD L^{-1}, and lagged accumulation peaks were observed on day 15 in the Inhibited and 5 II groups in the first and second batches. This indicated more severely inhibited methanogenesis processes in the ammonia experiment, which was supported by the obviously extended lag-phase time (λ) estimated using modified Gompertz equation (Table 3-2) compared to the salt-inhibited experiment. The reason for this discrepancy in inhibition severity may be the different inhibition mechanisms of ammonia and salt. For salt, overdosing changes the osmotic pressure in the cell, leading to cell disintegration, reduced metabolic enzyme activity, and CH_4 production (Li et al., 2024). For ammonia, not only the changes in osmotic pressure caused by large dosages but also the two forms of the substance themselves (i.e., FAN and NH_4^+) inhibit methanogenesis in different ways by competing with enzymatic reactions for intracellular protons and interfering with interactions at the Ca^{2+} and Mg^{2+} sites of enzymes participating in CH_4 synthesis (Li et al., 2023), which explains the severe overall VFA accumulation in ammonium-inhibited experiments. In addition, the poor CH_4 production performance of the Inhibited group in all three batches of both inhibitors can be explained by Fig. 3-4b and 3-4d, as the final accumulated total VFA concentrations were evidently higher than those of the other bioaugmented groups. Moreover, propionate accumulation was observed in the

Inhibited groups of both inhibitors at the end of the first batch; for example, propionate accounted for 72.8% of the total VFA accumulation in the salt-inhibited experiment. This agrees with the results of Duc et al. (2022), who claimed that propionate is a deterministic factor affecting CH_4 production and is prone to accumulation under high ammonia or salt concentrations. However, in the subsequent second and third batches of both inhibitor experiments, the proportion of propionate in the accumulated total VFA sharply decreased not only in the Inhibited groups but also in all bioaugmented groups. Further evidence is needed to explain whether this phenomenon is due to enhanced propionate-utilizing ability or deteriorated production ability.

Table 3-3 Total VFA and sCOD concentrations in repeated batch experiments.

		Ammonia experiment			Salt experiment		
		Total VFA on day 27 (mg L^{-1})	sCOD on day 27 (mg L^{-1})	Total VFA+CH_4 on day 8 (mgL^{-1})	Total VFA on day 27 (mg L^{-1})	sCOD on day 27 (mg L^{-1})	Total VFA+CH_4 on day 8 (mg L^{-1})
Control	B1	0	2200.0	5061.70	0	2200.0	5061.70
	B2	37.17	537.5	5434.55	37.17	537.5	5434.55
	B3	53.74	225.0	4470.79	53.74	225.0	4470.79
Inhibited	B1	1210.50	2712.5	4557.02	1434.57	1750.0	4409.80
	B2	437.73	2912.5	2262.80	537.16	B.D.	2236.41
	B3	396.92	2325.0	2854.95	201.64	325.0	3608.40
2.5 I	B1	469.41	2200.0	4662.67	255.42	425.0	4850.42
	B2	55.86	2875.0	3560.60	99.84	B.D.	2729.60
	B3	176.00	2000.0	4350.87	92.17	B.D.	3631.21
2.5 RB	B1	425.97	1675.0	4639.89	338.33	1025.0	4870.21
	B2	156.80	2425.0	3360.93	112.90	550.0	3229.38
	B3	291.00	2725.0	3620.02	187.55	225.0	3843.49
5 I	B1	201.63	1662.5	4422.14	95.34	1325.0	5040.19
	B2	106.42	3187.5	3998.68	114.94	1350.0	3295.94
	B3	235.55	1875.0	3446.16	188.52	675.0	3709.16
7.5 I	B1	189.51	1750.0	4389.37	110.17	625.0	5085.44
	B2	137.14	2487.5	4135.71	143.38	1825.0	3826.81
	B3	178.88	1925.0	3483.66	157.89	437.5	3896.43
5 II	B1	929.85	2550.0	4681.96	1383.43	2087.5	4410.89
	B2	109.23	3337.5	2730.41	150.44	1025.0	3474.94
	B3	99.42	2512.5	3764.92	60.60	600.0	3608.14

B: batch; B.D.: below detection; sCOD: soluble chemical oxygen demand; VFA: volatile fatty acid

As mentioned prior, a trend of performance convergence was observed in most of the experimental groups for both inhibitors, while better performance was achieved for different experimental groups before deterioration occurred at different timings. Scrutiny of the overall status of the system when deterioration occurs would be indicative, and the monitored VFA data would provide important information for a single experimental group during operation. As shown in Fig. 3-2, four common deteriorations in performance were observed for both inhibitors: (1) the 5 I group in the second batch, (2) 7.5 I group in the second batch, (3) 2.5 RB group in the third batch, and (4) 5 II group in the third batch. Regarding the deterioration of the 2.5 RB group in the third batch, an enhanced total VFA concentration was observed by comparing the data from the end of the second batch to the third batch of both inhibitors, as shown in Fig. 3-4 and Table 3-3. In the ammonium-inhibited experiment, the final accumulated total VFA increased from 156.8 mg COD L^{-1} in the second batch to 291.0 mg COD L^{-1} in the third batch. As for the salt-inhibited experiment, the accumulated total VFA increased from 112.9 mg COD L^{-1} to 187.6 mg COD L^{-1}. This suggests that the weakened ability to utilize VFAs resulted in the deterioration of the 2.5 RB group. For the 5 I and 7.5 I groups, a comparable final accumulation of total VFA concentrations between the first and second batches can be observed in Table 3-3, suggesting that the utilization of VFAs was not the key to impaired CH_4 production. Meanwhile, the final sCOD concentrations in the second batch were evidently higher than those in the first batch in these two groups of both inhibitors; for example, the sCOD concentration of the 5 I group in the ammonium-inhibited experiment increased from 1662.5 mg COD

L^{-1} in the first batch to 3187.5 mg COD L^{-1} in the second batch, and the value of the 7.5 I group in salt-inhibited experiment increased from 625.0 mg COD L^{-1} in the first batch to 1825.0 mg COD L^{-1} in the second batch, suggesting that the problem may stem from the upstream of VFAs metabolisms, i.e., hydrolysis and acidogenesis. This proposal was supported by actual VFAs production data on day 8, as shown in Table 3-3. Actual VFA production was calculated by adding the COD equivalents of the total VFA and CH_4 produced, according to Q. Li et al. (2015). The actual production on day 8 in the second batch was evidently lower than that in the first batch in these two groups of both inhibitors; for example, the actual VFA production of the 5 I group in the ammonium-inhibited experiment decreased from 4422.1 mg COD L^{-1} in the first batch to 3998.7 mg COD L^{-1} in the second batch, whereas VFA production of the 7.5 I group in the salt-inhibited experiment decreased from 5085.4 mg COD L^{-1} in the first batch to 3826.8 mg COD L^{-1} in the second batch, indicating weakened VFA production in the second batch. Despite the relatively high tolerance of acidogenic bacteria to inhibitors compared with methanogens (Li et al., 2022), their abundance and activity can be influenced by other changes in ambient parameters, such as the introduction of exotic microorganisms during bioaugmentation. However, the deterioration of the 5 II group in the third batch did not fall into the above two patterns and thus remained unexplained using the existing VFA data.

3.3.3 Microbial community succession

The biomass samples were collected from each bottle before the start of the experiment

and at the end of each batch. Subsequently, 16S rRNA amplicon sequencing was performed on each sample, enabling observation of the microbial community succession of a single group as well as comparison between different groups in a single batch. Alpha diversity based on the Shannon index showed continuous declining trends (Table 3-4) in all the bioaugmented groups, as well as the Inhibited group for both inhibitors, as the batch number increased. In the ammonium-inhibited experiment, the Shannon index of the 7.5 I group decreased from 4.33 in the first batch to 2.06 in the second batch and 1.40 in the third batch, indicating that the introduction of a bioaugmentation inoculum, as well as inhibiting conditions, shaped the anaerobic system to a less diversified global microbial community with dedicated functions.

Table 3-4 Changes in the Shannon index in each experimental group.

Group	Ammonia experiment			Salt experiment		
	first batch	second batch	third batch	first batch	second batch	third batch
Control	3.78	4.18	3.83	3.78	4.18	3.83
Inhibited	4.33	4.49	4.19	4.11	3.72	3.19
2.5 I	4.50	4.41	2.84	4.06	3.69	3.34
2.5 RB	4.48	3.29	1.46	4.03	3.58	3.37
5 I	4.36	2.12	1.72	4.05	3.67	3.47
7.5 I	4.33	2.06	1.40	3.97	3.70	3.36

(1) archaeal community

The archaeal community succession of each experimental group in the ammonium- and salt-inhibited experiments is shown in Fig. 3-5a and 3-5b, respectively. The dominant genus in the seed sludge was *Methanosaeta*, which is a typical aceticlastic methanogen vulnerable to ammonium and salt inhibition (Yan et al., 2019; Zhang et al., 2016). For the pre-acclimated enrichments used as bioaugmentation inocula for both inhibitors, the most abundant genus was *Methanosarcina*, a facultative methanogen known to perform both aceticlastic and hydrogenotrophic pathways (Tian et al., 2018), followed by the hydrogenotrophic methanogens *Methanobacterium* and *Methanoculleus*. As shown in Fig. 3-5, all experimental groups except for the Control group experienced intense archaeal community changes at the end of the first batch compared to the seed sludge for both inhibitors, which exhibited great capability for bioaugmentation as well as inhibiting conditions to shape the archaeal microbial community. *Methanosarcina* dominated all drastically changed communities (over 60% in the bioaugmented groups in the ammonia experiment and over 40% in the bioaugmented groups in the salt experiment) in replacement to *Methanosaeta*, regardless of the inhibitor type. At the end of the first batch, the abundance of *Methanobacterium* considerably increased in the bioaugmented groups for both inhibitors. The abundance increased from 0.42% in the seed sludge to 5.27% (2.5 I group), 9.52% (5 I group), and 11.02% (7.5 I group) in the ammonium-inhibited experiment, while the abundance increased to 6.76% (2.5 I group), 8.63% (5 I group), and 9.54% (7.5 I group) in the salt-inhibited experiment. The abundance of *Methanobacterium* was positively correlated with bioaugmentation

inoculum dosage but remained unchanged in both Inhibited groups (0.96% in the ammonia experiment and 0.65% in the salt experiment), suggesting that the abundance of *Methanobacterium* can be regarded as an indicator of the extent of bioaugmentation. In contrast, the abundance of *Methanoculleus* increased irrespective of the bioaugmented groups and Inhibited groups, which may be attributed to the superior resilience of *Methanoculleus* compared to other methanogens (Capson-Tojo et al., 2020). *Methanosaeta*, which was the dominant genus accounting for over 65% of the abundance in the seed sludge, decreased to below 7% in all the experimental groups with inhibitors at the end of the first batch, as it was outcompeted by other tolerant methanogens, which agrees with the results of Yan et al. (2020).

Within the bioaugmented groups in both inhibiting experiments, the structure of the archaeal communities was quickly shaped into their respective pre-acclimated enrichments at the end of the first batch. *Methanosarcina*, *Methanoculleus*, and *Methanobacterium* were the most abundant genera in all bioaugmented groups, as well as in the enrichment groups, and the predominance of these three genera was sustained during further operation, although their relative abundances changed during succession. In the salt-inhibited experiment, almost identical archaeal communities were shaped in all the bioaugmented groups at the end of the first batch, with the sum of the relative abundances of the three dominant genera in the four bioaugmented groups (2.5 I, 5 I, 7.5 I, and 2.5 RB) varying in a small range from 68.67% to 73.82%, despite the performance discrepancies among those groups. At the end of the second batch, the relative abundance of *Methanosarcina* in three of the four bioaugmented groups

declined by approximately 10%, except for a 5% increase in the 2.5 RB group, which seemed to be the reason for the better performance of the 2.5 RB group compared to all other groups. However, despite another 5% increase in *Methanosarcina* abundance in the 2.5 RB group observed at the end of the third batch, the performance converged with that of the other bioaugmented groups. In addition, a relatively distinct structure of the archaeal community was shaped in the 5 II group throughout the operation, with an even higher *Methanosarcina* abundance (over 65%), which did not prevent the convergence of performance in the 5 II group in the third batch. In the ammonium-inhibited experiment, despite the exceptional positive performance of the 2.5 I group, the succession of the archaeal community showed no peculiarity when compared to the 5 I and 7.5 I groups in all three batches. In addition, the abundance of *Methanobacterium* was positively correlated with the bioaugmentation inoculum dosages throughout the experiment, whereas the performance was completely reversed after the end of the first batch. In summary, the above results suggest that the archaeal community associated directly with CH_4 production was not the crux of performance change in this study.

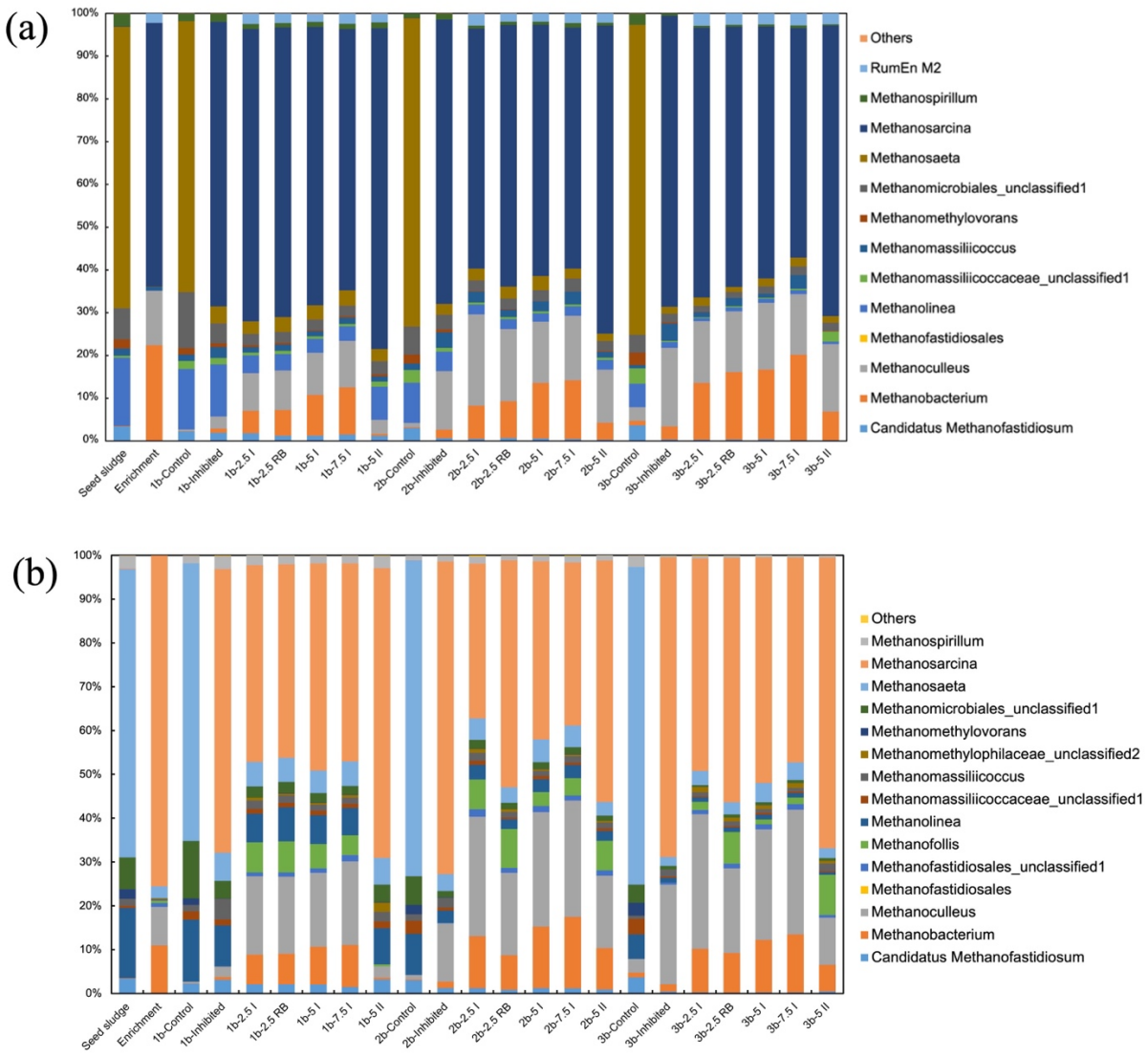

Fig. 3-5 Relative abundance of archaeal communities in the repeated batch experiment of (a) ammonium-inhibited experiment and (b) salt-inhibited experiment at the genus level. Genera under 1% relative abundance were allocated to “Others”. “b” in the sample names stands for “batch”.

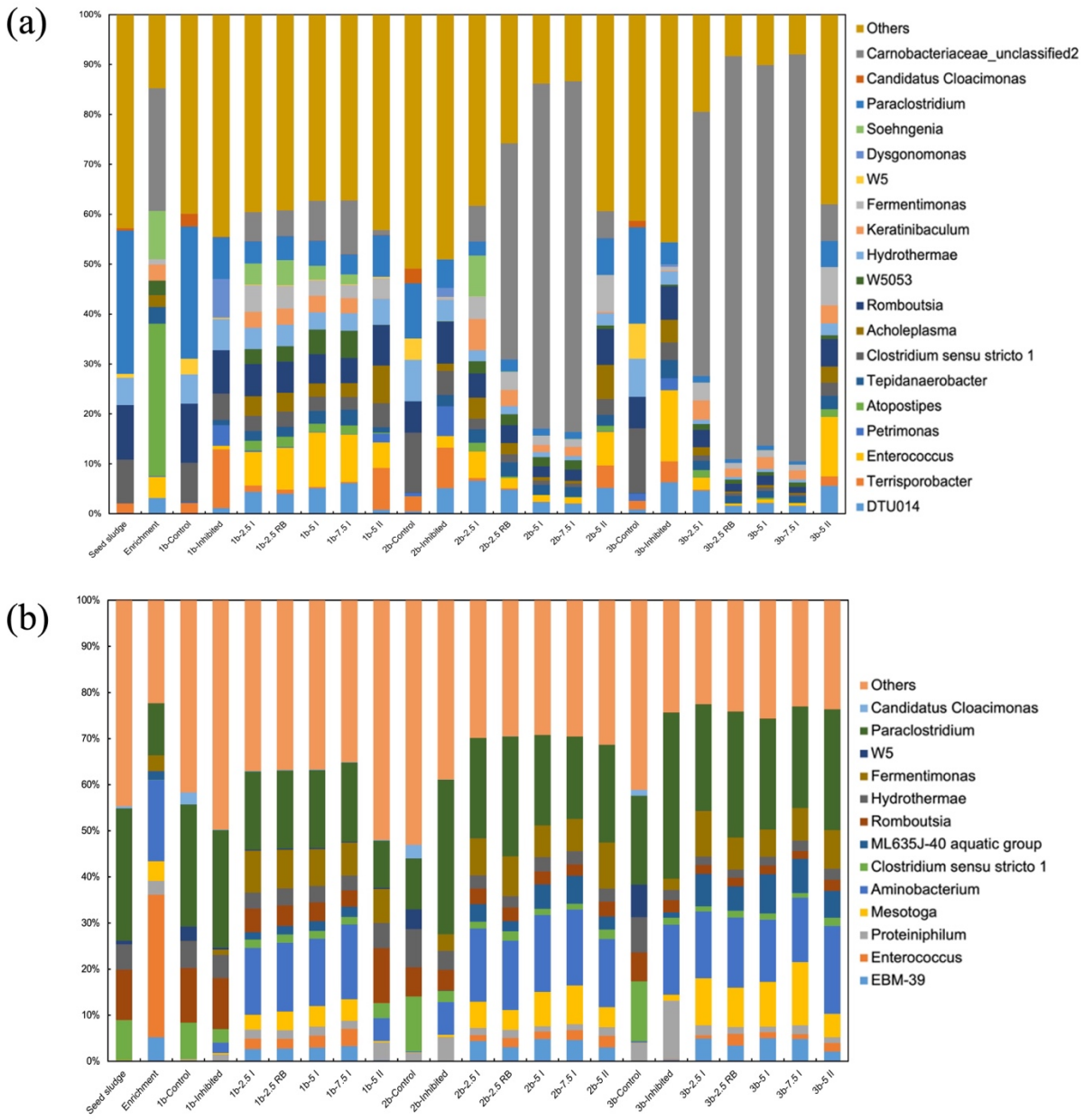

Fig. 3-6 Relative abundance of bacterial communities in the repeated batch experiment of (a) ammonium-inhibited experiment and (b) salt-inhibited experiment at the genus level. Genera under 5% relative abundance were allocated to "Others". "b" in the sample names stands for "batch".

(2) bacterial community

Bacteria play a major role in the hydrolysis, acidogenic, and acetogenic stages of the AD system (Wang et al., 2023), thus displaying a more complicated community structure than archaea. The succession of the bacterial communities in each experimental group in the ammonium- and salt-inhibited experiments is shown in Fig. 3-6a and 3-6b, respectively. The dominant bacteria in the seed sludge were *Paraclostridium* (28.7%), *Romboutsia* (10.9%), and *Clostridium sensu stricto* 1 (8.7%). For the enrichment pre-acclimated to ammonia, the dominant bacteria were *Atopostipes* (30.5%), *Carnobacteriaceae_unclassified2* (24.6%), and *Soehngenia* (9.7%). Regarding salt-acclimated enrichment, *Enterococcus* (30.9%), *Aminobacterium* (17.6%), and *Paraclostridium* (11.3%) were the dominant genera. Most of the above bacteria have been annotated as capable of mediating processes such as fermentation (Cai et al., 2021), acid production (Khafipour et al., 2020) and acid oxidation (Wang et al., 2019). The diverse dominant bacteria in the different enrichments can be attributed to the functional diversity and redundancy that exist ubiquitously in the bacterial community (Zhang et al., 2022). As shown in Fig. 3-5a and 3-5b, the abundance of the most dominant archaea in the enrichments was enhanced in the bioaugmented groups at the end of the first batch. However, only a limited number of bacteria were strengthened by the bioaugmentation inoculum for both inhibitors (e.g., *Carnobacteriaceae_unclassified2* in the ammonium-inhibited experiment and *Aminobacterium* in the salt-inhibited experiment). The succession patterns of the bacterial community in the ammonium- and salt-inhibited experiments were also

distinct, indicating that the bacterial community influenced reactor performance.

In the ammonium-inhibited experiment, balanced and diversified bacterial communities were formed for all bioaugmented groups at the end of the first batch, with the most dominant genus constituting approximately 10% abundance (Fig. 3-6a) and the Shannon index reaching a peak of approximately 4.5 (Table 3-4). However, this balance was disrupted by an abrupt increase in *Carnobacteriaceae_unclassified2*. The relative abundance of *Carnobacteriaceae_unclassified2* increased to 69.1% and 70.3%, along with Shannon indexes declining to 2.12 and 2.06 for the 5 I and 7.5 I groups, respectively, at the end of the second batch as a consequence. Although *Carnobacteriaceae_unclassified2* has been reported to be involved in the degradation of substrates, such as polysaccharides and sugars (Banti et al., 2023), other biochemical processes can be weakened by an overly homogeneous bacterial community. It can be speculated that the deterioration in the performance of the 5 I and 7.5 I groups was related to the drastic changes in the bacterial community occurring in the second batch. At the end of the third batch, the relative abundance of *Carnobacteriaceae_unclassified2* in the 2.5 RB group also increased to a comparable value (80.7%) to those in the 5 I and 7.5 I groups, and a similar deterioration in performance was also observed in the 2.5 RB group. In contrast, with respect to the exceptional positive performance of the 2.5 I group in CH_4 production, the relative abundance of *Carnobacteriaceae_unclassified2* increased relatively slowly (7.2% and 52.9% at the end of the second and third batches, respectively), presumably because the lowest dosage of bioaugmentation inoculum was introduced. Additionally, the

abundance of *Carnobacteriaceae_unclassified2* in the 5 II group showed little difference (5.4% and 7.4% at the end of the second and third batches, respectively) as the operation progressed. Moreover, the overall structure of the bacterial community of the 5 II group was dissimilar from that of the other bioaugmented groups, which can be attributed to the altered interactions among bacteria caused by the delayed introduction of the bioaugmentation inoculum. Evidence supporting these proposals based on VFAs data can also be found in the microbial succession process. For the enhanced accumulation of VFAs in the 2.5 RB group in the third batch, the abundance of the acid-oxidizing bacteria *Acholeplasma* (L. Li et al., 2015) and *Tepidanaerobacter* (Wang et al., 2023) decreased from 2.22% to 0.36% and from 2.85% to 1.48%, respectively. Additionally, as weakened VFAs production ability was suspected to be the cause of the deterioration occurred in the 5 I and 7.5 I groups in the second batch, a decreased abundance of the acid-producing bacteria *Enterococcus* (Woraruthai et al., 2024) and *Romboutsia* (Castro-Ramos et al., 2022) in both groups was confirmed. The abundance of *Enterococcus* decreased sharply from 10.88% to 1.32% in the 5 I group and from 9.50% to 1.20% in the 7.5 I group. Meanwhile, the abundance of *Romboutsia* also decreased from 5.90% to 2.16% in the 5 I group and from 5.07% to 2.23% in the 7.5 I group.

In the salt-inhibited experiment, similar balanced and diversified bacterial communities were formed for all bioaugmented groups at the end of the first batch, as in the ammonium-inhibited experiment. However, even if subsequent succession did not change drastically, as in the ammonium-inhibited experiment, similar performance

deterioration was observed. Evidence supporting these proposals based on VFAs data can also be found in salt-inhibited experiments. Regarding the suspected weakened VFA utilizing ability of 2.5 RB group, the abundance of the acid-oxidizing bacterium *Fermentimonas* (Ziganshina and Ziganshin, 2022) decreased from 8.64% to 6.97% in the third batch, whereas regarding the suspected weakened VFA producing ability, the acid-producing bacteria *Enterococcus* and *Romboutsia* also decreased in the 5 I, 7.5 I, and 2.5 I groups in the second batch. In addition, unlike in the ammonium-inhibited experiment, the bacterial structure of the 5 II group converged with that of the other bioaugmented groups at the end of the third batch. This may be attributed to the relatively mild inhibition severity of salt compared to that in the ammonium-inhibited experiment. In conclusion, the change in performance in different experimental groups can be explained by the succession of bacterial communities, which also supports proposals based on VFAs data.

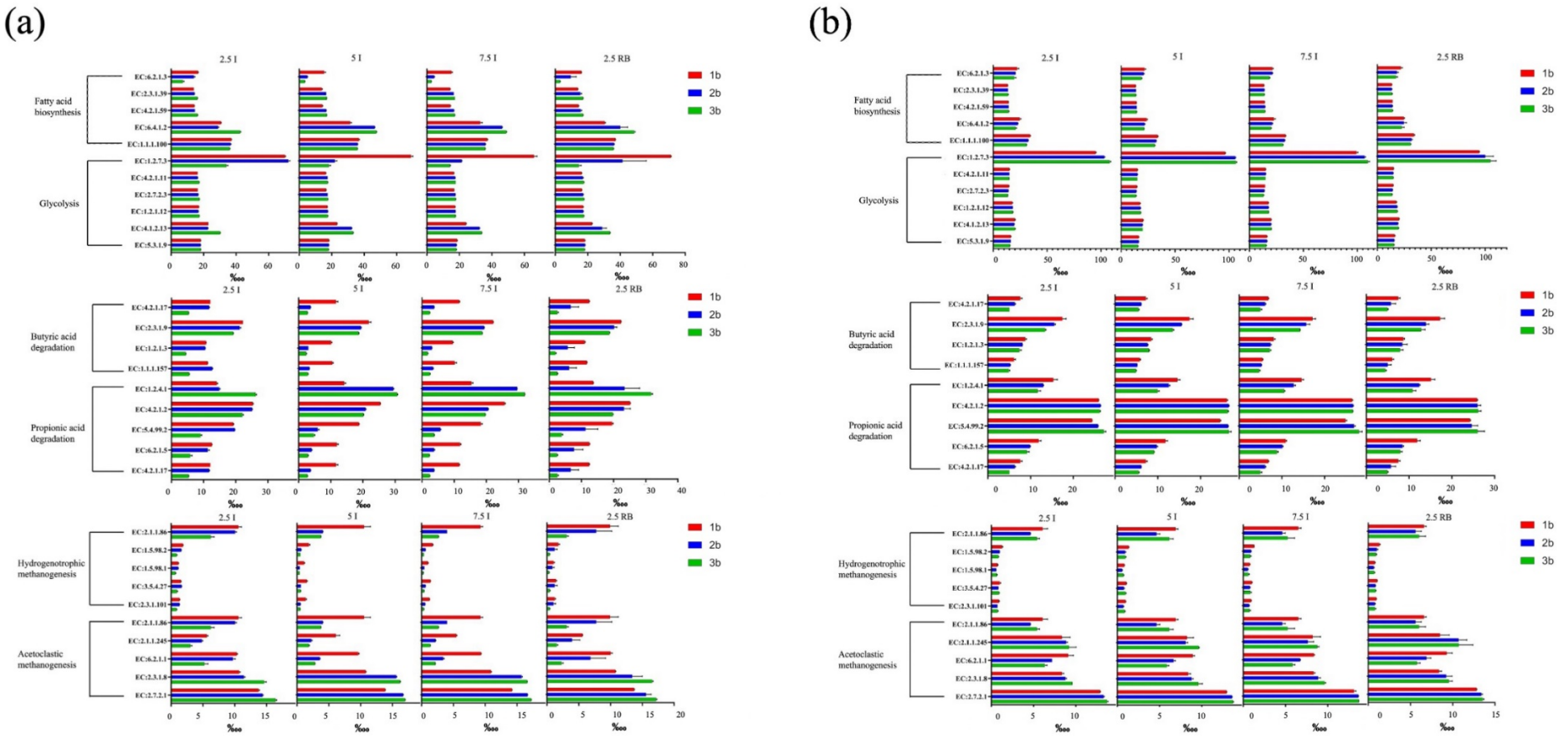

Fig. 3-7 The predicted relative abundance of key enzymes related to acidogenesis, acetogenesis and methanogenesis steps in anaerobic digestion of (a) ammonium-inhibited experiment and (b) salt-inhibited experiment using PICRUSt2 method. Error bars represent the standard deviation of the mean for each duplicate experiment.

3.3.4 Functional prediction based on 16S rRNA amplicon sequencing

For a more comprehensive understanding of the potential functional changes that occur during operation, the PICRUSt2 method was used to predict the relative abundances of key enzymes related to anaerobic digestion. As shown in Fig. 3-7, a total of eleven, nine, and ten enzyme genes were selected for acidogenesis, acetogenesis, and methanogenesis in the AD process, respectively, owing to their relatively large abundance. More specifically, acidogenesis was further subdivided into glycolysis and fatty acid biosynthesis pathways. Similarly, the acetogenesis step was subdivided into propionic acid and butyric acid degradation pathways, and the methanogenesis step was subdivided into aceticlastic and hydrogenotrophic methanogenesis pathways.

In the ammonium-inhibited experiment, the abundances of key enzymes for all three steps in the 5 I and 7.5 I groups showed synchronous changes in every batch. In the acidogenesis step, 2-oxoglutarate synthase (EC:1.2.7.3), which oxidatively decarboxylates pyruvate to acetyl-CoA (Zhao et al., 2023), was the most abundant enzyme gene constituting 68.78‰ and 65.61‰ in the 5 I and 7.5 I groups, respectively, at the end of the first batch, whereas the relative abundance decreased sharply to 21.90‰ and 21.41‰ at the end of the second batch. Additionally, the relative abundance of long-chain fatty acid-CoA ligase (EC:6.2.1.3) decreased sharply to approximately 0.35-fold in both 5 I and 7.5 I groups at the end of the second batch compared to that in the first batch. These results confirmed a previous proposal that weakened VFAs production ability was the major cause of performance deterioration

while the relative abundances of other related enzyme-encoding genes remained unchanged or increased slightly in the second batch. In addition to acidogenesis, a decreasing trend of key enzyme abundance was also observed in the acetogenesis and methanogenesis steps in the 5 I and 7.5 I groups. For example, the relative abundances of enoyl-CoA hydratase (EC:4.2.1.17) and methylmalonyl-CoA mutase (EC:5.4.99.2) in the acidogenesis step, as well as tetrahydromethanopterin S-methyltransferase (EC:2.1.1.86) and Co-methyltransferase (EC:2.1.1.245) in the methanogenesis step, decreased to less than 0.5-fold at the end of the second batch compared to those in the first batch in both 5 I and 7.5 I groups. This indicates that an overall decline in all three steps occurred in the 5 I and 7.5 I groups at the end of the second batch. The key enzyme abundance in the 2.5 RB group was relatively sustained at the end of the second batch, as the relative abundance of the dominant 2-oxoglutarate synthase (EC:1.2.7.3) decreased to 41.44‰ in comparison with ~20‰ in the 5 I and 7.5 I groups. In the third batch, weakened VFA utilization ability could be speculated to be due to the relative abundance of key enzymes in acetogenesis, and the other two steps declined sharply and converged with 5 I and 7.5 I, which also explained the deterioration of performance in the 2.5 RB group at the end of the third batch. Regarding the exceptional positive performance of CH_4 production in the 2.5 I group, supporting evidence can be found in the relative abundance of numerous key enzymes sustained throughout the experiment. For example, the relative abundance of the dominant 2-oxoglutarate synthase (EC:1.2.7.3) first increased to 72.25‰ in the second batch and then decreased to 33.95‰, in comparison to 14.21‰ in the 7.5 I group at the end of third batch.

For the salt-inhibited experiment, the discrepancies in relative abundance among different batches, as well as among different groups, were much smaller than those in the ammonium-inhibited experiment, which can be attributed to the mild inhibition severity of salt compared to the ammonium-inhibited experiment. A slight decrease in the relative abundance of numerous key enzyme genes was observed in all three steps. More specifically, a decreased relative abundance of acetyl-CoA carboxylase (EC:6.4.1.2) and 3-oxoacyl-[acyl-carrier-protein] reductase (EC:1.1.1.100) was observed in the acidogenesis step at the end of the second batch in the 5 I and 7.5 I groups, which supported the previous suspicion of decreased VFA production. Additionally, a decreased relative abundance of pyruvate dehydrogenase (acetyl-transferring) (EC:1.2.4.1) and acetyl-CoA C-acetyltransferase (EC:2.3.1.9) in the acetogenesis step was observed at the end of the third batch in group 2.5 RB, thereby supporting the previous suspicion of decreased VFA utilization ability. In summary, functional prediction based on 16S rRNA amplicon sequencing data suggested an overall decline in all three steps of the AD process in most experimental groups, regardless of the inhibitor, which resulted in converged and deteriorated performance for groups with different bioaugmentation regimes.

3.3.5 Steady state for bioaugmentation

According to the microbial community analysis results (Figs. 3-5 and 3-6), an evident trend of convergence was observed for the bioaugmented groups, resulting in similar CH_4 production performance irrespective of the inhibitor type. Despite the temporary CH_4 production performance divergence occurred in the first batch, the discrepancy

among the bioaugmented groups diminished as the succession of the microbial community reached a steady state (Fig. 3-2). This was also supported by the PCA results (Fig. 3-8). The relative distances between groups with different bioaugmentation regimes in both archaeal and bacterial communities decreased as the number of batches increased, regardless of the inhibitor, indicating a converging trend for the microbial communities. It can be speculated that the groups with higher inoculum doses promptly reached a steady state. For the 2.5 I group, in the ammonium-inhibited experiment, the small dosage introduced slowed the succession process, thus rendering exceptional positive performance in CH_4 production. It is expected that the performance of the 2.5 I group will converge with that of other bioaugmented groups in the near future, as the abundance of *Carnobacteriaceae_unclassified2* increased sharply in the third batch (Fig. 3-6a). The proposal of a steady state also conforms to the observation of a diminishing marginal effect for the repetitive introduction of the inoculum. The more the microbial community approached a steady-state structure, the smaller the role of the bioaugmentation inoculum in shaping the microbial community. However, for systems discharging sludge periodically (e.g., continuous stirred-tank reactors), the characteristics of the repetitive introduction of inoculum may be different, as it replenishes the microorganisms flushed away. Regarding the timing of bioaugmentation, distinct results were obtained in the ammonium- and salt-inhibited experiments. The bacterial community of group 5 II in the salt-inhibited experiment converged with other bioaugmented groups, whereas in the ammonium-inhibited experiment, a completely dissimilar community was formed by the end of the third batch (Fig. 3-6). It can be

speculated that the microbial community was shaped by cooperative interactions between the inhibiting conditions, seed sludge, and bioaugmentation inoculum. As the microbial community of the seed sludge changed drastically at the end of the first batch, it is reasonable to assume that the microbial community in the final steady state varied accordingly. The performance in CH_4 production depended on the microbial community in the final steady state for both inhibitors, whereas the performance of the transition state in the first batch exceeded the performance in the final steady state. This can be explained by the trend of inhibiting the shaping of the anaerobic system into a less diversified global microbial community with dedicated functions (Table 3-4), which deteriorates the functional diversity and redundancy of microorganisms, particularly the bacterial community. If this phenomenon is confirmed in more scenarios, maintaining the transition state by periodically discharging the fermentation bulk liquid and introducing inoculum in continuous-mode reactors may be ideal for maintaining the mitigating effects of bioaugmentation in AD reactors. An additional merit of operating in continuous-mode reactors is that the toxicant accumulation of byproducts is mitigated by the daily input and output of the bulk liquid, which may help maintain a suitable environment for the growth of various microorganisms (Tian et al., 2017).

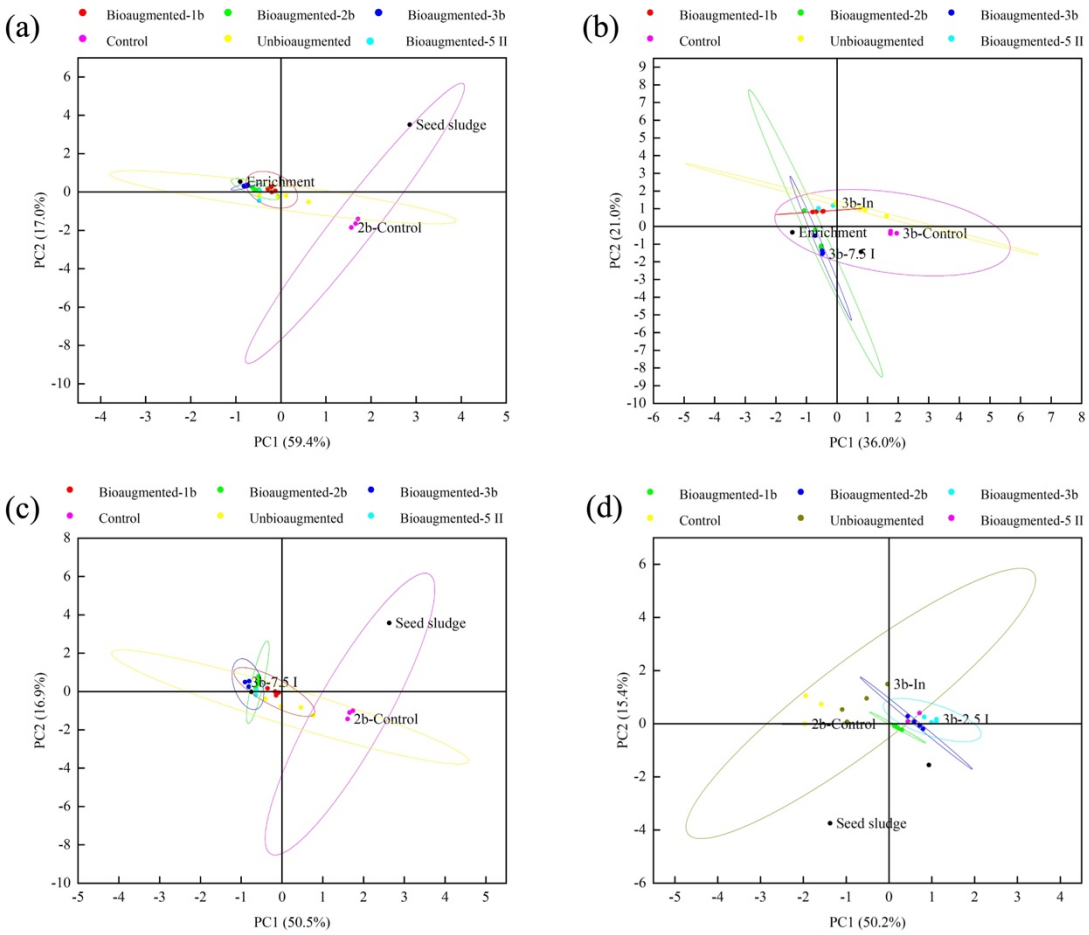

Fig. 3-8 Principal component analysis (PCA) based on the 16S rRNA amplicon sequencing results for different experimental groups in different batches: (a) archaeal communities in the ammonium-inhibited group, (b) bacterial communities in the ammonium-inhibited group, (c) archaeal communities in the salt-inhibited group, and (d) bacterial communities in the salt-inhibited group. “b” stands for “batch.” PC1 and PC2 represent the principal components 1 and 2, respectively.

3.4 Summary

The effects of bioaugmentation regimes of dosage, repetition, and timing under both ammonium- and salt-inhibited conditions were investigated using repeated batch reactors. The results revealed the temporality of the positive correlation between reactor performance and bioaugmentation inoculum dosages, as well as the diminishing marginal effect of the repetitive introduction of inoculum. Most of the bioaugmented groups in both inhibition experiments converged to a steady state in the microbial community, whereas different bioaugmentation timings resulted in markedly different microbial communities. The results of the key enzyme abundance prediction further suggested an overall decline in all three steps of anaerobic digestion for both inhibitors during operation. An overly homogeneous bacterial community caused by a drastic increase in the relative abundance of *Carnobacteriaceae_unclassified2* was the reason for the decline of CH_4 production performance in the ammonia inhibition experiment, and a balanced and diversified bacterial community is key for active CH_4 production. It can be speculated that the microbial community was shaped by cooperative interactions between the inhibiting conditions, seed sludge, and bioaugmentation inoculum. Maintaining the microbial community in a transition state by periodic discharging and the introduction of an inoculum may be ideal for maintaining high system performance. Overall, the results of this study provide guidance for regulating bioaugmentation to mitigate the inhibition of AD systems.

Chapter 4

Summary and conclusions

As previous studies showed that bioaugmentation stood out among various technologies in mitigating ammonium inhibition in AD reactors, whether bioaugmentation can also be applied on mitigating salt inhibition remains to be investigated. Besides, as unsuccessful bioaugmentation results (e.g., operation failure, temporary effect) were occasionally reported, bioaugmentation mitigating inhibition effect in AD reactors is still at a nascent stage in which the bioaugmentation regimes (i.e., dosage, repetition, and timing) need to be optimized to ensure its effectiveness. Although some previous studies have investigated the optimal dosage and meliority of single or routine dosing of bioaugmentation, most have focused only on short-term effects and some have reached conflicting conclusions.

Therefore, the objective of this study is to investigate the feasibility of applying bioaugmentation on mitigating salt inhibition in AD process and further to optimize bioaugmentation regimes in both ammonium- and salt-inhibited conditions.

In Chapter 1, literature review was conducted on principles and current status of AD process and bioaugmentation to AD process for mitigating inhibitory effects caused by ammonia/salt. Based on the review of previous studies, the objective of this study was set as mentioned above.

In Chapter 2, Bioaugmentation using pre-acclimated MSCs was conducted to alleviate the inhibitory effects of ammonia and salt stresses on CH_4 production in AD. Compared with non-bioaugmentation, bioaugmentation increased cumulative CH_4 production by 25% under salt stress. It also shortened the lag time of the second phase to enable AD smoothly under ammonia stress. The complement of SPOB, interspecies electron transfers, and *Methanoculleus* through bioaugmentation with MSCs possibly allowed efficient propionate degradation and CH_4 production. This study proves the feasibility of applying bioaugmentation on salt inhibition in AD reactors. It also provides novel insights into the establishment of effective bioaugmentation strategies under both ammonia and salt stresses.

In Chapter 3, The effects of bioaugmentation regimes of dosage, repetition, and timing on AD performance under both ammonium- and salt-inhibited conditions were investigated using repeated batch reactors. The results revealed the temporality of the positive correlation between reactor performance and bioaugmentation inoculum dosages, as well as the diminishing marginal effect of the repetitive introduction of inoculum in both inhibition experiments. Most of the bioaugmented groups in both inhibition experiments converged to a steady state in the microbial community, whereas different bioaugmentation timings resulted in markedly different microbial communities in ammonium-inhibited experiment. The results of the key enzyme abundance prediction further suggested an overall decline in all three steps of anaerobic digestion for both inhibitors during operation. A balanced and diversified bacterial community is key for active CH_4 production. It can be speculated that the microbial

community was shaped by cooperative interactions between the inhibiting conditions, seed sludge, and bioaugmentation inoculum. Maintaining the microbial community in a transition state by periodic discharging and the introduction of an inoculum may be ideal for maintaining high system performance.

Despite the confirmation of the feasibility of applying bioaugmentation on mitigating salt inhibition in AD process as well as the stressing of the importance of a balanced and diversified bacterial community for maintaining active CH_4 production under different stresses, further studies for conducting the full-scale application of bioaugmentation on mitigating inhibition effects in AD process are required for establishing the practical bioaugmentation technologies. Following studies are proposed to be carried out forward the practical application of bioaugmentation.

(1) To investigate the feasibility of bioaugmentation mitigating the inhibiting effect caused by the co-occurrence of high concentrations of ammonia and salt in AD reactors.

(2) To operate the continuous mode AD reactors to confirm whether maintaining the microbial community in a transition state by periodically discharging the fermentation bulk liquid and introducing bioaugmentation inoculum enable to maintain high system performance for longer time.

(3) To develop methods for efficiently enriching the tolerant consortia for further reducing the cost for bioaugmentation inoculum preparation: the use of a mixed

culture is recommended because of the relatively low requirements for cultivation compared to pure strains.

(4) To investigate the feasibility of applying supporting materials which enables biofilm formation and biomass retention to improve the effectiveness of the bioaugmentation.

References

Agyeman, F.O., Han, Y., Tao, W., 2021. Elucidating the kinetics of ammonia inhibition to anaerobic digestion through extended batch experiments and stimulation-inhibition modeling. Bioresour. Technol. 340, 125744. https://doi.org/10.1016/j.biortech.2021.125744

Ali, M., Elreedy, A., Fujii, M., Tawfik, A., 2021. Co-metabolism based adaptation of anaerobes to phenolic saline wastewater in a two-phase reactor enables efficient treatment and bioenergy recovery. Energy Convers. Manag. 247, 114722. https://doi.org/10.1016/j.enconman.2021.114722

Alsouleman, K., 2019. Effect of increasing amounts of ammonium nitrogen induced by consecutive mixture of poultry manure and cattle slurry on the microbial community during thermophilic anaerobic digestion. J. Microbiol. Biotechnol. 29, 1993–2005. https://doi.org/10.4014/jmb.1909.09023

Angelidaki, I., Karakashev, D., Batstone, D.J., Plugge, C.M., Stams, A.J.M., 2011. Biomethanation and Its Potential, in: Methods in Enzymology. Elsevier, pp. 327–351. https://doi.org/10.1016/B978-0-12-385112-3.00016-0

APHA, 2012. Standard methods for the examination of water and wastewater, 22nd ed. American public health association, American water works association, water environmental federation, Washington, DC.

Aramrueang, N., Zhang, R., Liu, X., 2022. Application of biochar and alkalis for recovery of sour anaerobic digesters. J. Environ. Manage. 307, 114538. https://doi.org/10.1016/j.jenvman.2022.114538

Banerjee, S., Schlaeppi, K., Van Der Heijden, M.G.A., 2018. Keystone taxa as drivers of microbiome structure and functioning. Nat. Rev. Microbiol. 16, 567–576. https://doi.org/10.1038/s41579-018-0024-1

Banti, D., Samaras, P., Chioti, A., Mitsopoulos, A., Tsangas, M., Zorpas, A., Sfetsas, T., 2023. Improvement of MBBR performance by the addition of 3D-printed biocarriers fabricated with 13X and bentonite. Resources 12, 81. https://doi.org/10.3390/resources12070081

Bastian, M., Heymann, S., Jacomy, M., 2009. Gephi: An open source software for exploring and manipulating networks. Proc. Int. AAAI Conf. Web Soc. Media 3, 361–362. https://doi.org/10.1609/icwsm.v3i1.13937

Bencoova, B., Grosos, R.,Gomory, M., Bacova, K., Michalkova, S., 2021. Use of biogas plants on a national and international scale. Acta Montan. Slovaca 139–148. https://doi.org/10.46544/AMS.v26i1.12

Berninghaus, A.E., Radniecki, T.S., 2022. Fats, oils, and greases increase the sensitivity of anaerobic mono- and co-digester inoculum to ammonia toxicity. Environ. Eng. Sci. 39, 512–522. https://doi.org/10.1089/ees.2021.0119

Cai, G., Zhao, L., Wang, T., Lv, N., Li, J., Ning, J., Pan, X., Zhu, G., 2021. Variation of volatile fatty acid oxidation and methane production during the bioaugmentation of anaerobic digestion system: Microbial community analysis revealing the influence of microbial interactions on metabolic pathways. Sci. Total Environ. 754, 142425. https://doi.org/10.1016/j.scitotenv.2020.142425

Caicedo, H.H., Hashimoto, D.A., Caicedo, J.C., Pentland, A., Pisano, G.P., 2020. Overcoming barriers to early disease intervention. Nat. Biotechnol. 38, 669–673. https://doi.org/10.1038/s41587-020-0550-z

Cao, L., Cox, C.D., He, Q., 2021. Patterns of syntrophic interactions in methanogenic conversion of propionate. Appl. Microbiol. Biotechnol. 105, 8937–8949. https://doi.org/10.1007/s00253-021-11645-9

Capson-Tojo, G., Moscoviz, R., Astals, S., Robles, Á., Steyer, J.-P., 2020. Unraveling the literature chaos around free ammonia inhibition in anaerobic digestion. Renew. Sustain. Energy Rev. 117, 109487. https://doi.org/10.1016/j.rser.2019.109487

Castro-Ramos, J.J., Solís-Oba, A., Solís-Oba, M., Calderón-Vázquez, C.L., Higuera-Rubio, J.M., Castro-Rivera, R., 2022. Effect of the initial pH on the anaerobic digestion process of dairy cattle manure. AMB Express 12, 162. https://doi.org/10.1186/s13568-022-01486-8

Chandra, R., 2012. Methane production from lignocellulosic agricultural crop wastes: A review in context to second generation of biofuel production. Renew. Sustain. Energy Rev. 15.

Chen, H., Wang, W., Xue, L., Chen, C., Liu, G., Zhang, R., 2016. Effects of ammonia on anaerobic digestion of food waste: Process performance and microbial community. Energy Fuels 30, 5749–5757. https://doi.org/10.1021/acs.energyfuels.6b00715

Chen, Q., Liu, C., Liu, X., Sun, D., Li, P., Qiu, B., Dang, Y., Karpinski, N.A., Smith, J.A., Holmes, D.E., 2020. Magnetite enhances anaerobic digestion of high salinity organic wastewater. Environ. Res. 189, 109884. https://doi.org/10.1016/j.envres.2020.109884

Chen, Y., Cheng, J.J., Creamer, K.S., 2008. Inhibition of anaerobic digestion process: A review. Bioresour. Technol. 99, 4044–4064. https://doi.org/10.1016/j.biortech.2007.01.057

Christou, M.L., Vasileiadis, S., Karpouzas, D.G., Angelidaki, I., Kotsopoulos, T.A., 2021. Effects of organic loading rate and hydraulic retention time on bioaugmentation performance to tackle ammonia inhibition in anaerobic digestion. Bioresour. Technol. 334, 125246. https://doi.org/10.1016/j.biortech.2021.125246

Climenhaga, M.A., Banks, C.J., 2008. Anaerobic digestion of catering wastes: Effect of micronutrients and retention time. Water Sci. Technol. 57, 687–692. https://doi.org/10.2166/wst.2008.092

Darestani, M., Haigh, V., Couperthwaite, S.J., Millar, G.J., Nghiem, L.D., 2017. Hollow fibre membrane contactors for ammonia recovery: Current status and future developments. J. Environ. Chem. Eng. 5, 1349–1359. https://doi.org/10.1016/j.jece.2017.02.016

De Vrieze, J., Smet, D., Klok, J., Colsen, J., Angenent, L.T., Vlaeminck, S.E., 2016. Thermophilic sludge digestion improves energy balance and nutrient recovery potential in full-scale municipal wastewater treatment plants. Bioresour. Technol. 218, 1237–1245. https://doi.org/10.1016/j.biortech.2016.06.119

De Vrieze, J., Verstraete, W., 2016. Perspectives for microbial community composition in anaerobic digestion: from abundance and activity to connectivity. Environ.

Microbiol. 18, 2797–2809. https://doi.org/10.1111/1462-2920.13437
Duc, L.V., Miyagawa, Y., Inoue, D., Ike, M., 2022. Identification of key steps and associated microbial populations for efficient anaerobic digestion under high ammonium or salinity conditions. Bioresour. Technol. 360, 127571. https://doi.org/10.1016/j.biortech.2022.127571
Fernandes, T.V., Keesman, K.J., Zeeman, G., van Lier, J.B., 2012. Effect of ammonia on the anaerobic hydrolysis of cellulose and tributyrin. Biomass Bioenergy 47, 316–323. https://doi.org/10.1016/j.biombioe.2012.09.029
Fernández-Rodríguez, J., Pérez, M., Romero, L.I., 2016. Semicontinuous temperature-phased anaerobic digestion (TPAD) of organic fraction of municipal solid waste (OFMSW). Comparison with single-stage processes. Chem. Eng. J. 285, 409–416. https://doi.org/10.1016/j.cej.2015.10.027
Fotidis, I.A., Karakashev, D., Angelidaki, I., 2013. Bioaugmentation with an acetate-oxidising consortium as a tool to tackle ammonia inhibition of anaerobic digestion. Bioresour. Technol. 146, 57–62. https://doi.org/10.1016/j.biortech.2013.07.041
Fotidis, I.A., Treu, L., Angelidaki, I., 2017. Enriched ammonia-tolerant methanogenic cultures as bioaugmentation inocula in continuous biomethanation processes. J. Clean. Prod. 166, 1305–1313. https://doi.org/10.1016/j.jclepro.2017.08.151
Fotidis, I.A., Wang, H., Fiedel, N.R., Luo, G., Karakashev, D.B., Angelidaki, I., 2014. Bioaugmentation as a solution to increase methane production from an ammonia-rich substrate. Environ. Sci. Technol. 48, 7669–7676. https://doi.org/10.1021/es5017075
Freilich, M.A., Wieters, E., Broitman, B.R., Marquet, P.A., Navarrete, S.A., 2018. Species co-occurrence networks: Can they reveal trophic and non-trophic interactions in ecological communities? Ecology 99, 690–699. https://doi.org/10.1002/ecy.2142
Gallert, C., Winter, J., 1997. Mesophilic and thermophilic anaerobic digestion of source-sorted organic wastes: effect of ammonia on glucose degradation and methane production. Appl. Microbiol. Biotechnol. 48, 405–410. https://doi.org/10.1007/s002530051071
Gao, S., Zhao, M., Chen, Y., Yu, M., Ruan, W., 2015. Tolerance response to in situ ammonia stress in a pilot-scale anaerobic digestion reactor for alleviating ammonia inhibition. Bioresour. Technol. 198, 372–379. https://doi.org/10.1016/j.biortech.2015.09.044
Gao, Y., Fang, Z., Liang, P., Zhang, X., Qiu, Y., Kimura, K., Huang, X., 2019. Anaerobic digestion performance of concentrated municipal sewage by forward osmosis membrane: Focus on the impact of salt and ammonia nitrogen. Bioresour. Technol. 276, 204–210. https://doi.org/10.1016/j.biortech.2019.01.016
Grady, C.P.L., Daigger, G.T., Lim, H.C., 1999. Biological Wastewater Treatment, second. ed. Marcel Dekker, New York.
Hajjaji, N., Houas, A., Pons, M.-N., 2016. Thermodynamic feasibility and life cycle assessment of hydrogen production via reforming of poultry fat. J. Clean. Prod. 134, 600–612. https://doi.org/10.1016/j.jclepro.2015.12.018
Hansen, K.H., Angelidaki, I., Ahring, B.K., 1998. Anaerobic digestion of swine manure:

Inhibition by ammmonia. Water Res. 32, 5–12. https://doi.org/10.1016/S0043-1354(97)00201-7

Hardy, J., Bonin, P., Lazuka, A., Gonidec, E., Guasco, S., Valette, C., Lacroix, S., Cabrol, L., 2021. Similar methanogenic shift but divergent syntrophic partners in snaerobic digesters exposed to direct versus successive ammonium additions. Microbiol. Spectr. 9, e00805-21. https://doi.org/10.1128/Spectrum.00805-21

Harirchi, S., Wainaina, S., Sar, T., Nojoumi, S.A., Parchami, Milad, Parchami, Mohsen, Varjani, S., Khanal, S.K., Wong, J., Awasthi, M.K., Taherzadeh, M.J., 2022. Microbiological insights into anaerobic digestion for biogas, hydrogen or volatile fatty acids (VFAs): A review. Bioengineered 13, 6521–6557. https://doi.org/10.1080/21655979.2022.2035986

Holliger, C., Alves, M., Andrade, D., Angelidaki, I., Astals, S., Baier, U., Bougrier, C., Buffière, P., Carballa, M., De Wilde, V., Ebertseder, F., Fernández, B., Ficara, E., Fotidis, I., Frigon, J.-C., De Laclos, H.F., Ghasimi, D.S.M., Hack, G., Hartel, M., Heerenklage, J., Horvath, I.S., Jenicek, P., Koch, K., Krautwald, J., Lizasoain, J., Liu, J., Mosberger, L., Nistor, M., Oechsner, H., Oliveira, J.V., Paterson, M., Pauss, A., Pommier, S., Porqueddu, I., Raposo, F., Ribeiro, T., Rüsch Pfund, F., Strömberg, S., Torrijos, M., Van Eekert, M., Van Lier, J., Wedwitschka, H., Wierinck, I., 2016. Towards a standardization of biomethane potential tests. Water Sci. Technol. 74, 2515–2522. https://doi.org/10.2166/wst.2016.336

Holm-Nielsen, J.B., Al Seadi, T., Oleskowicz-Popiel, P., 2009. The future of anaerobic digestion and biogas utilization. Bioresour. Technol. 100, 5478–5484. https://doi.org/10.1016/j.biortech.2008.12.046

Hupfauf, S., Plattner, P., Wagner, A.O., Kaufmann, R., Insam, H., Podmirseg, S.M., 2018. Temperature shapes the microbiota in anaerobic digestion and drives efficiency to a maximum at 45 °C. Bioresour. Technol. 269, 309–318. https://doi.org/10.1016/j.biortech.2018.08.106

Jiang, Y., McAdam, E., Zhang, Y., Heaven, S., Banks, C., Longhurst, P., 2019. Ammonia inhibition and toxicity in anaerobic digestion: A critical review. J. Water Process Eng. 32, 100899. https://doi.org/10.1016/j.jwpe.2019.100899

Jo, Y., Rhee, C., Choi, H., Shin, J., Shin, S.G., Lee, C., 2021. Long-term effectiveness of bioaugmentation with rumen culture in continuous anaerobic digestion of food and vegetable wastes under feed composition fluctuations. Bioresour. Technol. 338, 125500. https://doi.org/10.1016/j.biortech.2021.125500

Khafipour, A., Jordaan, E.M., Flores-Orozco, D., Khafipour, E., Levin, D.B., Sparling, R., Cicek, N., 2020. Response of microbial community to induced failure of anaerobic digesters through overloading with propionic acid followed by process recovery. Front. Bioeng. Biotechnol. 8, 604838. https://doi.org/10.3389/fbioe.2020.604838

Khanal, S.K. (Ed.), 2008. Anaerobic Biotechnology for Bioenergy Production: principles and Applications. Wiley-Blackwell, Ames, Iowa.

Kim, E., Lee, J., Han, G., Hwang, S., 2018. Comprehensive analysis of microbial communities in full-scale mesophilic and thermophilic anaerobic digesters treating food waste-recycling wastewater. Bioresour. Technol. 259, 442–450.

https://doi.org/10.1016/j.biortech.2018.03.079
Kovács, E., Wirth, R., Maróti, G., Bagi, Z., Nagy, K., Minárovits, J., Rákhely, G., Kovács, K.L., 2015. Augmented biogas production from protein-rich substrates and associated metagenomic changes. Bioresour. Technol. 178, 254–261. https://doi.org/10.1016/j.biortech.2014.08.111
Kugelman, I.J., McCarty, P.L., 1965. Cation toxicity and stimulation in anaerobic waste treatment. J. Water Pollut. Control Fed. 37, 97–116.
Lai, M.C., Gunsalus, R.P., 1992. Glycine betaine and potassium ion are the major compatible solutes in the extremely halophilic methanogen *Methanohalophilus* strain Z7302. J. Bacteriol. 174, 7474–7477. https://doi.org/10.1128/jb.174.22.7474-7477.1992
Lay, J.-J., Li, Y.-Y., Noike, T., 1997. Influences of pH and moisture content on the methane production in high-solids sludge digestion. Water Res. 31, 1518–1524. https://doi.org/10.1016/S0043-1354(96)00413-7
Lee, J., Kim, E., Hwang, S., 2021. Effects of inhibitions by sodium ion and ammonia and different inocula on acetate-utilizing methanogenesis: Methanogenic activity and succession of methanogens. Bioresour. Technol. 334, 125202. https://doi.org/10.1016/j.biortech.2021.125202
Lee, J.T.E., Dutta, N., Zhang, L., Tsui, T.T.H., Lim, S., Tio, Z.K., Lim, E.Y., Sun, J., Zhang, J., Wang, C.-H., Ok, Y.S., Ahring, B.K., Tong, Y.W., 2022. Bioaugmentation of *Methanosarcina thermophila* grown on biochar particles during semi-continuous thermophilic food waste anaerobic digestion under two different bioaugmentation regimes. Bioresour. Technol. 360, 127590. https://doi.org/10.1016/j.biortech.2022.127590
Lei, Y., Sun, D., Dang, Y., Feng, X., Huo, D., Liu, C., Zheng, K., Holmes, D.E., 2019. Metagenomic analysis reveals that activated carbon aids anaerobic digestion of raw incineration leachate by promoting direct interspecies electron transfer. Water Res. 161, 570–580. https://doi.org/10.1016/j.watres.2019.06.038
Leven, L., Eriksson, A.R.B., SchnÃ¼rer, A., 2007. Effect of process temperature on bacterial and archaeal communities in two methanogenic bioreactors treating organic household waste: Temperature effects on microbial communities in bioreactors. FEMS Microbiol. Ecol. 59, 683–693. https://doi.org/10.1111/j.1574-6941.2006.00263.x
Li, L., He, Q., Ma, Y., Wang, X., Peng, X., 2015. Dynamics of microbial community in a mesophilic anaerobic digester treating food waste: Relationship between community structure and process stability. Bioresour. Technol. 189, 113–120. https://doi.org/10.1016/j.biortech.2015.04.015
Li, Q., Qiao, W., Wang, X., Takayanagi, K., Shofie, M., Li, Y.-Y., 2015. Kinetic characterization of thermophilic and mesophilic anaerobic digestion for coffee grounds and waste activated sludge. Waste Manag. 36, 77–85. https://doi.org/10.1016/j.wasman.2014.11.016
Li, Q., Xu, M., Wang, G., Chen, R., Qiao, W., Wang, X., 2018. Sludge under high feedstock to seed sludge ratio in batch experiment. Bioresour. Technol. 249, 1009-1016.

Li, Wang, C., Xu, X., Sun, Y., Xing, T., 2022. Bioaugmentation with a propionate-degrading methanogenic culture to improve methane production from chicken manure. Bioresour. Technol. 346, 126607. https://doi.org/10.1016/j.biortech.2021.126607

Li, Y., Zhang, Y., Sun, Y., Wu, S., Kong, X., Yuan, Z., Dong, R., 2017. The performance efficiency of bioaugmentation to prevent anaerobic digestion failure from ammonia and propionate inhibition. Bioresour. Technol. 231, 94–100. https://doi.org/10.1016/j.biortech.2017.01.068

Li, Z.-Y., Inoue, D., Ike, M., 2023. Mitigating ammonia-inhibition in anaerobic digestion by bioaugmentation: A review. J. Water Process Eng. 52, 103506. https://doi.org/10.1016/j.jwpe.2023.103506

Li, Z.-Y., Nagao, S., Inoue, D., Ike, M., 2024. Different inhibition patterns of ammonia and salt revealed by kinetic analysis of their combined inhibitory effect on methanogenesis of hydrogen: A preliminary study. Biochem. Eng. J. 205, 109263. https://doi.org/10.1016/j.bej.2024.109263

Liao, X., Zhao, P., Hou, L., Adyari, B., Xu, E.G., Huang, Q., Hu, A., 2023. Network analysis reveals significant joint effects of microplastics and tetracycline on the gut than the gill microbiome of marine medaka. J. Hazard. Mater. 442, 129996. https://doi.org/10.1016/j.jhazmat.2022.129996

Linsong, H., Lianhua, L., Ying, L., Changrui, W., Yongming, S., 2022. Bioaugmentation with methanogenic culture to improve methane production from chicken manure in batch anaerobic digestion. Chemosphere 303, 135127. https://doi.org/10.1016/j.chemosphere.2022.135127

Liu, C., Yuan, X., Zeng, G., Li, W., Li, J., 2008. Prediction of methane yield at optimum pH for anaerobic digestion of organic fraction of municipal solid waste. Bioresour. Technol. 99, 882–888. https://doi.org/10.1016/j.biortech.2007.01.013

Liu, T., Sung, S., 2002. Ammonia inhibition on thermophilic aceticlastic methanogens. Water Sci. Technol. 45, 113–120. https://doi.org/10.2166/wst.2002.0304

Liu, Y., Boone, D.R., 1991. Effects of salinity on methanogenic decomposition. Bioresour. Technol. 35, 271–273. https://doi.org/10.1016/0960-8524(91)90124-3

Madigou, C., Lê Cao, K.-A., Bureau, C., Mazéas, L., Déjean, S., Chapleur, O., 2019. Ecological consequences of abrupt temperature changes in anaerobic digesters. Chem. Eng. J. 361, 266–277. https://doi.org/10.1016/j.cej.2018.12.003

Manzoor, S., Bongcam-Rudloff, E., Schnürer, A., Müller, B., 2016. Genome-guided analysis and whole transcriptome profiling of the mesophilic syntrophic acetate oxidising bacterium *Syntrophaceticus schinkii*. PLOS ONE 11, e0166520. https://doi.org/10.1371/journal.pone.0166520

Mao, C., Feng, Y., Wang, X., Ren, G., 2015. Review on research achievements of biogas from anaerobic digestion. Renew. Sustain. Energy Rev. 45, 540–555. https://doi.org/10.1016/j.rser.2015.02.032

Maroušek, J., Strunecký, O., Kolář, L., Vochozka, M., Kopecký, M., Maroušková, A., Batt, J., Poliak, M., Šoch, M., Bartoš, P., Klieštik, T., Filip, M., Konvalina, P., Moudrý, J., Peterka, J., Suchý, K., Zoubek, T., Cera, E., 2020. Advances in nutrient management make it possible to accelerate biogas production and thus improve the

economy of food waste processing. Energy Sources Part Recovery Util. Environ. Eff. 1–10. https://doi.org/10.1080/15567036.2020.1776796

Maus, I., Wibberg, D., Stantscheff, R., Stolze, Y., Blom, J., Eikmeyer, F.-G., Fracowiak, J., König, H., Pühler, A., Schlüter, A., 2015. Insights into the annotated genome sequence of *Methanoculleus bourgensis* MS2T, related to dominant methanogens in biogas-producing plants. J. Biotechnol. 201, 43–53. https://doi.org/10.1016/j.jbiotec.2014.11.020

McCarty, P.L., McKinney, R.E., 1961. Salt Toxicity in Anaerobic Digestion. J. WPCF. 33, 399-415.

Miura, T., Kita, A., Okamura, Y., Aki, T., Matsumura, Y., Tajima, T., Kato, J., Nakashimada, Y., 2015. Effect of salinity on methanogenic propionate degradation by acclimated marine sediment-derived culture. Appl. Biochem. Biotechnol. 177, 1541–1552. https://doi.org/10.1007/s12010-015-1834-5

MoE, 2021. 2020 Present Status of organic waste biogasification facilities. Minitry of Environment, Korea.

Nakakubo, R., Møller, H.B., Nielsen, A.M., Matsuda, J., 2008. Ammonia inhibition of methanogenesis and identification of process indicators during anaerobic digestion. Environ. Eng. Sci. 25, 1487–1496. https://doi.org/10.1089/ees.2007.0282

Nielsen, H. B., Angelidaki, I., 2008. Codigestion of manure and industrial organic waste at centralized biogas plants: Process imbalances and limitations. Water Sci. Technol. 58, 1521–1528. https://doi.org/10.2166/wst.2008.507

Nielsen, Henrik Bangsø, Angelidaki, I., 2008. Strategies for optimizing recovery of the biogas process following ammonia inhibition. Bioresour. Technol. 99, 7995–8001. https://doi.org/10.1016/j.biortech.2008.03.049

Niu, Q., Hojo, T., Qiao, W., Qiang, H., Li, Y.-Y., 2014. Characterization of methanogenesis, acidogenesis and hydrolysis in thermophilic methane fermentation of chicken manure. Chem. Eng. J. 244, 587–596. https://doi.org/10.1016/j.cej.2013.11.074

Niu, Q., Kubota, K., Qiao, W., Jing, Z., Zhang, Y., Yu-You, L., 2015. Effect of ammonia inhibition on microbial community dynamic and process functional resilience in mesophilic methane fermentation of chicken manure: Effect of ammonia inhibition on microbial community dynamic. J. Chem. Technol. Biotechnol. 90, 2161–2169. https://doi.org/10.1002/jctb.4527

Ortega-Bravo, J.C., Pavez, J., Hidalgo, V., Reyes-Caniupán, I., Torres-Aravena, Á., Jeison, D., 2022. Biogas production from concentrated municipal sewage by forward osmosis, micro and ultrafiltration. Sustainability 14, 2629. https://doi.org/10.3390/su14052629

Pan, X., Zhao, L., Li, C., Angelidaki, I., Lv, N., Ning, J., Cai, G., Zhu, G., 2021. Deep insights into the network of acetate metabolism in anaerobic digestion: focusing on syntrophic acetate oxidation and homoacetogenesis. Water Res. 190, 116774. https://doi.org/10.1016/j.watres.2020.116774

Pardilhó, S., Pires, J.C., Boaventura, R., Almeida, M., Maia Dias, J., 2022. Biogas production from residual marine macroalgae biomass: Kinetic modelling approach. Bioresour. Technol. 359, 127473. https://doi.org/10.1016/j.biortech.2022.127473

Peces, M., Astals, S., Jensen, P.D., Clarke, W.P., 2018. Deterministic mechanisms define the long-term anaerobic digestion microbiome and its functionality regardless of the initial microbial community. Water Res. 141, 366–376. https://doi.org/10.1016/j.watres.2018.05.028

Peiffer, J.A., Spor, A., Koren, O., Jin, Z., Tringe, S.G., Dangl, J.L., Buckler, E.S., Ley, R.E., 2013. Diversity and heritability of the maize rhizosphere microbiome under field conditions. Proc. Natl. Acad. Sci. 110, 6548–6553. https://doi.org/10.1073/pnas.1302837110

Peng, H., Zhang, Y., Tan, D., Zhao, Z., Zhao, H., Quan, X., 2018. Roles of magnetite and granular activated carbon in improvement of anaerobic sludge digestion. Bioresour. Technol. 249, 666–672. https://doi.org/10.1016/j.biortech.2017.10.047

Peng, X., Zhang, S., Li, L., Zhao, X., Ma, Y., Shi, D., 2018. Long-term high-solids anaerobic digestion of food waste: Effects of ammonia on process performance and microbial community. Bioresour. Technol. 262, 148–158. https://doi.org/10.1016/j.biortech.2018.04.076

Poggi-Varaldo, H.M., Rodríguez-Vázquez, R., Fernández-Villagóme, G., Esparza-García, F., 1997. Inhibition of mesophilic solid-substrate anaerobic digestion by ammonia nitrogen. Appl. Microbiol. Biotechnol. 47, 284–291. https://doi.org/10.1007/s002530050928

Rajagopal, R., Massé, D.I., Singh, G., 2013. A critical review on inhibition of anaerobic digestion process by excess ammonia. Bioresour. Technol. 143, 632–641. https://doi.org/10.1016/j.biortech.2013.06.030

Romero-Güiza, M.S., Vila, J., Mata-Alvarez, J., Chimenos, J.M., Astals, S., 2016. The role of additives on anaerobic digestion: A review. Renew. Sustain. Energy Rev. 58, 1486–1499. https://doi.org/10.1016/j.rser.2015.12.094

Saha, S., Kurade, M.B., Ha, G.-S., Lee, S.S., Roh, H.-S., Park, Y.-K., Jeon, B.-H., 2021. Syntrophic metabolism facilitates *Methanosarcina*-led methanation in the anaerobic digestion of lipidic slaughterhouse waste. Bioresour. Technol. 335, 125250. https://doi.org/10.1016/j.biortech.2021.125250

Sasaki, K., Morita, M., Hirano, S., Ohmura, N., Igarashi, Y., 2011. Decreasing ammonia inhibition in thermophilic methanogenic bioreactors using carbon fiber textiles. Appl. Microbiol. Biotechnol. 90, 1555–1561. https://doi.org/10.1007/s00253-011-3215-5

Schmack, D., Reuter, M., n.d. Generating biogas e.g. methane from biomass in a fermentation reactor comprises adding a microorganism of the species *Methanoculleus bourgensis* to the biomass. WO2010115424-A1; DE102009003780-A1; DE102009003780-B4.

Shanmugam, P., Horan, N.J., 2009. Optimising the biogas production from leather fleshing waste by co-digestion with MSW. Bioresour. Technol. 100, 4117–4120. https://doi.org/10.1016/j.biortech.2009.03.052

Shi, X., Ng, K.K., Li, X.-R., Ng, H.Y., 2015. Investigation of intertidal wetland sediment as a novel inoculation source for anaerobic aaline wastewater treatment. Environ. Sci. Technol. 49, 6231–6239. https://doi.org/10.1021/acs.est.5b00546

Sohail, M., Khan, A., Badshah, M., Degen, A., Yang, G., Liu, H., Zhou, J., Long, R.,

2022. Yak rumen fluid inoculum increases biogas production from sheep manure substrate. Bioresour. Technol. 362, 127801. https://doi.org/10.1016/j.biortech.2022.127801

Soto, M., Méndez, R., Lema, J.M., 1993. Methanogenic and non-methanogenic activity tests. Theoretical basis and experimental set up. Water Res. 27, 1361–1376. https://doi.org/10.1016/0043-1354(93)90224-6

Sprott, G.D., Patel, G.B., 1986. Ammonia toxicity in pure cultures of methanogenic bacteria. Syst. Appl. Microbiol. 7, 358–363. https://doi.org/10.1016/S0723-2020(86)80034-0

Sung, S., Liu, T., 2003. Ammonia inhibition on thermophilic anaerobic digestion. Chemosphere 53, 43–52. https://doi.org/10.1016/S0045-6535(03)00434-X

Tale, V.P., Maki, J.S., Zitomer, D.H., 2015. Bioaugmentation of overloaded anaerobic digesters restores function and archaeal community. Water Res. 70, 138–147. https://doi.org/10.1016/j.watres.2014.11.037

Tao, Y., Ersahin, M.E., Ghasimi, D.S.M., Ozgun, H., Wang, H., Zhang, X., Guo, M., Yang, Y., Stuckey, D.C., van Lier, J.B., 2020. Biogas productivity of anaerobic digestion process is governed by a core bacterial microbiota. Chem. Eng. J. 380, 122425. https://doi.org/10.1016/j.cej.2019.122425

Tian, H., Fotidis, I.A., Mancini, E., Angelidaki, I., 2017. Different cultivation methods to acclimatise ammonia-tolerant methanogenic consortia. Bioresour. Technol. 232, 1–9. https://doi.org/10.1016/j.biortech.2017.02.034

Tian, H., Fotidis, I.A., Mancini, E., Treu, L., Mahdy, A., Ballesteros, M., González-Fernández, C., Angelidaki, I., 2018. Acclimation to extremely high ammonia levels in continuous biomethanation process and the associated microbial community dynamics. Bioresour. Technol. 247, 616–623. https://doi.org/10.1016/j.biortech.2017.09.148

Tian, H., Yan, M., Treu, L., Angelidaki, I., Fotidis, I.A., 2019. Hydrogenotrophic methanogens are the key for a successful bioaugmentation to alleviate ammonia inhibition in thermophilic anaerobic digesters. Bioresour. Technol. 293, 122070. https://doi.org/10.1016/j.biortech.2019.122070

Tiwari, B.R., Rouissi, T., Brar, S.K., Surampalli, R.Y., 2021. Critical insights into psychrophilic anaerobic digestion: Novel strategies for improving biogas production. Waste Manag. 131, 513–526. https://doi.org/10.1016/j.wasman.2021.07.002

Town, J.R., Dumonceaux, T.J., 2016. Laboratory-scale bioaugmentation relieves acetate accumulation and stimulates methane production in stalled anaerobic digesters. Appl. Microbiol. Biotechnol. 100, 1009–1017. https://doi.org/10.1007/s00253-015-7058-3

Turcios, A.E., Cayenne, A., Uellendahl, H., Papenbrock, J., 2021. Halophyte plants and their residues as feedstock for biogas production—Chances and challenges. Appl. Sci. 11, 2746. https://doi.org/10.3390/app11062746

Usman, M., Salama, E.-S., Arif, M., Jeon, B.-H., Li, X., 2020. Determination of the inhibitory concentration level of fat, oil, and grease (FOG) towards bacterial and archaeal communities in anaerobic digestion. Renew. Sustain. Energy Rev. 131,

110032. https://doi.org/10.1016/j.rser.2020.110032
Venkiteshwaran, K., Milferstedt, K., Hamelin, J., Zitomer, D.H., 2016. Anaerobic digester bioaugmentation influences quasi steady state performance and microbial community. Water Res. 104, 128–136. https://doi.org/10.1016/j.watres.2016.08.012
Wang, H., Fotidis, I.A., Angelidaki, I., 2015. Ammonia effect on hydrogenotrophic methanogens and syntrophic acetate-oxidizing bacteria. FEMS Microbiol. Ecol. 91, fiv130. https://doi.org/10.1093/femsec/fiv130
Wang, H.-Z., Lv, X.-M., Yi, Y., Zheng, D., Gou, M., Nie, Y., Hu, B., Nobu, M.K., Narihiro, T., Tang, Y.-Q., 2019. Using DNA-based stable isotope probing to reveal novel propionate- and acetate-oxidizing bacteria in propionate-fed mesophilic anaerobic chemostats. Sci. Rep. 9, 17396. https://doi.org/10.1038/s41598-019-53849-0
Wang, S., Wang, Z., Usman, M., Zheng, Z., Zhao, X., Meng, X., Hu, K., Shen, X., Wang, X., Cai, Y., 2023. Two microbial consortia obtained through purposive acclimatization as biological additives to relieve ammonia inhibition in anaerobic digestion. Water Res. 230, 119583. https://doi.org/10.1016/j.watres.2023.119583
Westerholm, M., Levén, L., Schnürer, A., 2012. Bioaugmentation of syntrophic acetate-oxidizing culture in biogas reactors exposed to increasing levels of ammonia. Appl. Environ. Microbiol. 78, 7619–7625. https://doi.org/10.1128/AEM.01637-12
Wilén, B.-M., Jin, B., Lant, P., 2003. The influence of key chemical constituents in activated sludge on surface and flocculating properties. Water Res. 37, 2127–2139. https://doi.org/10.1016/S0043-1354(02)00629-2
Wilson, L.P., 2016. Enhanced anaerobic digestion performance via combined solids- and leachate-based hydrolysis reactor inoculation. Bioresour. Technol. 10.
Wilson, L.P., H.Loetscher, L., E.Sharvelle, S., De Long, S.K., 2013. Microbial community acclimation enhances waste hydrolysis rates under elevated ammonia and salinity conditions. Bioresour. Technol. 146, 15–22. https://doi.org/10.1016/j.biortech.2013.06.081
Wood, J.M., 2015. Bacterial responses to osmotic challenges. J. Gen. Physiol. 145, 381–388. https://doi.org/10.1085/jgp.201411296
Woraruthai, T., Supawatkorn, C., Uthaipaisanwong, P., Kusonmano, K., Wongsurawat, T., Jenjaroenpun, P., Chaiyen, P., Wongnate, T., 2024. Isolation and characterization of *Enterococcus faecalis* isolate VT-H1: A highly efficient hydrogen-producing bacterium from palm oil mill effluent (POME). Int. J. Hydrog. Energy 49, 295–309. https://doi.org/10.1016/j.ijhydene.2023.08.017
Wu, L., Yang, Y., Chen, S., Zhao, M., Zhu, Z., Yang, S., Qu, Y., Ma, Q., He, Z., Zhou, J., He, Q., 2016. Long-term successional dynamics of microbial association networks in anaerobic digestion processes. Water Res. 104, 1–10. https://doi.org/10.1016/j.watres.2016.07.072
Xu, J., Kumar Khanal, S., Kang, Y., Zhu, J., Huang, X., Zong, Y., Pang, W., Surendra, K.C., Xie, L., 2022. Role of interspecies electron transfer stimulation in enhancing anaerobic digestion under ammonia stress: Mechanisms, advances, and

perspectives. Bioresour. Technol. 360, 127558. https://doi.org/10.1016/j.biortech.2022.127558

Xu, X., Sun, Yong, Sun, Yongming, Li, Y., 2022. Bioaugmentation improves batch psychrophilic anaerobic co-digestion of cattle manure and corn straw. Bioresour. Technol. 343, 126118. https://doi.org/10.1016/j.biortech.2021.126118

Yan, M., Fotidis, I.A., Tian, H., Khoshnevisan, B., Treu, L., Tsapekos, P., Angelidaki, I., 2019. Acclimatization contributes to stable anaerobic digestion of organic fraction of municipal solid waste under extreme ammonia levels: Focusing on microbial community dynamics. Bioresour. Technol. 286, 121376. https://doi.org/10.1016/j.biortech.2019.121376

Yan, M., Treu, L., Zhu, X., Tian, H., Basile, A., Fotidis, I.A., Campanaro, S., Angelidaki, I., 2020. Insights into ammonia adaptation and methanogenic precursor oxidation by genome-centric analysis. Environ. Sci. Technol. 54, 12568–12582. https://doi.org/10.1021/acs.est.0c01945

Yan, M., Zhu, X., Treu, L., Ravenni, G., Campanaro, S., Goonesekera, E.M., Ferrigno, R., Jacobsen, C.S., Zervas, A., Angelidaki, I., Fotidis, I.A., 2021. Comprehensive evaluation of different strategies to recover methanogenic performance in ammonia-stressed reactors. Bioresour. Technol. 336, 125329. https://doi.org/10.1016/j.biortech.2021.125329

Yang, Z., Guo, R., Xu, X., Wang, L., Dai, M., 2016. Enhanced methane production via repeated batch bioaugmentation pattern of enriched microbial consortia. Bioresour. Technol. 216, 471–477. https://doi.org/10.1016/j.biortech.2016.05.062

Yang, Z., Sun, H., Zhao, Q., Kurbonova, M., Zhang, R., Liu, G., Wang, W., 2020. Long-term evaluation of bioaugmentation to alleviate ammonia inhibition during anaerobic digestion: Process monitoring, microbial community response, and methanogenic pathway modeling. Chem. Eng. J. 399, 125765. https://doi.org/10.1016/j.cej.2020.125765

Yerkes, D.W., Boonyakitsombut, S., Speece, R.E., 1997. Antagonism of sodium toxicity by the compatible solute betaine in anaerobic methanogenic systems. Wat. Sci. Tech. 36, 15-24.

Yu, D., Zhang, J., Chulu, B., Yang, M., Nopens, I., Wei, Y., 2020. Ammonia stress decreased biomarker genes of acetoclastic methanogenesis and second peak of production rates during anaerobic digestion of swine manure. Bioresour. Technol. 317, 124012. https://doi.org/10.1016/j.biortech.2020.124012

Yu, D., Zhang, Q., De Jaegher, B., Liu, J., Sui, Q., Zheng, X., Wei, Y., 2021. Effect of proton pump inhibitor on microbial community, function, and kinetics in anaerobic digestion with ammonia stress. Bioresour. Technol. 319, 124118. https://doi.org/10.1016/j.biortech.2020.124118

Yuan, H., Zhu, N., 2016. Progress in inhibition mechanisms and process control of intermediates and by-products in sewage sludge anaerobic digestion. Renew. Sustain. Energy Rev. 58, 429–438. https://doi.org/10.1016/j.rser.2015.12.261

Zeb, I., Ma, J., Mehboob, F., Kafle, G.K., Amin, B.A.Z., Nazir, R., Ndegwa, P., Frear, C., 2019. Kinetic and microbial analysis of methane production from dairy wastewater anaerobic digester under ammonia and salinity stresses. J. Clean. Prod.

219, 797–808. https://doi.org/10.1016/j.jclepro.2019.01.295
Zhang, H., Yuan, W., Dong, Q., Wu, D., Yang, P., Peng, Y., Li, L., Peng, X., 2022. Integrated multi-omics analyses reveal the key microbial phylotypes affecting anaerobic digestion performance under ammonia stress. Water Res. 213, 118152. https://doi.org/10.1016/j.watres.2022.118152
Zhang, J., Mao, L., Zhang, L., Loh, K.-C., Dai, Y., Tong, Y.W., 2017. Metagenomic insight into the microbial networks and metabolic mechanism in anaerobic digesters for food waste by incorporating activated carbon. Sci. Rep. 7, 11293. https://doi.org/10.1038/s41598-017-11826-5
https://doi.org/10.1016/j.jbiosc.2019.11.011
Zhang, L., Zhu, K., Li, A., 2016. Differentiated effects of osmoprotectants on anaerobic syntrophic microbial populations at saline conditions and its engineering aspects. Chem. Eng. J. 288, 116–125. https://doi.org/10.1016/j.cej.2015.11.100
Zhang, S., Chang, J., Liu, W., Pan, Y., Cui, K., Chen, X., Liang, P., Zhang, X., Wu, Q., Qiu, Y., Huang, X., 2018. A novel bioaugmentation strategy to accelerate methanogenesis via adding *Geobacter sulfurreducens* PCA in anaerobic digestion system. Sci. Total Environ. 642, 322–326. https://doi.org/10.1016/j.scitotenv.2018.06.043
Zhao, W., Chen, Z., Xia, D., Lv, Q., Li, S., 2023. Biogas production characteristics of lignite and related metabolic functions with indigenous microbes from different coal seams. Fuel 349, 128598. https://doi.org/10.1016/j.fuel.2023.128598
Ziganshina, E.E., Ziganshin, A.M., 2022. Anaerobic digestion of chicken manure in the presence of magnetite, granular activated carbon, and biochar: Operation of anaerobic reactors and microbial community structure. Microorganisms 10, 1422. https://doi.org/10.3390/microorganisms10071422.

Appendix

Kinetic analysis of the combined inhibitory effect of ammonia and salt on methanogenesis of hydrogen

Introduction

Although studies on the inhibition of ammonia and salt on anaerobic digestion (AD) have been reported, most focused on a single factor or few experimental groups and failed to derive any kinetic parameters (Duc et al., 2023; Lee et al., 2021; Oh et al., 2008). To provide a full profile of the combined inhibitory effect of ammonia and salt on methanogenesis of hydrogen, following three questions should be considered: (1) What is the inhibition pattern of ammonia/salt at various concentrations? (2) What are their combined inhibition effects through a wide concentration range? (3) Is there a parameter that unifies ammonia and salt inhibition? To answer these questions and resultantly to be an assist in this doctoral dissertation research, hydrogen-fed SMA (specific methanogenic activity) tests were conducted with different concentrations of ammonia and salt, and their combined inhibitory effects on CH_4 production were analyzed.

Material and methods

Specific methanogenetic activity test setup

Seed AD sludge was collected from a mesophilic continuous anaerobic digester in central Japan. The sludge concentration was adjusted to 3.5 g VSS L^{-1} and washed twice with 0.9% NaCl solution. Basal anaerobic medium containing no organics (Table A-1) was selected as the culture medium for the SMA test. A series of anaerobic batch tests were conducted with five different nominal concentrations of ammonia (0, 1.25, 2.5, 3.75, and 5 g NH_4-N L^{-1}) and salt (0, 7.5, 15, 22.5, and 30 g NaCl L^{-1}). Duplicate samples were prepared for each test group, resulting in 51 bottles (50 test groups and a blank group without inhibitor or substrate addition). For each group, 20 mL of the stabilized seed sludge/culture medium mixture was added to a 137 mL serum bottle. After an anaerobic condition was obtained by sealing each bottle with a butyl rubber stopper and flushing with N_2 gas for 8 min, 30 mL of N_2 gas was drawn out before 50 mL of H_2/CO_2 mixture gas (80%/20% v/v) was injected as the substrate for methanogenesis. All groups were cultivated as mentioned previously for 6 days without pH control. Biogas production was monitored once or twice a day depending on the production rate. Liquid samples for pH, TAN, and salinity analyses were collected on days 0, 2, and 6.

Table A-1 Composition of basal anaerobic medium used in SMA tests.

Substance	Concentration	Unit
KH_2PO_4	0.28	g L^{-1}
NaCl	1	g L^{-1}
KCl	0.5	g L^{-1}
NH_4Cl	0.3	g L^{-1}
$MgCl_2 \cdot 6H_2O$	0.5	g L^{-1}
$CaCl_2 \cdot 2H_2O$	0.015	g L^{-1}
$NaHCO_3$	2.6	g L^{-1}
NaOH	0.5	mg L^{-1}
$FeCl_2 \cdot 4H_2O$	1.5	mg L^{-1}
$CoCl_2 \cdot 6H_2O$	0.19	mg L^{-1}
$MnCl_2 \cdot 4H_2O$	0.1	mg L^{-1}
$ZnCl_2$	0.07	mg L^{-1}
$Na_2MoO_4 \cdot 2H_2O$	0.036	mg L^{-1}
$NiCl_2 \cdot 6H_2O$	0.024	mg L^{-1}
$Na_2WO_4 \cdot 2H_2O$	0.008	mg L^{-1}
H_3BO_3	0.006	mg L^{-1}
$Na_2SeO_3 \cdot 5H_2O$	0.006	mg L^{-1}
$CuCl_2 \cdot 2H_2O$	0.002	mg L^{-1}
Biotin	0.02	mg L^{-1}
Folic acid	0.02	mg L^{-1}
Pyridoxine hydrochloride	0.1	mg L^{-1}
Riboflavin	0.05	mg L^{-1}
Thiamine	0.05	mg L^{-1}
Nicotinic acid	0.05	mg L^{-1}
Pantothenic acid	0.05	mg L^{-1}
Vitamin B12	0.001	mg L^{-1}
p-Aminobenzoic acid	0.05	mg L^{-1}
Thioctic acid	0.05	mg L^{-1}
$Na_2S \cdot 9H_2O$	0.048	g L^{-1}
L-cysteine	0.031	g L^{-1}

Analytical method

The total suspended solids and VSS were determined using methods introduced in Chapter 2. For biogas sampling, the positive pressure in the serum bottles was measured at the start of experiments, with all the gas pushed back to the system after recording the value. As the pressure decreased following H_2/CO_2 consumption, N_2 gas was supplied to maintain the pressure at 1 atm when negative pressure formed. Thereafter, headspace gas samples were collected, and the CH_4 concentration was determined using gas chromatography same as in Chapter 2. No gas was discharged from the system during operation, so accumulative CH_4 production was calculated by multiplying the measured headspace and CH_4 concentration. The pH and salinity were measured using portable pH (Toko Chemical Laboratories, Japan) and salinity (Atago, Japan) meters, respectively. The TAN concentration was determined using a coulometric titration ammonia meter (Central Kagaku, Japan).

Kinetic analysis

The Modified Gompertz model (Eq. (2-1)), which is a common choice describing a mono-sigmoidal pattern in batch AD experiments, was selected to describe the accumulative CH_4 production in the SMA test, where R' is the SMA (mL CH_4 g VSS^{-1} day^{-1}). Kinetic parameters were estimated with nonlinear curve fitting using the solver tool in Microsoft Excel (version 16.70).

The extended Monod equation (Eq. (A-1)), a generalized form of the basic Monod equation accounting for different types of inhibition, was selected to describe the inhibition effect of ammonia/salt on SMA:

$$R' = R_m \left(1 - \frac{I}{I^*}\right)^n \left[\frac{S}{S + K_S\,(1-(I/I^*))^m}\right] \quad \text{(A-1)}$$

where R' is the SMA at the inhibitor concentration of I (mL CH_4 g VSS^{-1} day^{-1} as in Eq. (2-1)), R_m is the maximum SMA without inhibition (mL CH_4 g VSS^{-1} day^{-1}), S is the substrate concentration (g L^{-1} as COD), K_s is the half-saturation constant (g L^{-1} as COD), I is the inhibitor concentration (g L^{-1}); I^* is the lethal concentration (g L^{-1}), and n and m are coefficients that determine the inhibition pattern. Before the fitting of the extended Monod equation, a series of batch tests was conducted to estimate the baseline Monod parameter (K_s). The same setups as used in the SMA test, except for different H_2/CO_2 mixture gas volumes of 10–50 mL with no inhibition addition, were applied. The accumulative CH_4 results were fitted with the Gompertz model, and K_s was estimated to be 1.04 g COD L^{-1} using the Monod equation (Fig. A-1).

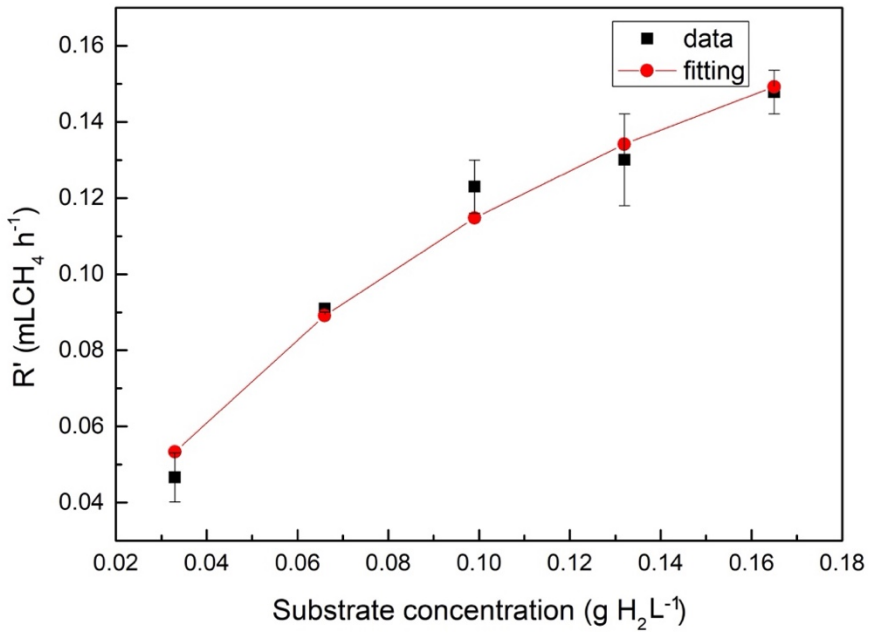

Fig. A-1 Fitting results of different substrate concentration groups using the Monod equation. *Ks* was estimated to be 1.04 g COD L^{-1}; error bars represent the standard deviation of the mean for each duplicate experiment.

A 3-D contour with peripheral area padded with predicted SMA data from the extended Monod equation was depicted as follows: For ammonium-inhibition groups, five extended Monod-fitted curves predicting the relationships of SMA values and ammonia inhibition concentration were conducted at five different salt concentrations based on experimental SMA results. The ammonium concentration range was then divided by 40 equidistant concentrations, and the extended Monod equation was re-applied for each ammonium concentration for salt-inhibition group prediction based on the five data points on the original five fitted curves. Finally, a 40 × 40 SMA dataset was created, and the 3-D contour was built on it.

Results and discussion

Kinetic analysis of specific methanogenetic activity test

The measured data of accumulative CH_4 production (background CH_4 produced in blank group was negligible) in the SMA tests were fitted to the modified Gompertz model. The parameters P, λ, and R' in the model were determined. The model showed a good fit for most samples ($R^2 > 0.95$ with low RMSE) (Table A-2). The R' value was further used for fitting the extended Monod equation. In the extended Monod equation fitting, R_m, I^*, m, and n were taken as parameters to be determined. A good fit was attained in both ammonium and salt-inhibition groups ($R^2 > 0.95$ with low RMSE) (Table A-3).

Table A-2 Fitting results of Gompertz model. (A), (B) present the data from duplicate groups.

(A)

Group	Nominal ammonia concentration (g NH_4-N L^{-1})	Nominal salt concentration (g NaCl L^{-1})	P (mL)	λ (h)	R' (mL CH_4 g VSS^{-1} day^{-1})	R^2
A0S0	0	0	12.0	64.1	102.34	0.965
A1S0	1.25	0	10.0	61.6	40.13	0.976
A2S0	2.50	0	11.8	95.0	23.51	0.975
A3S0	3.75	0	6.8	80.0	28.52	0.982
A4S0	5.00	0	0.8	98.4	5.49	0.966
A0S1	0	7.5	10.0	59.5	48.75	0.994
A1S1	1.25	7.5	10.0	71.6	37.93	0.976
A2S1	2.50	7.5	8.0	97.8	23.33	0.977
A3S1	3.75	7.5	0.1	51.5	2.80	0.979
A4S1	5.00	7.5	0.1	51.4	2.27	0.988
A0S2	0	15.0	8.0	102.0	19.80	0.990
A1S2	1.25	15.0	N.A.	N.A.	N.A.	N.A.
A2S2	2.50	15.0	8.0	141.8	14.05	0.968
A3S2	3.75	15.0	0.1	49.2	1.60	0.980
A4S2	5.00	15.0	0.1	49.6	3.08	0.962
A0S3	0	22.5	7.8	146.2	13.22	0.950
A1S3	1.25	22.5	5.0	122.0	9.65	0.963
A2S3	2.50	22.5	0.1	40.7	1.69	0.987
A3S3	3.75	22.5	0.3	40.2	2.26	0.942
A4S3	5.00	22.5	0	-	0	-
A0S4	0	30.0	0.2	50.4	3.18	0.969
A1S4	1.25	30.0	0.1	53.0	3.08	0.986
A2S4	2.50	30.0	0.2	38.0	2.02	0.992
A3S4	3.75	30.0	0	-	0	-
A4S4	5.00	30.0	0	-	0	-

- : not applicable; N.A.: data unavailable

(B)

Group	Nominal ammonia concentration (g NH_4-N L^{-1})	Nominal salt concentration (g NaCl L^{-1})	P (mL)	λ (h)	R' (mL CH_4 g VSS^{-1} day^{-1})	R^2
A0S0	0	0	12.0	54.4	77.83	0.999
A1S0	1.25	0	10.0	73.4	39.96	0.982
A2S0	2.50	0	10.0	76.4	40.83	0.973
A3S0	3.75	0	10.0	118.8	24.91	0.989
A4S0	5.00	0	0.4	71.0	7.87	0.999
A0S1	0	7.5	N.A.	N.A.	N.A.	N.A.
A1S1	1.25	7.5	10.0	81.3	33.58	0.980
A2S1	2.50	7.5	10.0	128.4	24.02	0.972
A3S1	3.75	7.5	0	-	0	-
A4S1	5.00	7.5	0	-	0	-
A0S2	0	15.0	5.0	73.9	27.46	0.990
A1S2	1.25	15.0	5.0	120.0	15.66	0.980
A2S2	2.50	15.0	2.5	118.8	12.56	0.995
A3S2	3.75	15.0	0.1	74.4	1.48	0.991
A4S2	5.00	15.0	0	-	0	-
A0S3	0	22.5	3.5	112.9	9.96	0.928
A1S3	1.25	22.5	1.5	100.1	7.65	0.912
A2S3	2.50	22.5	0	-	0	-
A3S3	3.75	22.5	0	-	0	-
A4S3	5.00	22.5	0	-	0	-
A0S4	0	30.0	5.0	135.4	10.57	0.916
A1S4	1.25	30.0	0	-	0	-
A2S4	2.50	30.0	0	-	0	-
A3S4	3.75	30.0	0	-	0	-
A4S4	5.00	30.0	0	-	0	-

- : not applicable; N.A.: data unavailable

Table A-3 Fitting results of kinetic parameters of I^*, R_m, n, and m for the extended Monod equation of ammonium inhibition groups and salt inhibition groups

Salt concentration (g NaCl L^{-1})	I^* (g L^{-1})	R_m (ml CH_4 g VSS^{-1} day^{-1})	n	m	R^2	Ammonia concentration (g NH_4-N L^{-1})	I^* (g L^{-1})	R_m (ml CH_4 g VSS^{-1} day^{-1})	n	m	R^2
0	25.0	154.2	9.41	-0.50	0.929	0	80.0	210.0	6.08	0	0.999
7.5	4.0	86.4	0.60	-0.20	0.998	1.25	28.1	83.6	0.84	0	0.962
15	4.0	40.3	0.52	-0.15	0.977	2.5	23.3	63.7	0.65	0	0.999
22.5	2.6	20.8	0.20	-0.51	0.992	3.75	10.9	45.0	0.50	0	0.995
30	1.7	12.4	0.48	-0.98	0.978	5	8.5	13.7	0.27	0	0.962

I^*, lethal concentration; R_m, maximum SMA without inhibition; n and m, coefficients that determine the inhibition pattern; R^2, R-square.

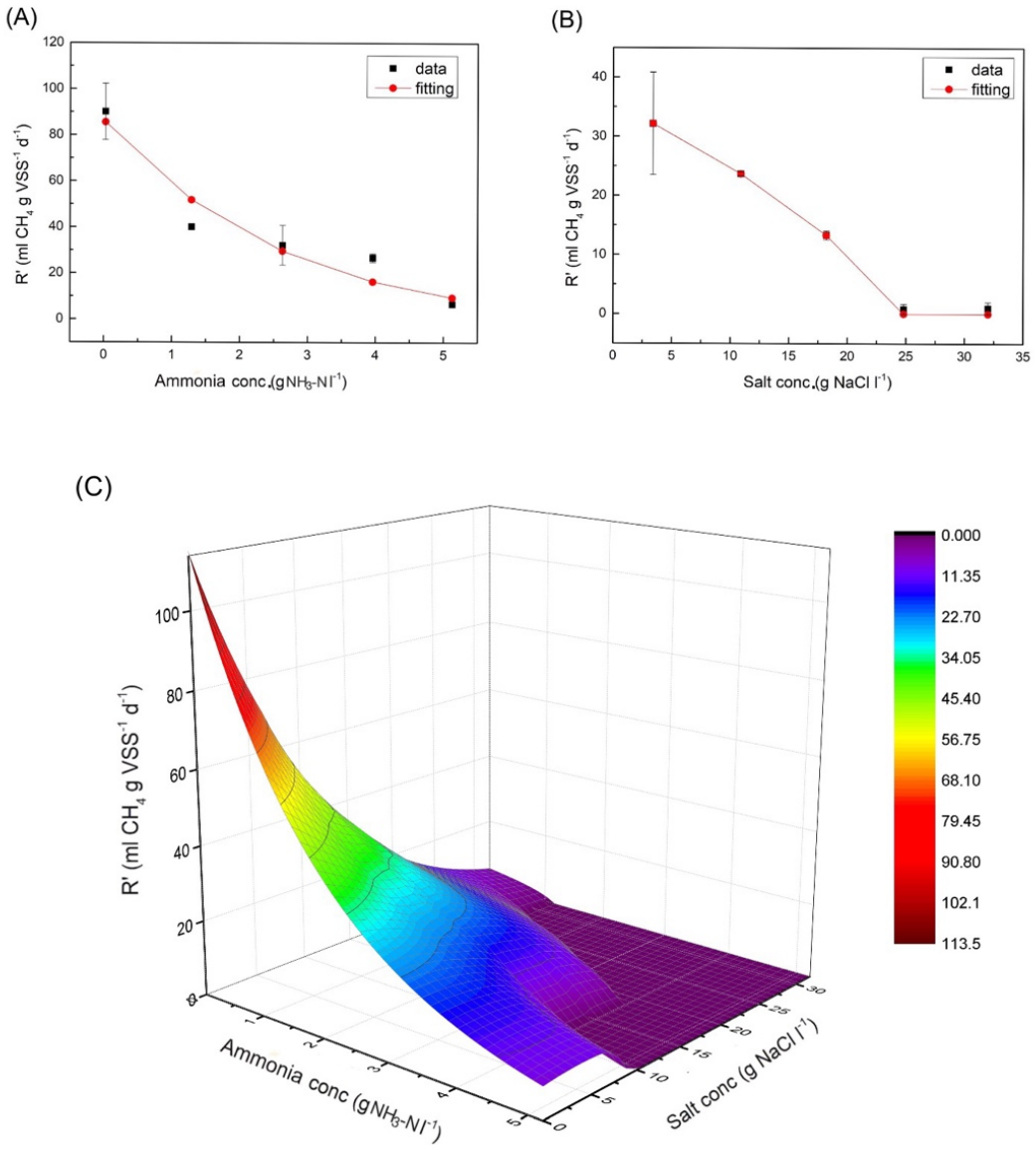

Fig. A-2 Typical fitting results of inhibition groups using extended Monod equation and 3-D contour prediction of SMA at various inhibition concentration based on fitting results, (A): ammonium inhibition groups at a nominal salt concentration of 0 g NaCl L^{-1}; (B): salt inhibition groups at a nominal ammonia concentration of 2.5 g NH_4-N L^{-1}, error bars represent standard deviation of the mean for each duplicate experiment, (C): 3-D contour prediction of SMA at various inhibition concentration.

The typical fitting results of ammonium and salt-inhibition groups using the extended Monod equation are shown in Fig. A-2(A) and Fig. A-2(B), respectively. The maximum SMA in the non-inhibitory condition was 85.57 mL CH_4 g VSS^{-1} day^{-1}, which was comparable to previous results (13.8–81.4 mL CH_4 g VSS^{-1} day^{-1} with different operating conditions) (Lu et al., 2018).

For the ammonium-inhibition group, SMA decreased sharply to 44.4% of the non-inhibitory condition level as the ammonium concentration increased from 0.02 to 1.29 g NH_4-N L^{-1}. The decreasing trend slowed when the ammonium concentration increased further: 29.7% of the non-inhibited SMA remained when the concentration reached 3.96 g NH_4-N L^{-1}. For the salt-inhibition group, an almost linear SMA decrease was observed as the salt concentration increased. Inhibition was almost complete when the salt concentration reached 24.8 g NaCl L^{-1}. The best-fit model parameters are summarized in Table A-3. *m* and *n* were <0 and >0, respectively, for ammonium inhibition, indicating mixed inhibition patterns, whereas *m* and *n* were 0 and >0, respectively, for salt inhibition, which is a characteristic of noncompetitive inhibition patterns (Grady et al., 1999).

Combined inhibitory effect of ammonia and salt

A 3-D contour padded with predicted SMA data from the extended Monod equation is shown in Fig. A-2(C). Monotonical decreases in SMA were observed along both axes, indicating increased severity of inhibition with both increasing ammonium and salt levels. Moreover, a bump area appeared at 2–4 g NH_4-N L^{-1}, indicating a relative insensitivity of the CH_4 production rate to the ammonium increase in the moderate

inhibition range. Conversely, no evident change in decrease rate was observed in the salt-inhibition groups. Thus, the combined inhibitory effect of ammonia and salt could not be summarized simply as additive or synergetic. It varied with the respective concentrations of ammonia and salt. Moreover, ammonia and salt showed different inhibition characteristics. An evident slowing of the declining trend in the CH_4 production rate in the moderate inhibition range was observed for ammonium inhibition, but it was not observed for salt inhibition, which aligned with the above results. The slowed declining trend may be attributed to the tolerance of HMs to ammonia inhibition. Despite sharing a weak cell wall structure lacking peptidoglycan with acetoclastic methanogens (Capson-Tojo et al., 2020), HMs such as *Methanoculleus thermophilus* showed no evident decrease in CH_4 production as ammonia increased from 3 to 5 g NH_4-N L^{-1} (Wang et al., 2015), which is comparable to the current results. According to Yan et al. (2020), the advantageous Gibbs free energies and the multiple energy-converting hydrogenase levels for homeostatic regulation contribute to the superior ammonium tolerance of HMs.

To describe the combined inhibition of ammonia and salt, salinity was selected as a unified parameter because of its ease of measurement. Ammonia addition also substantially contributed to the overall salinity, and all the data points fell into a logarithmic strip, irrespective of the different inhibition patterns of ammonia and salt (Fig. A-3). A threshold of 3.5% was determined, beyond which no CH_4 production was observed. Salinity strongly affects the osmotic pressure in a cell and leads to cell plasmolysis and even cell death (Zhang et al., 2020). This might explain the

predominant logarithmic impact of salinity on SMA, despite the deviating effect from respective characteristic impacts of ammonia and salt. A logarithmic model fit the data points well, with $R^2 > 0.95$, indicating that salinity can be applied as a unified parameter to predict the combined inhibition of ammonia and salt in methanogenesis of hydrogen.

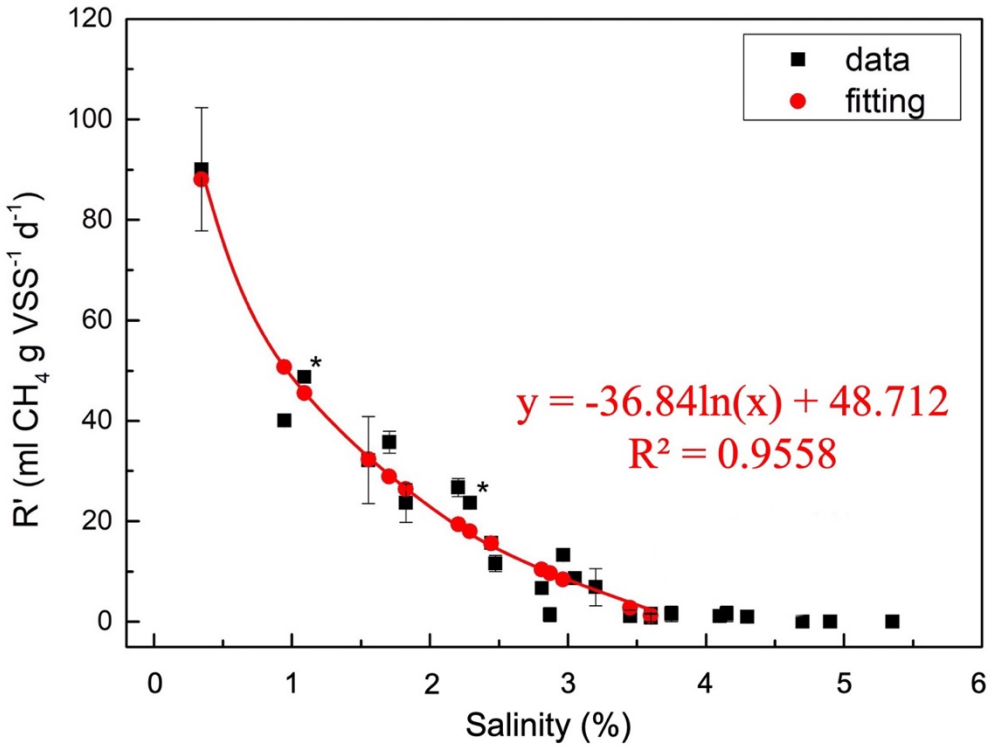

Fig. A-3 SMA at various salinity concentration, * represents duplicate data unavailable, error bars represent standard deviation of the mean for each duplicate experiment.

Summary

The combined inhibitory effect of ammonia and salt on methanogenesis of hydrogen was preliminarily investigated through kinetic analysis of SMA tests. The results demonstrated different inhibition patterns of ammonia and salt, despite both inhibitors decreasing SMA monotonically. The combined inhibitory effect was predicted using a 3-D contour and SMA data generated from the extended Monod model. Salinity was used as a unified parameter to predict the combined inhibition of ammonia and salt. This study provides a detailed perspective on the combined inhibitory effect of ammonia and salt on methanogenesis of hydrogen.

Reference

Capson-Tojo, G., Moscoviz, R., Astals, S., Robles, Á., Steyer, J.-P., 2020. Unraveling the literature chaos around free ammonia inhibition in anaerobic digestion. Renew. Sustain. Energy Rev. 117, 109487. https://doi.org/10.1016/j.rser.2019.109487

Duc, L.V., Nagao, S., Mojarrad, M., Miyagawa, Y., Li, Z.-Y., Inoue, D., Tajima, T., Ike, M., 2023. Bioaugmentation with marine sediment-derived microbial consortia in mesophilic anaerobic digestion for enhancing methane production under ammonium or salinity stress. Bioresour. Technol. 376, 128853. https://doi.org/10.1016/j.biortech.2023.128853

Grady, C.P.L., Daigger, G.T., Lim, H.C., 1999. Biological Wastewater Treatment, second. ed. Marcel Dekker, New York.

Lee, J., Kim, E., Hwang, S., 2021. Effects of inhibitions by sodium ion and ammonia and different inocula on acetate-utilizing methanogenesis: Methanogenic activity and succession of methanogens. Bioresour. Technol. 334, 125202. https://doi.org/10.1016/j.biortech.2021.125202

Lu, Y., Liaquat, R., Astals, S., Jensen, P.D., Batstone, D.J., Tait, S., 2018. Relationship between microbial community, operational factors and ammonia inhibition resilience in anaerobic digesters at low and moderate ammonia background concentrations. New Biotechnol. 44, 23–30. https://doi.org/10.1016/j.nbt.2018.02.013

Oh, G., Zhang, L., Jahng, D., 2008. Osmoprotectants enhance methane production from the anaerobic digestion of food wastes containing a high content of salt. J. Chem.

Technol. Biotechnol. 83, 1204–1210. https://doi.org/10.1002/jctb.1923
Wang, H., Fotidis, I.A., Angelidaki, I., 2015. Ammonia effect on hydrogenotrophic methanogens and syntrophic acetate-oxidizing bacteria. FEMS Microbiol. Ecol. 91, fiv130. https://doi.org/10.1093/femsec/fiv130
Yan, M., Treu, L., Zhu, X., Tian, H., Basile, A., Fotidis, I.A., Campanaro, S., Angelidaki, I., 2020. Insights into ammonia adaptation and methanogenic precursor oxidation by genome-centric analysis. Environ. Sci. Technol. 54, 12568–12582. https://doi.org/10.1021/acs.est.0c01945
Zhang, J., Zhang, R., He, Q., Ji, B., Wang, H., Yang, K., 2020. Adaptation to salinity: Response of biogas production and microbial communities in anaerobic digestion of kitchen waste to salinity stress. J. Biosci. Bioeng. 130, 173–178.

Achievements

Publications

1. **Li, Z.-Y.**, Inoue, D., Ike, M., 2023. Mitigating ammonia-inhibition in anaerobic digestion by bioaugmentation: A review. Journal of Water Process Engineering 52, 103506. https://doi.org/10.1016/j.jwpe.2023.103506
2. Duc, L.V., Nagao, S., Mojarrad, M., Miyagawa, Y., **Li, Z.-Y.**, Inoue, D., Tajima, T., Ike, M., 2023. Bioaugmentation with marine sediment-derived microbial consortia in mesophilic anaerobic digestion for enhancing methane production under ammonium or salinity stress. Bioresource Technology 376, 128853. https://doi.org/10.1016/j.biortech.2023.128853
3. **Li, Z.-Y.**, Nagao, S., Inoue, D., Ike, M., 2024. Different inhibition patterns of ammonia and salt revealed by kinetic analysis of their combined inhibitory effect on methanogenesis of hydrogen: A preliminary study. Biochemical Engineering Journal 205 (2024) 109263. https://doi.org/10.1016/j.bej.2024.109263
4. **Li, Z.-Y.**, Nagao, S., Inoue, D., Ike, M. Different bioaugmentation regimes for mitigating ammonium/salt inhibition in repeated batch anaerobic digestion: the generic converging trend of microbial community. Journal of Cleaner Production (Under review)

International conferences

1. **Li, Z.-Y.**, Nagao, S., Inoue, D., Ike, M. Dosage Investigation of the Bioaugmentation Inoculum for Ammonium Inhibition in Anaerobic Digestion

Process. The Water and Environment Technology Conference 2023 (WET2023), online, July 2023. Poster.

2. **Li, Z.-Y.**, Nagao, S., Inoue, D., Ike, M. Determination of Effective Inoculum Dosage of Bioaugmentation in Anaerobic Digestion for Mitigating Ammonium Inhibition. The 15th International Joint Workshop on Advanced Engineering Technology for Environment and Energy (AETEE), Osaka, Japan, August 2023. Oral presentation
3. **Li, Z.-Y.**, Nagao, S., Inoue, D., Ike, M. Determination of Effective Inoculum Dosage of Bioaugmentation in Anaerobic Digestion for Mitigating Ammonium Inhibition. The 13th International Conference on Environmental Engineering, Science and Management (EEAT), Khon Kaen, Thailand, May 2024. Oral presentation

Acknowledgments

Time has come to put a period to my study life in Osaka University. The start was not that smooth because of the influence of the pandemic. Luckily, with the help from many people that I can finally fulfill this research work.

Firstly, I would like to extend my sincere gratitude to my supervisor **Prof. Michihiko Ike** for his instructive support and advice to my research. His acute foresight and conscientiousness in conducting research work impressed and encouraged me a lot during my doctoral course.

Then, I would like to thank **Associate Prof. Daisuke Inoue** for his great support on my daily experiments and paper writing work. I would not be able to finish those manuscripts so smoothly without his guidance.

I would like to thank **Prof. Akihiro Tokai** for the precious comments and suggestions as a reviewer for this thesis.

I would like to thank **Associate Prof. Takahisa Tajima** from Hiroshima University for providing the marine sediments used in Chapter 2.

I also would like to thank **Mrs. Maki Morita** for the daily support on creating a convenient environment in the laboratory.

I would like to thank my partner in conducting experiments, **Mr. Shintaro Nagao**, for his impressive and diligent work.

I would like to thank my mentor, **Miss Yu Ren** for her generous support when I first came to Japan and her continuous care and kindness during my staying.

I would like to thank my friends, **Jing Cai, Tomoya Ishibashi, Shinpei Fujiwara Tomomi Sugiyama and Hanrui Chen** for their support and encouragement. I also want to thank other genial members in our laboratory for their kindness and help.

I would like to thank **New Energy and Industrial Technology Development Organization (NEDO)** of Japan for the financial support for this research. I also would like to thank the **China Scholarship Council** for providing the personal financial support.

I would like to thank **Osaka University Football Club** for accepting me as a member to participate trainings for over one year.

I would like to thank my friends in China, **Xin Chen**, **Lidan He** and **Qiuyi Dong** for their help and kindness.

At last, I would like to thank my family for their support.